Université d'Ottawa · University of Ottawa

Université d'Ottawa · University of Ottawa

FACULTÉ DES ÉTUDES SUPÉRIEURES ET POSTDOCTORALES

FACULTY OF GRADUATE AND POSTDOCTORAL STUDIES

Brian Richard SCOTT

AUTEUR DE LA THÈSE - AUTHOR OF THESIS

M.Sc. (Biochemistry)

GRADE - DEGREE

Department of Biochemistry, Microbiology and Immunology

FACULTÉ, ÉCOLE, DÉPARTEMENT - FACULTY, SCHOOL, DEPARTMENT

TITRE DE LA THÈSE - TITLE OF THE THESIS

Structure-Function Relationships of Human Apolipoprotein A-1: Role of the Amino-Terminal Amphipathic alpha-Helices

Y. Marcel

DIRECTEUR DE LA THÈSE - THESIS SUPERVISOR

CO-DIRECTEUR DE LA THÈSE - THESIS CO-SUPERVISOR

EXAMINATEURS DE LA THÈSE - THESIS EXAMINERS

D. Carrier

R. Parks

Z. Yao

J.-M. De Koninck, Ph.D.

LE DOYEN DE LA FACULTÉ DES ÉTUDES SUPÉRIEURES ET POSTDOCTORALES

DEAN OF THE FACULTY OF GRADUATE AND POSTDOCTORAL STUDIES

Structure-Function Relationships of Human Apolipoprotein A-I: Role of the Amino-Terminal Amphipathic α-Helices

by

Brian R. Scott

Thesis submitted to the Department of Biochemistry, Microbiology and Immunology in partial fulfillment of the requirements for the degree of Masters in Science

University of Ottawa
Ottawa, Ontario, Canada
November 2001

Your file Votre référence
ISBN: 0-494-10700-6
Our file Notre référence
ISBN: 0-494-10700-6

SUMMARY

To investigate the role(s) of the globular domain (residues 1-43) and the first class A helix (residues 44-65) of apolipoprotein A-I (apoA-I) in the metabolism of high density lipoproteins (HDL), we have taken a combined *in vitro* and *in vivo* approach. This work demonstrates that both the globular domain and helix 1 of apoA-I are important for the maturation of HDL. Deletions of these domains were associated with progressive impairments in the ability of apoA-I to activate lecithin:cholesterol acyltransferase (LCAT) and form cholesteryl ester rich HDL. While phospholipid binding was significantly reduced for both apoA-I mutants relative to wild-type apoA-I, cholesterol efflux was not affected by these deletions. We propose both the globular domain and helix 1 are critical LCAT activating domains of apoA-I and are required for the maturation of HDL *in vivo*.

DEDICATION

I dedicate my thesis to my family and friends whose constant support made this work possible. James Richard Scott, Lynda Scott, Barry Scott and Colleen Sweet have provided a guiding light and encouragement without which my efforts would have been fruitless. Furthermore, I dedicate this work to my grandparents Stanley and Jean Joynt and Grace Scott whose "joie de vie" is an inspiration to us all.

"Our doubts are traitors,
And make us lose the good we oft might win
By fearing to attempt."

William Shakespeare (Measure by Measure)

ACKNOWLEDGEMENTS

I would like to thank my supervisor and teacher Dr. Yves Marcel for his guidance, support and encouragement and Dan McManus who has provided invaluable tutelage and friendship. The expert assistance and timely advise of Vivian Franklin made my work more efficient and enjoyable. I would also like to acknowledge Dr. James Burgess for his expert academic and technical suggestions. Other members of the Lipoprotein and Atherosclerosis Group at the University of Ottawa Heart Institute made significant contributions to this work, including Andrea MacKenzie, Dr. Robert Scott Kiss, Dr. Phillippe Frank, Susha Zachariah and Cheryl Dollard. Furthermore, I would like to thank Dr. Daniel Sparks, Tracey Neville, Dr. Khai Tran and Jelena Vukmirica for their contributions, as well. Finally, I would like to acknowledge the remaining members of my thesis advisory committee, Dr. Ross Milne and Dr. James Van Huysse.

TABLE OF CONTENTS

LIST OF TABLES

LIST OF FIGURES AND ILLUSTRATIONS

ABBREVIATIONS

Δ7-43 ApoA-I: ApoA-I with deletion of residues 7-43
Δ7-43 ApoA-I Ad5: Δ7-43 apoA-I adenovirus
Δ7-65 ApoA-I: ApoA-I with deletion of residues 7-65
Δ7-65 ApoA-I Ad5: Δ7-65 apoA-I adenovirus
ABCA1: ATP Binding Cassette Transporter A1
AcLDL: Acetylated Low Density Lipoprotein
ApoA-I: Apolipoprotein A-I
ApoB-48: Apolipoprotein B-48
ApoB-100: Apolipoprotein B-100
ApoC-I: Apolipoprotein C-I
ApoC-II: Apolipoprotein C-II
ApoC-III: Apolipoprotein C-III
ApoE: Apolipoprotein E
ApoLp-III: Apolipophorin III
AppK_m: Apparent K_m
BSA: Bovine Serum Albumin
CAD: Coronary Artery Disease
CE: Cholesteryl Ester
CETP: Cholesteryl Ester Transfer Protein
DMEM: Dulbecco's Modified Eagle's Medium
DMPC: Dimyristoylphosphatidylcholine
FBS: Fetal Bovine Serum

FC: Free Cholesterol
FCR: Fractional Catabolic Rate
FED: Fish Eye Disease
FFA: Free Fatty Acids
FLD: Familial LCAT Deficiency
FPLC: Fraction Partition Liquid Chromatography
HDL: High Density Lipoproteins
HEK: Human Embryonic Kidney Cells
His-Δ1-43 ApoA-I: Histidine-Tagged ApoA-I with deletion of residues 1-43
His-Δ1-65 ApoA-I: Histidine-Tagged ApoA-I with deletion of residues 1-65
His-Δ210-243 ApoA-I: Histidine-Tagged ApoA-I with deletion of residues 210-243
His-Wt ApoA-I: Histidine-Tagged Wild-Type ApoA-I
HL: Hepatic Lipase
HRP: Horse Radish Peroxidase
HSPG: Heparin Sulfate Proteoglycans
IDL: Intermediate Density Lipoprotein
IgG: Immunoglobulin G
IPTG: Isopropyl-β-D-thiogalactopyranoside
LCAT: Lecithin:Cholesterol Acyltransferase
LDL: Low Density Lipoprotein
LDLr: Low Density Lipoprotein Receptor
LPL: Lipoprotein Lipase
NTA: Nickel Nitrilotriacetic
OxLDL: Oxidized Low Density Lipoprotein
PBS: Phosphate Buffered Saline
PC: Phosphatidylcholine
P.F.U.: Plaque Forming Units
PKA: Protein Kinase A
PKC: Protein Kinase C
PL: Phospholipid
PLTP: Phospholipid Transfer Protein
RCT: Reverse Cholesterol Transport
ROS: Reactive Oxygen Species
SDS-PAGE: Sodium Dodecylsulfate Polyacrylamide Gel Electrophoresis
SDS-PAGGE: Sodium Dodecylsulfate Polyacrylamide Gradient Gel Electrophoresis
SM: Sphingomyelin
SMC: Smooth Muscle Cells
SR-AI / A-II: Scavenger Receptor Class A Type I / Type II
SR-BI: Scavenger Receptor Class B Type I
TC: Total Cholesterol
TD: Tangier Disease
TG: Triglyceride
TMS: Transmembrane Sequence
TRL: Triglyceride-Rich Lipoprotein
VLDL: Very Low Density Lipoprotein
Wt ApoA-I: Wild-Type ApoA-I
Wt ApoA-I Ad5: Wild-Type ApoA-I

CHAPTER 1: INTRODUCTION

1.1 Pathogenesis of Atherosclerosis

In 1973, Ross and Glomset proposed the 'Response to Injury Hypothesis' to describe the pathogenesis of the atherosclerotic lesion (1). In this model, oxidatively modified low density lipoproteins (LDL) are retained within the intimal layer of the artery where they elicit complex immune responses causing the recruitment of macrophages and smooth muscle cells from the bloodstream and media, respectively. Subsequent accumulation of extracellular lipid, fibrous elements and a calcium-phosphate matrix are hallmarks of an advanced atheroma that penetrates the arterial lumen restricting blood flow. Thrombosis is highly associated with the rupture of such lesions, occlusion of the arterial lumen and clinical presentation of the disease.

LDL, the major cholesterol containing lipoprotein in the blood, passively diffuses from the circulation to the intima in all areas of all healthy arteries. However, regions of specific arteries prone to atherosclerosis, predominantly areas of arterial branching or curvature, exhibit enhanced retention of LDL via direct interaction between apoB and extracellular matrix proteoglycans (2,3). Limited oxidation of LDL then occurs as reactive oxygen species (ROS), derived from vascular cells, modify the phospholipid component of LDL (4). Oxidized LDL is constitutively endocytosed via interaction with the macrophage scavenger receptors, SR-AI/II and CD36. This process is critical to lipid accumulation within the atherosclerotic lesion as mice lacking either receptor exhibit significantly less atherosclerosis (5,6). Constitutive endocytosis of oxidized LDL induces the formation of large intracellular cholesterol droplets and are consequently referred to as foam cells. Foam cells are the hallmark of the early atherogenic lesion and are responsible for the continual accumulation of cholesterol throughout lesion development.

Inflammatory cytokines secreted from both macrophage and T cells stimulate the proliferation and migration of smooth muscle cells (SMC) from the media to the intima. SMC secrete an extracellular matrix that provides structural support and a fibrous cap to a growing mass of extracellular lipid derived from the death of macrophage foam cells termed the 'necrotic core'. The necrotic core contains, in addition to cholesterol and cell debris, a varying degree of calcification. At this point the lesion size increases first in the direction of the adventitia until a critical point at which the fibrous plaque expands into the arterial lumen restricting blood flow. This thickening of the atherosclerotic plaque contributes to arterial stenosis that further alters arterial hemostasis.

However, thrombosis is highly associated with plaque instability rather than the degree of arterial stenosis. Plaque instability stems from breakdown of the SMC derived extracellular matrix by several well-characterized enzymes secreted from macrophages, including interstitial collagenase, gelatinases, stromolysin and the cathepsins (7). Furthermore, T cells produce IFN-γ that inhibits SMC matrix production. Subsequent to destabilization, plaques can fissure exposing tissue factor to the necrotic core making these sites for platelet attachment. Thrombi of significant size can occlude blood flow in a coronary artery causing unstable angina and myocardial infarction.

1.2 Human Plasma Lipoproteins: General Physical Properties

This section describes the lipid and apolipoprotein composition of the plasma lipoproteins. The information presented here was compiled from previously published review papers and book chapters (8,9). Lipoproteins are microemulsions consisting of a core of neutral lipid, predominantly cholesteryl ester (CE) and triacylglycerol (TG),

surrounded by a phospholipid (PL) monolayer also containing free cholesterol (FC) (Fig. 1-1). All surface lipids are amphipathic and are oriented with their hydrophobic moiety directed towards the lipoprotein core and hydrophilic moiety exposed to the aqueous environment. The apolipoproteins are also amphipathic and situate within the PL monolayer such that hydrophobic domains interact with surface lipid and stabilize the lipoprotein structure while polar residues are exposed to the aqueous environment. The plasma lipoproteins contain exchangeable (apoA-I, apoA-IV, apoC-I, apoC-II, apoC-III and apoE) and/or non-exchangeable (apoB-48 and apoB-100) apolipoproteins. While apoA-II is normally considered an exchangable apolipoprotein, it remains to be determined how this apolipoprotein is secreted and associated with lipoproteins. Exchangeable apolipoproteins are water soluble in the absence of lipids while non-exchangeable apolipoproteins are insoluble. Thus, *in vivo*, exchangeable apolipoproteins are able to dissociate from one lipoprotein particle and reassociate with another via a lipid-free intermediate. Non-exchangeable apolipoproteins are secreted in the context of a mature lipoprotein particle and remain associated with the lipid moiety until eventual catabolism.

Heterogeneous in size, density and lipid and protein composition (Table 1-1and 1-2), the plasma lipoproteins are divided into 5 classes and are involved in 3 distinct routes of cholesterol transport. Chylomicrons are the largest lipoprotein particles. Their molecular mass is on the range of 400 MDa and approximately 75-1200 nm in diameter. These lipoproteins are secreted from intestinal enterocytes and transport dietary triacylglycerol to sites of storage and utilization in the body. Due to the lipoprotein size and triacylglycerol content, these are the most buoyant lipoprotein species equilibrating at a density of 0.930 g/mL. The hepatic analogues of chylomicrons are the very low density lipoproteins (VLDL). VLDL are 10-80 MDa particles, range in diameter from 30-80 nm and are slightly

denser than chylomicrons (0.930-1.006 g/mL). These lipoproteins transport TG and cholesterol from the liver to sites of utilization and storage in the body. Hydrolysis of the VLDL TG core generates a smaller and denser lipoprotein particle named intermediate

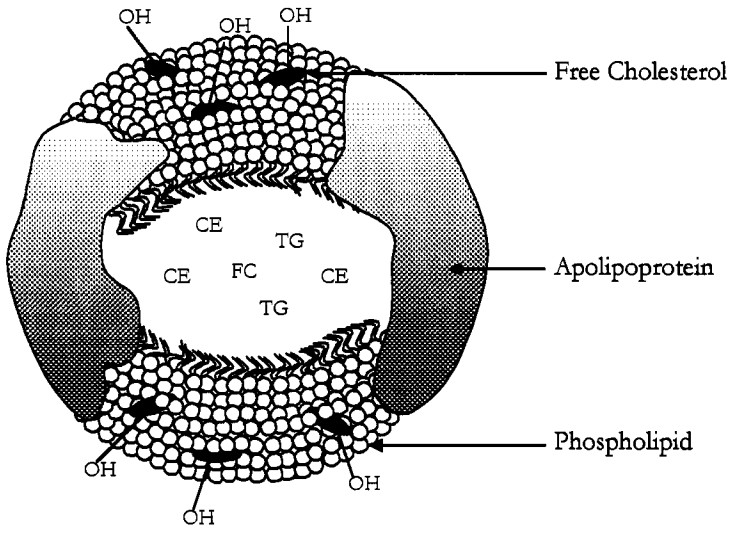

Figure 1-1: Model of a Spherical Lipoprotein

Lipoproteins are microemulsions assembled such that amphipathic lipid molecules form the surface monolayer while neutral lipids partition to the core and are excluded from the aqueous environment. Apolipoproteins contain amphipathic α-helices and interact with the lipoprotein surface to stabilize the overall structure and mediate interactions with cell surface receptors, lipolytic enzymes and lipid transfer proteins.

density lipoprotein (IDL). IDL are 5-10 MDa lipoproteins, are 25-35 nm in diameter and occupy a density of 1.006-1.019 g/mL. This lipoprotein class is intermediate in density between VLDL and the subsequent lipoprotein class, the low density lipoprotein (LDL). LDL are generated by the hydrolysis of IDL and, as such, are derived from VLDL initially secreted from the liver. These lipoproteins are approximately 2.3 MDa in size, 18-25 nm in diameter and equilibrate at a density of 1.019-1.063 g/mL. Finally, high density lipoproteins (HDL) are composed of two principal subclasses, HDL_2 and HDL_3. HDL are not assembled intracellularly and secreted as are chylomicrons and VLDL or derived from the

Table 1-1: Physical Properties of the Human Plasma Lipoproteins[a]

	Electrophoretic Definition[b]	Particle Size (nm)	Molecular Weight	Density (g/mL)
Chylomicron	Remains at Origin	75-1200	~400 000 000	0.930
VLDL	Pre-β Lipoprotein	30-80	10-80 000 000	0.930-1.006
IDL	Slow Pre-β Lipoprotein	25-35	5-10 000 000	1.006-1.019
LDL	β-Lipoprotein	18-25	2 300 000	1.019-1.063
HDL_2	α-Lipoprotein	9-12	360 000	1.063-1.125
HDL_3	α-Lipoprotein	5-9	175 000	1.125-1.210

[b]Migration by agarose gel electrophoresis
[a]Originally published in ref (8)
Reprinted with permission of Academic Press Inc.

Table 1-2: Chemical Composition of Post-Prandial Human Lipoproteins[a]

	Surface Components			Core Lipids	
	FC	PL	Apolipoprotein	TG	CE
			mol%		
Chylomicrons	35	63	2	95	5
VLDL	43	55	2	76	24
IDL	38	60	2	78	22
LDL	42	58	0.2	19	81
HDL_2	22	75	2	18	82
HDL_3	23	72	5	16	84

[a]Originally published. in ref (8)
Reprinted with permission of Academic Press Inc.

catabolism of precursors like IDL and LDL. HDL are assembled within the circulation from exchangeable apolipoprotein and lipid constituents. HDL also differ from other lipoprotein classes in that they transport lipid in the opposite direction as compared to the

apoB-100 containing lipoproteins, transporting excess lipid from peripheral tissues to the liver for biliary secretion and recycling. Furthermore, HDL cholesterol levels are inversely correlated with the risk of coronary artery disease as established in clinical studies.

1.3 HDL Metabolism

High density lipoproteins (HDL) are the smallest and most dense lipoprotein class and transport cholesterol from extra-hepatic cells to the liver for excretion in the bile and recycling, a process referred to as Reverse Cholesterol Transport (10). This pathway is widely accepted as the primary mechanism by which HDL exert their anti-atherogenic effects. This section is devoted to the description and interconversion of HDL subclasses, individual steps in the reverse cholesterol transport pathway and HDL catabolism.

1.3.1 Introduction to HDL Structure

This summary of HDL structure was compiled from previously published review articles (refer to refs (11,12) for a more detailed description). Plasma HDL particles range in diameter from 5-12 nm with molecular masses of 200-400 kDa. The organization of the lipid constituents in HDL is similar to other plasma lipoproteins and was illustrated in Fig. 1-1, spherical microemulsions assembled such that apolipoproteins and FC situate within the PL monolayer while neutral lipids, CE and TG, partition to the HDL core.

Due to the significantly smaller size of HDL, special consideration must be made to the relative contribution of core versus surface constituents as small lipoproteins have a greater surface area to volume ratio. The lipoprotein surface monolayer is 20 Å thick and accounts for a significant proportion of the lipid content and approximately 80-85% of the HDL particle volume. While chylomicron and VLDL mass is predominantly TG, 80% of

HDL mass is apolipoprotein and PL. The predominant apolipoprotein constituent of HDL is apoA-I, which accounts for approximately 70% of the protein mass while apoA-II and the apoCs constitute 20% and 10%, respectively.

HDL are perhaps the most underrated lipoprotein class due to the manner in which the plasma values are expressed. HDL plasma concentrations are expressed in terms of HDL cholesterol values as are LDL, the predominant cholesterol carrying lipoprotein particle in the plasma. However, HDL and LDL levels in plasma are similar with respect to total mass (lipid + protein) and, if HDL particle size is taken into account, plasma HDL particle concentration is 10-20 fold greater.

1.3.2 Identification of HDL Subclasses

The formation of HDL precursors and their subsequent conversion to spherical, CE-rich lipoproteins is referred to as HDL maturation. HDL are very heterogeneous in size, density, lipid and apolipoprotein content. The following considers individual HDL subclasses differing in these physical properties, their respective roles in HDL metabolism and reverse cholesterol transport.

1.3.2.1 HDL_1 / HDL_2 / HDL_3

Gofman and coworkers separated plasma HDL into three distinct pools by both non-denaturing gradient gel electrophoresis and density ultracentrifugation, which are referred to as HDL_1, HDL_2 and HDL_3 in an order of increasing density and decreasing size (13). Of these, HDL_2 and HDL_3 are by far the most abundant in normolipidemic humans. HDL_2 are 360 kDa in size, 9-12 nm in diameter and occupy a density of 1.063-1.125 g/mL. HDL_3 occupy a density ranging from 1.125-1.210 g/mL, are approximately 175 kDa in size

and 5-9 nm in diameter. The core volume of HDL_2 is 3.5-fold greater than HDL_3 while the increase in protein content is only 50%. The mass difference in protein content may correspond to the addition of one molecule of apoA-I (14) however this has not been demonstrated.

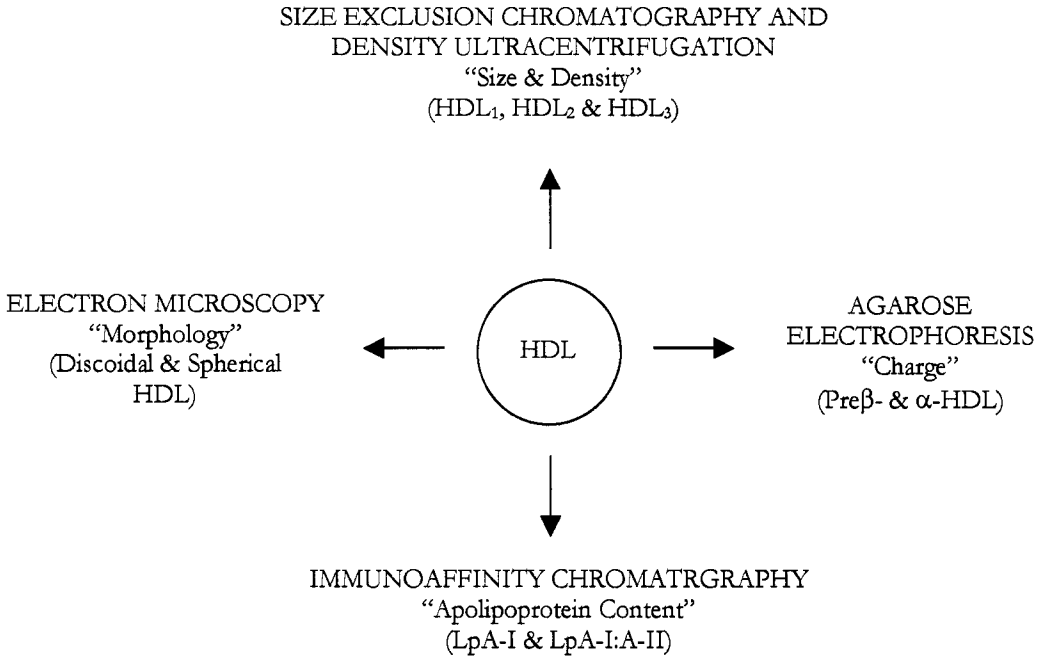

Figure 1-2: HDL Subclasses as Defined by Their Physical Properties and Separation Procedures
Adapted from Barrans *et al.* (15)

Interindividual variations in HDL concentrations are due predominantly to changes in HDL_2 but not HDL_3 levels. This may be related to LPL activity, which is in general proportional to HDL_2 levels (16-18). HDL_3 readily accept PL, FC and apolipoproteins from lipolyzed VLDL and cell membranes to generate an intermediate HDL_2 particle, referred to as HDL_{2a}. This step alone is insufficient for the formation of true HDL_2, referred to as HDL_{2b}, which requires the additional enrichment of LCAT-derived CE. Therefore, the conversion of HDL_3 to HDL_{2b} is thought to constitute a two-step process. The first step involves the transfer of LPL- and cell-derived surface components to HDL_3, and may be

reversible, while enrichment with CE mediated by LCAT is necessary for the ultimate conversion to HDL_2.

HDL_1 is an important lipoprotein constituent in rodents (19-21) and is present, but not abundant, in human plasma (22). This HDL subclass is larger than HDL_2 (13-14 nm in diameter) and differs significantly from $HDL_{2,3}$ as apoE accounts for an estimated 60% of the total protein content (21). These lipoproteins form in plasma, apparently from HDL_2, and represent a further progression in HDL maturation. Incubation of human plasma in the test tube at 37°C results in a pronounced increase in HDL_1 levels, presumably due to the accumulation of LCAT-derived CE in HDL (23). Thus, it appears that the conversion of HDL_2 to HDL_1 is governed by the same reactions that are responsible for the transformation of HDL_3 to HDL_2. The emergence of HDL_1-like particles in cholesterol-fed animals suggests that native HDL_1 form in response to the need to transport larger quantities of HDL cholesterol than are normally required (24). The replacement of apoA-I with apoE may result from the poor association of apoA-I with larger lipoprotein particles and the size of HDL_1 may represent the limit at which apoA-I is thermodynamically the favoured HDL protein constituent.

1.3.2.2 Preβ- and α- HDL

On the basis of their electrophoretic mobility in agarose, HDL are divided into those with α- and preβ- mobility describing their migration relative to α and β globulins and are referred to as α- and preβ-HDL (25,26). This technique separates plasma lipoproteins by surface charge, which is determined by both lipid and apolipoprotein constituents. Plasma HDL is predominantly α-migrating while preβ-HDL accounts for only 2-14% (25,27). By two-dimensional agarose/native PAGGE, α-migrating HDL were shown to consist of both

HDL_2 and HDL_3 while preβ-HDL consisted of 3 subfractions: $preβ_1$, $preβ_2$ and $preβ_3$-HDL (reviewed in ref (15)). The physical properties and metabolism of the α-migrating HDL includes the HDL_1, HDL_2 and HDL_3 subclasses described above whereas preβ-HDL are distinct from these forms and represent cholesterol-poor HDL precursors.

Preβ-HDL consist of apoA-I, PL, various amounts of FC and are generally devoid of CE. $Preβ_1$-HDL are 70-80 kDa in size and appoximately 5 nm in diameter (25) while $preβ_2$-HDL are significantly larger, on the order of 325 kDa and 10-12 nm in diameter (26,28). $Preβ_3$-HDL are slightly larger than $preβ_2$-HDL and are poorly characterized due to their very low abundance in human plasma.

The molecular basis accounting for the electrophoretic migration of α- and preβ-HDL was described by Davidson and coworkers (29). The difference between the two appears to be due to the presence of a neutral lipid core in α- but not preβ-HDL. While neutral lipids do not directly contribute to HDL surface charge, conformational changes in the surface apolipoproteins, primarily apoA-I, are believed to confer this effect. Some contribution may be made from phosphatidylinositol content, however, this has been disputed by some groups (15).

$Preβ_1$-HDL are the most effective acceptors of cellular cholesterol due to a lower FC to PL ratio relative to HDL_2 and HDL_3 (30). Yancey and coworkers suggested that apoA-I initially associates with the cell membrane to form apoA-I/PL complexes and these complexes subsequently serve as the acceptors for cholesterol efflux (31).

$Preβ_2$ and $preβ_3$-HDL are thought to represent subsequent stages in the maturation of $preβ_1$-HDL, those particles which have accumulated significant levels of FC and PL from cells. However, $preβ_{2,3}$-HDL may also be generated directly during TRL lipolysis or HDL

remodeling. Several studies suggest that preβ-HDL are converted into α-migrating HDL. When plasma is incubated at 37°C for 90 min, total preβ-HDL content decreases by 33% (32). Under conditions in which LCAT activity is inhibited, a decrease in preβ-HDL does not occur, suggesting conversion of FC to CE is necessary for the conversion of preβ- to α-migrating HDL. Other work indicates that during similar incubations the association of apoA-I with preβ-HDL decreases over time with a parallel increase in that associated with α-migrating HDL and this shift was prevented by LCAT inhibition (32).

1.3.2.3 LpA-I and LpA-I:A-II

The second major apolipoprotein of HDL, apoA-II, defines two HDL subclasses, those particles containing apoA-I without apoA-II (LpA-I) and those containing apoA-I and apoA-II (LpA-I:A-II). Elevated levels of LpA-I are associated with decreased risk of atherosclerosis while no correlation is observed for LpA-I:A-II (33-36) suggesting these subclasses differ in their functional properties.

ApoA-II binds with greater affinity to PL than apoA-I and displaces apoA-I from HDL *in vitro* (37). However, when an apoA-II to apoA-I ratio in the physiological range (0.5:1.0) was used, apoA-II induced a rearrangement in apoA-I structure, enhanced apoA-I susceptibility to denaturation and decreased LCAT reactivity without appreciable apoA-I displacement (38). Addition of apoA-II was also found to render the central domain of apoA-I (residues 99-187) more accessible to proteolytic digestion.

HDL containing only apoA-II are undetectable *in vivo* but are easily generated *in vitro* (39). LpA-I and LpA-I:A-II appear equivalent with respect to their capacity to promote cholesterol efflux in most studies (40,41) however, some reports consider LpA-I better acceptors of cellular cholesterol (42-44). Lipid-free apoA-II recruits PL from cell

membranes as efficiently as does apoA-I, however apoA-II/PL complexes cannot be transformed to α-HDL by LCAT. This suggests the contribution of apoA-II to the pool of HDL precursors (preβ-HDL) and subsequent generation of CE-rich HDL is limited.

ApoA-II appears to modulate the activity of factors involved in HDL metabolism. Studies with apoA-II transgenic (45,46) and knock-out (47) mice suggests apoA-II inhibits HL activity. Zhong *et al.* observed that coexpression of apoA-II with CETP resulted in TG-enriched HDL, resistant to reductions in size and apoA-I content, reflecting inhibition of HL by apoA-II (46). Thus apoA-II may be a physiological inhibitor of HL activity and maintain steady-state concentrations of HDL by inhibiting HL-mediated HDL remodeling and catabolism. *In vitro* studies addressing this issue are controversial and have shown apoA-II both stimulates (48) and inhibits (49) HL activity.

1.3.2.4 Discoidal and Spherical HDL

For a complete description of the methodology used for visualizing lipoproteins by negative stain electron microscopy please refer to a review by Forte *et al.* (50). Newly isolated plasma lipoproteins are traditionally visualized by the negative staining technique using an electron dense stain such as uranyl acetate, uranyl formate, ammonium molybdate and phosphotungstate. HDL are predominantly 'spheroidal' in morphology and, when applied at high concentrations, form hexagonal packing arrays. Examination of HDL from individuals with familial LCAT deficiency and fish-eye disease reveals the presence of predominantly 'disc-shaped' (discoidal) HDL. Discoidal HDL likely represent intermediates in the formation of spherical HDL. In support of this hypothesis, lymph HDL, which represent newly synthesized intestinal HDL precursors, are discoidal (51). Reconstituted HDL formed *in vitro* by the cholate dispersion method exhibit both preβ-mobility and

discoidal morphology (52,53). Incubation of both plasma from LCAT deficient patients and reconstituted discoidal HDL with purified human LCAT *in vitro* results in the formation of spherical HDL and a shift to α-electrophoretic mobility (54,55). Thus preβ- and α-migrating HDL may be synonymous with discoidal and spherical HDL, respectively.

1.3.3 The Reverse Cholesterol Transport Hypothesis

Research interest in HDL is derived from the findings of epidemiological studies which have established an inverse correlation between HDL cholesterol levels and the risk of coronary artery disease (56-62). In support of this protective effect, *in vitro* studies have described several potential anti-atherogenic mechanisms for HDL (Table 1-3). However, the most widely accepted explanation is that of the reverse cholesterol transport pathway. First proposed by Glomset in 1968, it has remained essentially the same since its inception (10). HDL acquire cholesterol from peripheral tissues, including cells within the arterial wall, and mediate its transport to the liver for biliary excretion and recycling (Fig. 1-3). By mitigating

Table 1-3: Activities Other Than Reverse Cholesterol Transport Attributed to ApoA-I and/or HDL*

Activity	Reference
Inhibits LDL oxidation[a]	(63,64)
Anticoagulant[a]	(65)
Inhibits endothelial expression of adhesion molecules[a]	(66)
Suppresses neutrophil activation[a]	(67)
Antiviral[a]	(68)
Inhibits platelet-dependent thrombus formation[a]	(69)
Inhibits membrane lysis by complement[a]	(68)
Inhibits bacterial endotoxin[a]	(70)
Induces trypanosomal lysis	(71-73)
Inhibits human anti-bacterial/cytotoxic peptide LL-37	(74)
Stimulates human placental lactogen production	(75)
Stabilizes prostacyclin	(76)
Stimulates apoE secretion in macrophages	(77)
Induces amyloidosis (apoA-I mutants)	(78)

[a]Potential anti-atherogenic properties of apoA-I / HDL aside from Reverse Cholesterol Transport
*Adapted from Brouillette *et al.* (79)

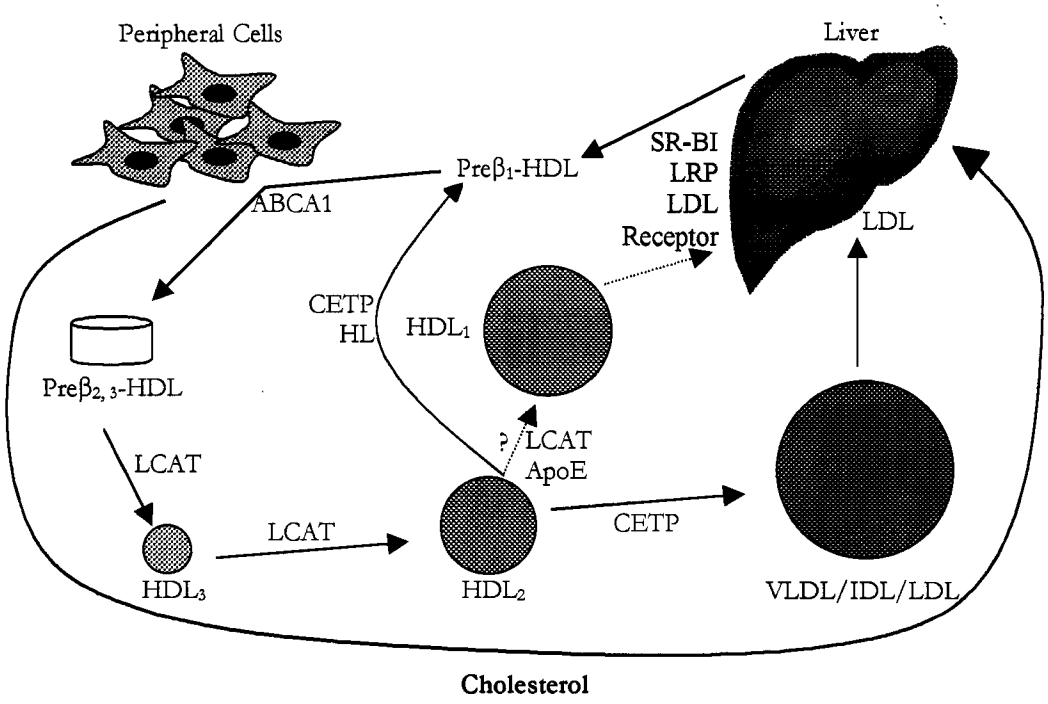

Figure 1-3: Schematic of the Reverse Cholesterol Transport Pathway

Nascent HDL (preβ$_1$-HDL) acquire FC and PL from peripheral cells by efflux mechanisms involving ABCA1 forming larger preβ$_{2,3}$-HDL. Discoidal, preβ-HDL are converted to spherical, α-migrating HDL$_{2,3}$ by the partitioning of LCAT-derived CE to the HDL core. HDL-CE is transferred to the apoB-100 containing lipoproteins and subsequently taken up by the liver via interaction with the LDL receptor. Alternatively, some HDL-CE may be taken up directly by selective uptake involving SR-BI or conversion of HDL$_2$ to HDL$_1$ and receptor-mediated endocytosis involving the LDL receptor and LRP.

the accumulation of excess cholesterol, HDL protect against the formation of cholesterol-engorged macrophages within the arterial wall and the subsequent development of atherosclerotic lesions. This section describes the key steps in this pathway.

1.3.3.1 Origins of HDL Precursors

As opposed to chylomicrons and VLDL that are assembled intracellularly and secreted, HDL appear to be assembled within the circulation from apolipoprotein and lipid constituents derived from various sources. Spherical, α-migrating HDL originate from HDL precursors, particles consisting of apoA-I and minimal amounts of lipid, referred to as nascent HDL.

Preliminary experiments using rat liver perfusion identified discoidal complexes, proposed to be nascent HDL (80). However, apoE but not apoA-I was the major apolipoprotein component of these structures suggesting they are not precursors to mature HDL, which contain predominantly apoA-I. Similarly, electron microscopic examination of intestinal lymph revealed the presence of discoidal structures. However, in contrast to hepatic perfusates, apoA-I was the predominant apolipoprotein (81).

The inability to detect mature HDL along the cellular secretory pathway in liver and intestinal cells further suggested these particles are not the secretory products of cells, while intact VLDL and chylomicrons were identified by this technique (80,82). Nonetheless, hepatic production rate of apoA-I is a major determinant of plasma HDL levels. Sorci-Thomas *et al.* demonstrated that isocaloric substitution of polyunsaturated fat reduced HDL concentrations in African green monkeys and correlated with reduced hepatic secretion of apoA-I during liver perfusion (83). Similarly, a comparison of cynomolgus and African green monkeys indicated that hepatic secretion rate of apoA-I was 5-fold greater in African green monkeys, which have 2- and 2.7-fold greater plasma levels of HDL cholesterol and apoA-I than cynomolgus monkeys (84). Furthermore, higher plasma levels of HDL correlated with a greater resistance to diet induced atherosclerosis in the African green monkey. These experiments suggest that while HDL may not be assembled within the cell, cellular production rate of apoA-I is responsive to dietary lipid status and directly related to plasma HDL levels.

Lipoprotein lipase (LPL) hydrolyzes core TG in chylomicrons and VLDL and its activity is dependent upon its cofactor apoC-II. Direct interaction of apoC-II with the N-terminal domain may represent the method of activation of LPL (85). LPL is localized

predominantly on the luminal side of endothelial cells, in proximity to sites of TG storage and utilization, adipose and muscle tissues that are the predominant sites of LPL synthesis.

LPL activity is directly related to plasma HDL concentrations and hydrolysis of chylomicron and VLDL core TG contributes surface components including PL, FC and apolipoproteins to the HDL pool (86,87). LPL or apoC-II deficiency is associated with elevated plasma TG, VLDL-C and apoB and low LDL-C and HDL-C consistent with impaired catabolism of TRL and impaired generation of HDL precursors.

The lipidation of nascent HDL was recently shown to depend upon phospholipid transfer protein (PLTP). PLTP is a 476 amino-acid glycoprotein (88) and a member of the lipopolysaccharide binding/lipid transfer protein family, which also includes cholesteryl ester transfer protein (CETP), lipopolysaccharide-binding protein (LBP) and bactericidal/permeability-increasing protein (BPI) (88,89).

In vitro studies have demonstrated that PLTP transfers PL (90), α-tocopherol (91), lipopolysaccharide (92) and FC (93) between lipoprotein particles. In doing so, PLTP modified HDL particle size distribution and, subsequently, was proposed to be important for HDL metabolism *in vivo*. The most convincing evidence for this has been published recently using PLTP transgenic and knock-out mouse models. Jiang *et al.* demonstrated that PLTP deficient mice were unable to transfer phosphatidylcholine from intravenously infused VLDL to HDL particles, which resulted in enhanced HDL catabolism and low HDL and apoA-I levels (94). However, studies in which PLTP was overexpressed were inconsistent with these observations. Transgenic mice or mice expressing high levels of human PLTP by adenovirus-mediated gene transfer exhibited decreased apoA-I and HDL levels (95-97). Human PLTP transgenic mice exhibited a 30-40% decrease in plasma levels of HDL and incubation of plasma from these mice at 37°C revealed a 2- to 3-fold increase in the

formation of preβ-HDL relative to wild-type mice (96). While preβ-HDL are normally a minor subfraction of HDL, this species is a very efficient acceptor of cellular cholesterol and

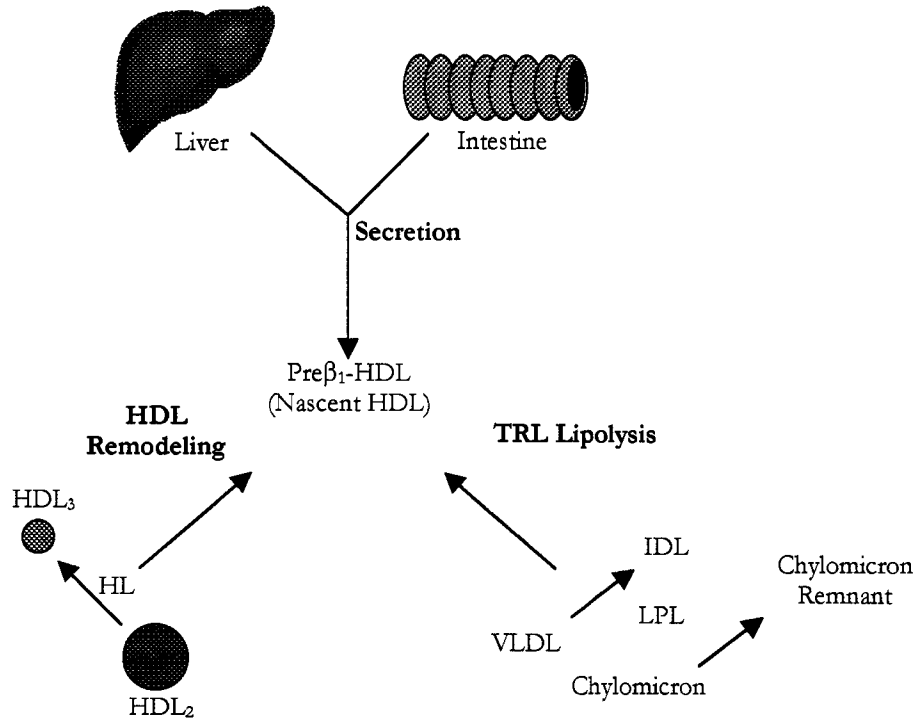

Figure 1-4: Sources of HDL Precursors

Nascent HDL are derived from hepatic and intestinal secretion, lipolysis of triglyceride-rich lipoproteins (TRL) and HDL remodeling.

a key component to reverse cholesterol transport. Therefore, PLTP is proposed to have an anti-atherogenic effect by mitigating accumulation of excess cholesterol via generation of preβ-HDL. Preβ-HDL are also generated by HDL remodeling involving CETP and HL and is described in Section 1.3.3.4. The sources of HDL precursors are summarized in Fig. 1-4.

1.3.3.2 HDL-Mediated Removal of Cellular Cholesterol: Tangier Disease and ABCA1

Cholesterol efflux refers to the net movement of cellular FC to an extracellular acceptor particle, a process that opposes the accumulation of excess cholesterol by cells *in*

vivo and is subdivided into two general forms (reviewed in ref (98)). The first is 'diffusional' efflux, which concerns the net movement of cholesterol from cell membranes to a lipoprotein or another acceptor particle through aqueous phase at below critical micelle concentration (99-101). The process is non-directional and the rate-limiting step is desorption of cholesterol from the plasma membrane. This varies depending upon cell type (102,103), properties of the cell membrane and LCAT activity, which maintains a concentration gradient of FC between the cell membrane and the lipoprotein surface driving the net transfer to the lipoprotein (10).

The finding that lipid-free apolipoproteins induced cellular cholesterol release (104) formulated the second type referred to as 'apolipoprotein-specific' cholesterol efflux sometimes referred to as binding and translocation dependent efflux. While this mechanism is only partially defined, it involves the direct interaction of exchangeable apolipoproteins with the cell followed by the efflux of cholesterol and PL to the acceptor protein. As opposed to the diffusional mechanism, the apolipoproteins initially recruit PL, probably from the cell surface, forming apolipoprotein/phospholipid complexes that subsequently recruit cholesterol forming HDL particles (105).

The classification of HDL as products of the remnants derived from the lipolysis of chylomicrons and VLDL (proposed by Eisenberg (106)) now seems inadequate. The importance of cellular lipid acquisition by HDL precursors has emerged following the identification of ABCA1 as the affected gene in Tangier disease. This discovery clearly demonstrated that cholesterol efflux mechanisms involving lipid-free/poor apolipoproteins are essential for maintenance of steady-state concentrations of HDL and supports the role of reverse cholesterol transport in cellular cholesterol homeostasis.

Tangier disease (TD) is an autosomal recessive disorder first identified in a kindred from Tangier Island, Virginia (recently reviewed in ref (107)). The most striking features of these individuals are hyperplastic, orange tonsils present in approximately one-third of the less than 100 cases documented to date. Clinical presentation of TD is variable and may involve splengomegaly, hypocholesterolemia, ocular abnormalities, peripheral neuropathy and coronary artery disease. Biochemical features include HDL deficiency, elevated plasma TG levels and peripheral storage of CE in various cell types. The most prominent cell types accumulating CE belong to the reticulo-endothelial system, however other cell types accumulate CE as well, including the fibroblasts of the cornea, melanocytes, Schwann cells, neurons and non-vascular smooth muscle cells.

The most prominent lipoprotein phenotype associated with this disease is the virtual absence of α-migrating HDL and apoA-I levels reduced to 1-3% of normal values (108) despite normal apoA-I structure and apoA-I synthetic rate (109). The only HDL species present in these patients is preβ_1-HDL, a lipid-poor HDL precursor normally of low abundance in plasma.

The accumulation of cholesterol in TD reflects an imbalance in cellular cholesterol homeostasis. In this regard, several laboratories demonstrated that fibroblasts isolated from Tangier patients had defective cholesterol efflux (110-112). Cell culture studies indicated that efflux of cholesterol to HDL and cyclodextrin (111) was normal in Tangier fibroblasts while efflux to apoA-I was virtually absent relative to controls (111,113).

In 1999, three groups identified mutations in the gene encoding for the ATP binding cassette transporter A1 (ABCA1) as the TD gene (114-116). This was a previously cloned member of a large protein family known as the ATP binding cassette transporters (reviewed in ref (117)). More recently, Marcil *et al.* demonstrated that mutations in ABCA1 are also

associated with many cases of hypoalphalipoproteinemia and familial HDL deficiency (FHD) (118).

The topology of ABCA1 is similar to that of the cystic fibrosis transmembrane conductance regulator (CFTR), consisting of 2 transmembrane domains each consisting of 6 putative transmembrane helices. Intracellularly, between the 6^{th} and 7^{th} transmembrane sequence are situated Walker A and Walker B motifs found in many proteins that utilize

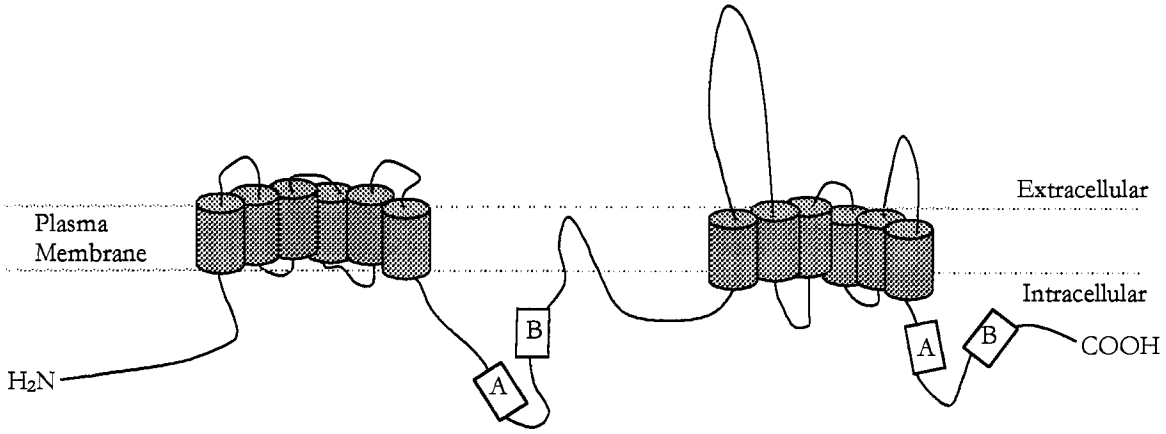

Figure 1-5: Putative Topology of the ATP Binding Cassette Transporter A1

The schematic of the ATP binding cassette transporter A1 (ABCA1) illustrates the 2 sets of 7 transmembrane helices and 2 sets of intracellular Walker A and B motifs. Distal to the first set of Walker motifs a hydrophobic loop is thought to penetrate into but not through the plasma membrane.
Adapted from Hayden *et al.* (119)

ATP (Fig. 1-5) (120). ABCA1 is associated predominantly with the plasma membrane where it may act as a PL (and cholesterol) 'flippase', transferring these molecules from the inner to the outer membrane leaflet where they are accessible to surface bound apolipoproteins (121,122). While the tertiary structure of ABCA1 is unknown, by analogy to a close family member, P-glycoprotein, this transporter likely forms a large aqueous pore in the plasma membrane in which the Walker A and B motifs are in close proximity (123). Lipid-free apolipoproteins may interact directly (124,125) or indirectly (126) with ABCA1, stimulating the mobilization of intracellular cholesterol in transport vesicles or 'rafts' in a Golgi-

dependent process to the plasma membrane. ABCA1 translocates the lipid domains to the exofacial side of the plasma membrane where they form structures protruding from the cell surface. Interaction of apolipoproteins solublizes these domains generating small HDL particles.

1.3.3.3 HDL Maturation: The Role of LCAT

Lecithin:cholesterol acyltransferase (LCAT) was first identified by Glomset in 1962 and is a plasma enzyme that catalyzes the hydrolysis and transfer of the sn-2 fatty acyl chain of phosphatidylcholine (lecithin) to FC forming lysophosphatidylcholine and CE (reviewed in refs (127,128)). CE is the predominant storage form of cholesterol both in cells and in lipoproteins. Furthermore, the majority of CE in plasma is derived from LCAT esterification. HDL is the preferred lipoprotein substrate for LCAT, which requires activation by apoA-I for maximal enzymatic activity. Due to increased hydrophobicity, esterification induces a repositioning of the cholesterol molecule from the HDL surface to the core where it is no longer directly exposed to the aqueous environment. The accumulation of CE in the HDL core *in vitro* is concomitant with the transformation of preβ- to α-migrating HDL and discoidal to spherical HDL.

LCAT is a glycoprotein with an apparent molecular weight of 60 kDa, of which glycosylation accounts for approximately 20%, synthesized in the liver and present both free in the circulation and bound to lipoprotein surfaces. The secondary structure of LCAT contains both β-sheet and α-helical elements organized into an α/β hydrolase fold similar to other members of the lipase gene family (129).

The importance of LCAT for formation of native HDL in plasma was first evidenced by the aberrant HDL metabolism in familial LCAT deficiency (FLD) and fish-eye

disease (FED) (reviewed in ref (130)). Both disorders are characterized by extremely low or nonexistent plasma LCAT activity, markedly decreased lipoprotein CE content, abnormal lipoprotein profiles and morphologically abnormal erythrocytes. In FED, LCAT activity associated with HDL is defective while LDL cholesterol is esterified normally, in contrast to FLD in which both activities are abnormal. Electron microscopic examination of HDL from these individuals indicated they were predominantly of discoidal morphology. Incubation of plasma from FLD and FED patients with purified human LCAT induced a transformation from discoidal to spherical morphology, suggesting plasma LCAT activity is required for the proper conversion of discoidal to spherical HDL *in vivo*.

Overexpression of human LCAT in mice and rabbits (131-134) results in high plasma LCAT activity and increased HDL cholesterol apparently due to decreased catabolism of large HDL by the liver and increased hepatic apoA-I production in transgenic rabbits (135). When fed a high cholesterol diet, LCAT transgenic rabbits were significantly protected from atherosclerosis as compared to controls not expressing human LCAT, while LCAT transgenic mice are more susceptible to diet induced atherogenesis (136,137). This appears to be due to the presence of CETP in rabbits and its absence in mice. The larger, cholesterol-rich HDL generated in the absence of CETP were cleared more slowly by the liver and were proatherogenic.

Therefore, plasma LCAT activity is critical for the conversion of lipid-poor HDL precursors, discoidal and preβ-HDL, to spherical α-migrating HDL_2 and HDL_3. Esterification of HDL free cholesterol maintains a concentration gradient driving the net transfer of cholesterol from cell membranes to HDL, a crucial step for reverse cholesterol transport.

1.3.3.4 HDL Remodeling

'Remodeling' refers to the processes that alter the biochemical and physical properties of CE-containing HDL in the circulation. This involves the combined actions of CETP, HL and PLTP, which modulate the lipid composition and plasma levels of HDL. These processes serve to transfer LCAT-derived CE from HDL to apoB-100 containing lipoproteins allowing subsequent uptake by the liver and regeneration of HDL precursors.

CETP is a hydrophobic glycoprotein with an apparent molecular weight of 70-74 kDa synthesized in liver, spleen, small intestines, adipose tissues, adrenal gland, kidney, heart and skeletal muscles (138,139). CETP expression varies greatly between species, being very low in mice and high in rabbits whereas activity in humans is intermediate (140). CETP reversibly associates with lipoproteins within the circulation and mediates bi-directional lipid exchange from one lipoprotein particle to another. CETP facilitates the transfer of CE from HDL to VLDL, IDL and LDL while TG moves simultaneously in the opposite direction in an equimolar ratio (138). IDL and LDL are catabolized in the liver and mediate the ultimate clearance of HDL cholesterol from the circulation via interation with the LDL receptor. This exchange also results in TG-enriched HDL subject to lipolysis by hepatic lipase.

HL is a lipolytic enzyme structurally similar to LPL that is synthesized in hepatocytes and bound to the basolateral surface of hepatocytes and hepatic endothelial cells facing the space of Disse (141,142). Unlike LPL, HL does not have an absolute requirement for an apolipoprotein cofactor for enzymatic activity. The substrate specificity of HL is broad *in vitro*, therefore designating a specific metabolic role for this enzyme has proved difficult.

In concert, CETP and HL serve to deplete large HDL particles of CE and regenerate preβ-HDL and HDL_3 species which can scavenge additional lipid from cellular membranes (Fig. 1-6). CE transferred to apoB-containing lipoproteins are taken up in the liver via

interaction with the LDL receptor by receptor-mediated endocytosis, serving as the final step in the HDL mediated retrograde transport of cholesterol.

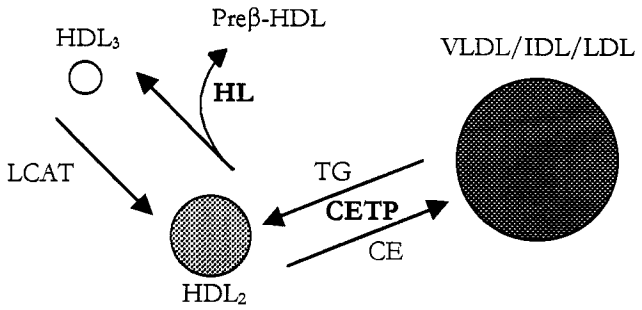

Figure 1-6: Combined Actions of CETP and HL in HDL Remodelling

CETP mediates the heterotypic exchange of HDL-CE for TG from VLDL, IDL and LDL resulting in the TG enrichment of HDL_2. The TG content of HDL_2 is subject to hydrolysis by HL resulting in the liberation of excess surface components, including FC, PL and apolipoproteins (apoA-I), forming nascent preβ-HDL and smaller HDL_3.

1.3.4 SR-B1: Selective Uptake of HDL Cholesterol

Scavenger receptors are a structurally diverse class of receptors that bind a wide range of chemically modified and native lipoproteins (reviewed in ref (143)). The best characterized of these are the scavenger receptors class A type I and type II (SR-AI/II) and CD36 which are expressed on macrophage and appear to play an important role in the uptake and accumulation of oxidized LDL. A novel mechanism of cellular cholesterol uptake from lipoproteins, called selective uptake, was first described in cell culture studies (144). This involves the cellular uptake of HDL CE in the absence of appreciable internalization of the HDL particle. The scavenger receptor class B type I (SR-BI) was cloned based upon its ability to bind acetylated LDL (145) but has also been shown to bind native lipoproteins including HDL and LDL. In addition to binding, SR-BI mediates the selective uptake of lipids from HDL (146) and LDL (147) in transfected cells. SR-BI is

abundant in liver and steroidogenic tissues and correlates with selective uptake activity of HDL cholesterol in these tissues.

The suggested importance of SR-BI in HDL metabolism is evidenced *in vivo* using adenovirus-mediated gene transfer and transgenic techniques. Overexpression of hepatic SR-BI significantly reduces HDL cholesterol and increases cholesterol in the bile (148,149). Genetic ablation of SR-BI resulted in increased plasma HDL cholesterol associated with larger HDL particles relative to wild-type animals (150). Furthermore, SR-BI deficient mice exhibited reductions in the cholesterol content in steroidogenic tissues (150). These results indicated that in the absence of SR-BI both liver and steroidogenic tissues exhibit reduced selective uptake of HDL CE. This suggests that, at least in mice, selective uptake of HDL cholesterol may be a major route for hepatic cholesterol clearance with respect to reverse cholesterol transport. However, there is no evidence that selective uptake of HDL cholesterol is a major route for hepatic clearance in humans.

1.3.5 HDL Catabolism

Several studies suggest that enhanced catabolism and not production rate is the principal metabolic determinant of plasma HDL levels (151,152). HDL clearance rates from plasma are inversely correlated to particle size, as smaller HDL have shorter residence times than larger HDL. Thus lipolytic enzyme (153) and lipid transfer protein activities can regulate the catabolic rate of HDL by changes in HDL particle composition.

TG-enrichment of HDL has been shown to increase lipolysis of HDL by HL, reduce HDL size and increase particle catabolism (154,155). Similarly, hypertriglyceridemia is often associated with low plasma HDL levels, TG-rich HDL and a greater fractional catabolic rate of apoA-I (156). Enrichment of HDL with TG *in vitro* followed by subsequent lipolysis with

LPL results in enhanced rate of clearance when infused into rabbits (157). *In vivo*, the plasma factor responsible for TG enrichment of HDL is CETP, which mediates the exchange of HDL CE for TG from VLDL, IDL and LDL. Subsequent hydrolysis by HL results in the formation of smaller HDL particles and the generation of nascent preβ-HDL. *In vitro*, hydrolysis of HDL TG promotes the dissociation of apoA-I (158), suggesting that HDL in hypertriglyceridemic individuals may contain a greater proportion of loosely associated apoA-I, which is more rapidly cleared from the circulation by renal filtration (157). Furthermore, Braschi *et al.* demonstrated that the charge and conformation of apoA-I in reconstituted lipoproteins may be key factors in determining the clearance rates of apoA-I and HDL from plasma (159).

1.4 Apolipoprotein A-I Structure and Function

Many of the functional and anti-atherogenic properties of HDL are conferred by its principal protein constituent, apoA-I. ApoA-I is a 243 a.a. plasma protein secreted from both liver and intestine and is one of the most abundant apolipoproteins in mammalian blood plasma. ApoA-I stimulates the removal of excess cholesterol from various cell types, serves as a cofactor for LCAT and thereby mediates the assembly of HDL within the circulation. This section describes in detail the gene organization, protein structure, structure-function relationships and animal models used to characterize apoA-I.

1.4.1 ApoA-I Gene Structure

The human apoA-I gene is located on the long arm of chromosome 11 (11q23) in a multigene complex with apoC-III and apoA-IV which spans over 15 kb (160,161). The gene is organized in a manner similar to the other mammalian exchangeable apolipoproteins with the exception of apoA-IV, consisting of 4 exons and 3 introns (Fig. 1-7) (reviewed in ref (162)). The first intron interrupts the 5' untranslated region while the second is situated within the coding sequence upstream of the signal peptidase cleavage site. The third intron interrupts the coding sequence at codon 43 and thus codons 44-243, which encode the remainder of apoA-I, are derived from exon 4. The first 3 exons are the most highly conserved amongst the exchangeable apolipoproteins while differences in mRNA length are mainly due to the length of exon 4. The remarkably similar genomic structure of this family supports the hypothesis that they evolved from a common ancestor by partial and complete gene duplications (Fig. 1-8).

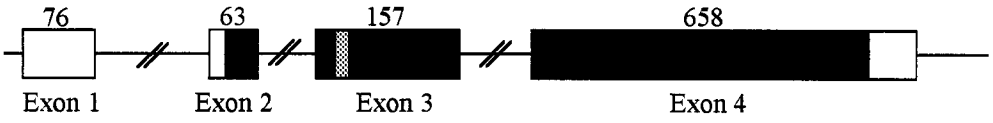

Figure 1-7: Intron / Exon Arrangement and Coding Sequences of the ApoA-I Gene

The wide bars represent exons while thin lines represent introns. Exons are further subdivided: the open bars represent the 5' and 3' untranslated regions, the hatched bars mark the region encoding the signal peptide and the black bars indicate the regions encoding the mature protein. In addition, the grey bar in exon 3 represents the 6 residue signal peptide. Adapted from Luo *et al.* (163).

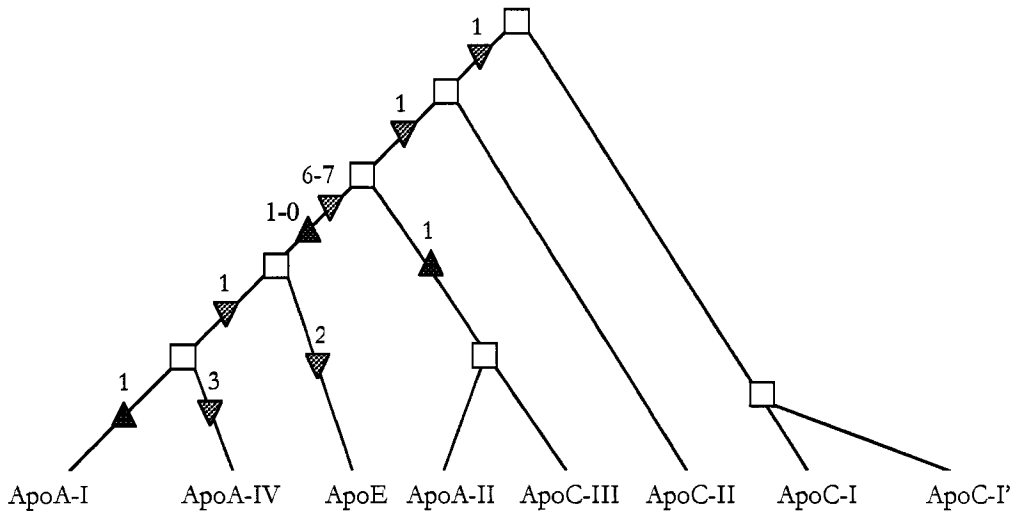

Figure 1-8: Evolutionary Tree of the Plasma Exchangeable Apolipoproteins

The initial ancestor was likely very similar to apoC-I in structure and length. Full gene duplications (□) followed by subsequent duplications of 22 or 11 codons (▼) and deletions of 11 codons (▲) generated the 6 other family members. Adapted from Luo *et al.* (163).

1.4.2 ApoA-I Protein Structure

This section serves to review the current models of apoA-I primary, secondary and tertiary structure. While some models suggest dimeric interactions of apoA-I may occur when bound to HDL, this has been poorly characterized and thus potential models of quaternary structure will not be considered aside from the putative lipid-bound topology.

1.4.2.1 ApoA-I Synthesis and Primary Structure

Plasma apoA-I is secreted from both human liver and intestine (106,164,165). Initially synthesized as a 267 a.a. preproprotein, the 18 a.a. pro-sequence is cleaved following ER translocation and apoA-I is secreted into the circulation as a 249 proprotein (reviewed in ref (166)). The hexapeptide pro-peptide is rapidly removed within the circulation by an unidentified enzyme generating the mature 243 a.a. protein. Recent work by Pyle *et al.*

suggests this enzyme is a metalloprotease, as the cleavage event was inhibited by metalloprotease inhibitors and was dependent upon calcium, and recognizes a consensus sequence encompassing residues –2 to +4 of proapoA-I (167). Furthermore, the work of Stoffel *et al.* suggests this cleavage may be dependent upon the conformation of this region (166).

ApoA-I from a number of species, ranging in size from 258-267 a.a., show considerable sequence similarity (45-55%) (Fig. 1-9) (162,168). A comparison of the aligned sequences indicates the amino-terminal domain (residues 1-98) is most highly conserved, consistent with the studies of Collet *et al.* demonstrating that the immunoreactivity of monoclonal antibodies is most highly conserved in this region while the remainder of apoA-I exhibits conservative substitutions (169). As indicated above, residues 1-43 of the mature sequence are encoded by exon 3 while the remainder of the protein is derived from exon 4. The primary structure encoded by exon 4 of the exchangeable apolipoproteins (exon 3 for apoA-IV) contains multiple repeats of 22 amino-acids which are punctuated by single Pro residues in most instances. The conservation of the 22-mer repeats and the positions of the prolines further suggest a common origin for the exchangeable apolipoprotein gene family.

1.4.2.2 ApoA-I Secondary Structure: The Amphipathic α-Helix

These tandem repeats of 22 amino-acids form amphipathic α-helices, which Segrest *et al.* first described as unique structural motifs in lipid interaction (170). An amphipathic helix is defined as an α-helix with opposing polar and non-polar faces oriented along the long axis of the helix and, while initial identification was confined only to the apolipoproteins, they have since been identified in many functionally diverse proteins.

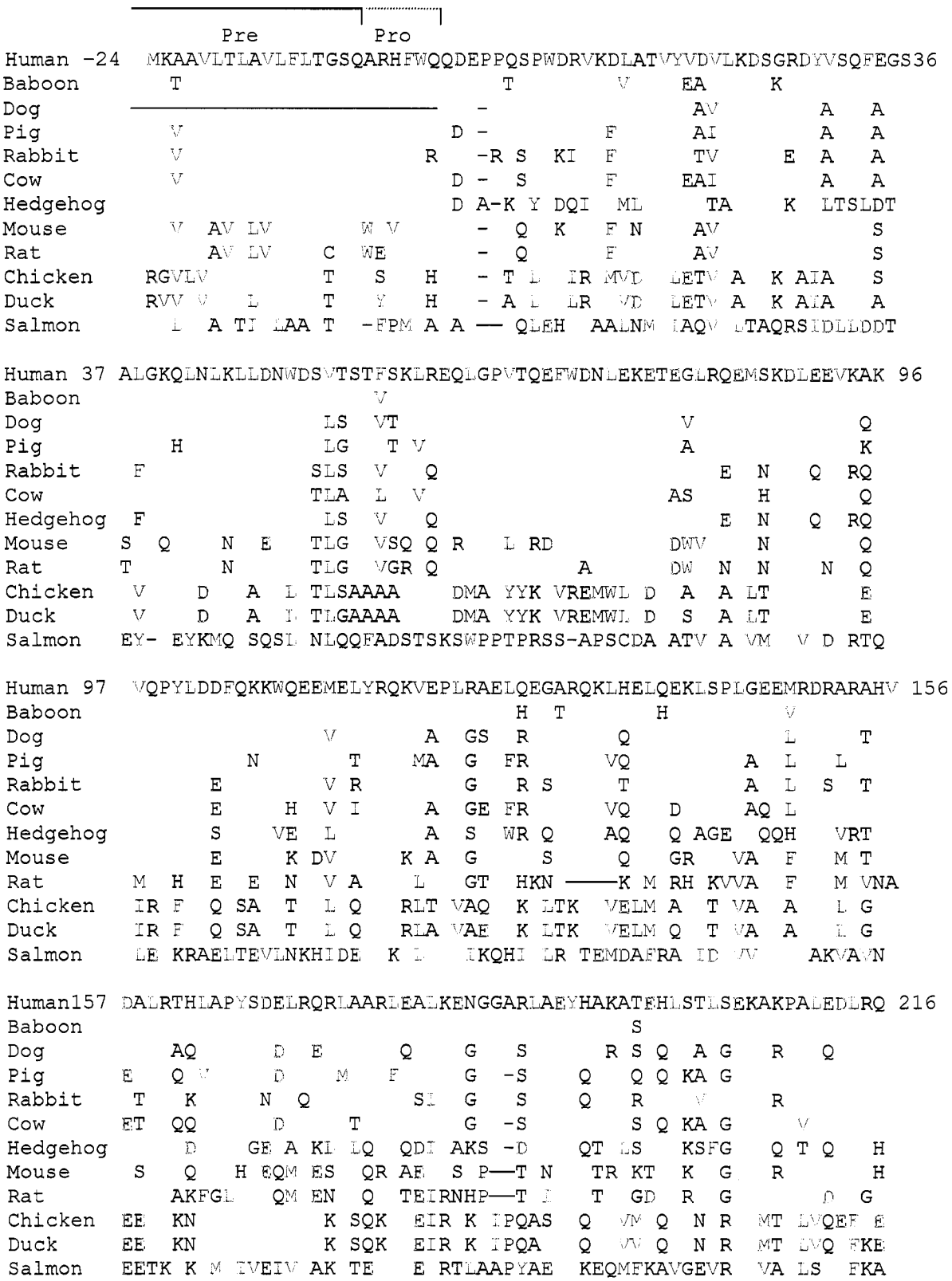
Pre
Pro
Human -24 MKAAVLTLAVLFLTGSQARHFWQQDEPPQSPWDRVKDLATVYVDVLKDSGRDYVSQFEGS 36
Baboon T T V EA K
Dog — - AV A A
Pig V D - F AI A A
Rabbit V R -R S KI F TV E A A
Cow V D - S F EAI A A
Hedgehog D A-K Y DQI ML TA K LTSLDT
Mouse V AV LV W V - Q K F N AV S
Rat AV LV C WE - Q F AV S
Chicken RGVLV T S H - T L IR MVL LETV A K AIA S
Duck RVV V L T Y H - A L LR VD LETV A K AIA A
Salmon L A TI LAA T -FPM A A — QLEH AALNM IAQV LTAQRSIDLLDDT
Human 37 ALGKQLNLKLLDNWDSVTSTFSKLREQLGPVTQEFWDNLEKETEGLRQEMSKDLEEVKAK 96
Baboon V
Dog LS VT V Q
Pig H LG T V A K
Rabbit F SLS V Q E N Q RQ
Cow TLA L V AS H Q
Hedgehog F LS V Q E N Q RQ
Mouse S Q N E TLG VSQ Q R L RD DWV N Q
Rat T N TLG VGR Q A DW N N N Q
Chicken V D A L TLSAAAA DMA YYK VREMWL D A A LT E
Duck V D A I TLGAAAA DMA YYK VREMWL D S A LT E
Salmon EY- EYKMQ SQSL NLQQFADSTSKSWPPTPRSS-APSCDA ATV A VM V D RTQ
Human 97 VQPYLDDFQKKWQEEMELYRQKVEPLRAELQEGARQKLHELQEKLSPLGEEMRDRARAHV 156
Baboon H T H V
Dog V A GS R Q L T
Pig N T MA G FR VQ A L L
Rabbit E V R G R S T A L S T
Cow E H V I A GE FR VQ D AQ L
Hedgehog S VE L A S WR Q AQ Q AGE QQH VRT
Mouse E K DV K A G S Q GR VA F M T
Rat M H E E N V A L GT HKN ———K M RH KVVA F M VNA
Chicken IR F Q SA T L Q RLT VAQ K LTK VELM A T VA A L G
Duck IR F Q SA T L Q RLA VAE K LTK VELM Q T VA A L G
Salmon LE KRAELTEVLNKHIDE K L IKQHI LR TEMDAFRA ID VV AKVAVN
Human157 DALRTHLAPYSDELRQRLAARLEALKENGGARLAEYHAKATEHLSTLSEKAKPALEDLRQ 216
Baboon S
Dog AQ D E Q G S R S Q A G R Q
Pig E Q V D M F G -S Q Q Q KA G
Rabbit T K N Q SI G S Q R V R
Cow ET QQ D T G -S S Q KA G V
Hedgehog D GE A KL LQ QDI AKS -D QT LS KSFG Q T Q H
Mouse S Q H EQM ES QR AE S P—T N TR KT K G R H
Rat AKFGL QM EN Q TEIRNHP—T I T GD R G D G
Chicken EE KN K SQK EIR K IPQAS Q VM Q N R MT LVQEF E
Duck EE KN K SQK EIR K IPQA Q VV Q N R MT LVQ FKE
Salmon EETK K M IVEIV AK TE E RTLAAPYAE KEQMFKAVGEVR VA LS FKA

```
Human  217 GLLPVLESFKVSFLSALEEYTKKLNTQ 243
Baboon                            S
Dog                     L A  D A     A
Pig                NL   I A ID AS    A
Rabbit                A VQNV D A
Cow                E L   I A ID AS    A
Hedgehog     E LW GI AGAM -M  LG    S
Mouse      S M M  TL TKAQ VIDKASET TA
Rat          M    AW AKIM MID AK    A-
Chicken    R T YA NL NRLI F D LQ SVA—
Duck       R T YA NL TR I L D LQ TVA—
Salmon     RWA PPRRPSK SWLSTRPSARP———
```

Figure 1-9: Alignment of Human ApoA-I with Sequences from 11 Species

The primary (prepro-) sequences of apoA-I from human (171), baboon (172), dog (173), pig (174), rabbit (175), cow (176), hedgehog (177), mouse (178), rat (179), chicken (180), duck (Swiss-Prot accession number, O42296) and salmon (181) are aligned. Colors indicate proline (purple, P), aspartic acid or glutamic acid (red, D and E), arginine or lysine (blue, R or K), and phenylalanine, isoleucine, leucine, methionine, valine, tryptophane, or tyrosine (green, F, I, L, M, V, W, and Y). The remaining amino acids, alanine, cysteine, glycine, histidine, asparagine, glutamine, serine, and threonine (A, C, G, H, N, Q, S, and T) are uncolored. The numbering of human apoA-I starts at –24 (signal peptide of apoA-I), residue 1 being the first of mature apoA-I.
Originally published by Frank *et al.* (182)
Reprinted with permission of Lipid Research Inc.

Early predictions of apoA-I secondary structure employed the sequence algorithms described by Chou and Fasman (183). These studies suggested residues 44-243 of apoA-I may be composed of 8-10 α-helices formed predominantly by 22-mer and 11-mer repeats while the N-terminus (a.a. 1-43) assumes a less well-defined globular structure (184,185). This was partially confirmed experimentally by circular dichroism and infrared spectroscopy (52,186,187). Structural analysis by Segrest *et al.* generated similar results with respect to the exon 4 encoded region and suggested that residues 8-33 form an amphipathic helix similar to those found in some globular proteins (188). More recently, 10 amphipathic helices spanning residues 44-243 have been identified in the crystal structure of an apoA-I deletion mutant lacking residues 1-43 (189).

The amphipathic helices were initially divided into seven varieties based upon the proteins in which they were first identified: class A (apolipoproteins), class H (polypeptide hormones), class L ("lytic" polypeptides), class G (globular proteins), class K (calmodulin-

regulated protein kinases), class C (coiled-coil proteins) and class M (transmembrane proteins) (reviewed in ref (190)). More recent work has indicated the apolipoproteins are composed of class A_1, class A_2, class Y (all slight variants of the original class A) and a class G variant (referred to as class G*) (188). The physical properties and distribution of charged residues in these helices are indicated in Table 1-4 and Fig. 1-10, respectively. Class A_1 and A_2 are very similar, positive charges are symmetrically distributed at +/- 100° while negative charges form a single cluster and are directly opposite the hydrophobic face for both classes. They differ structurally in that the positive-negative charge clustering is less well defined for A_1 than A_2 and, while the hydrophobicity of the nonpolar face is comparable, the hydrophobic moment and the Lys/Arg ratio is significantly lower for class A_1. Class Y differs significantly from both class A_1 and A_2 with respect to the organization of negative

Table 1-4: Properties of the Amphipathic α-Helices of ApoA-I[a]

Class	Mean $<\mu_H>$[b] per a.a.[c,d]	Hydrophobicity per a.a. of Nonpolar Face[d,e]		No. of + a.a.[c]	No. of − a.a.[c]	Lys/Arg Ratio[c]
		CON	CON/SNK	Per 11 a.a.		
A_1	0.34	0.71	0.72	2.0	2.1	0.5
A_2	0.43	0.74	0.75	1.9	1.8	4.8
Y	0.37	0.65	0.67	1.9	2.2	1.2
G*	0.44	0.68	0.61	1.6	1.6	1.0

[b]Hydrophobic moment
[c]Data derived from CONSENSUS analyses.
[d]Calculated using a normalized (unitless) GES hydrophobicity scale.
[e]Includes only the six residues centered on the nonpolar face.
[a]Adapted from Segrest *et al.* (188)

and positive charges on the polar face. An additional group of positively charged residues separates two clusters of negative charges and results in a hydrophobic moment and nonpolar face hydrophobicity intermediate as compared to other amphipathic helices. G*

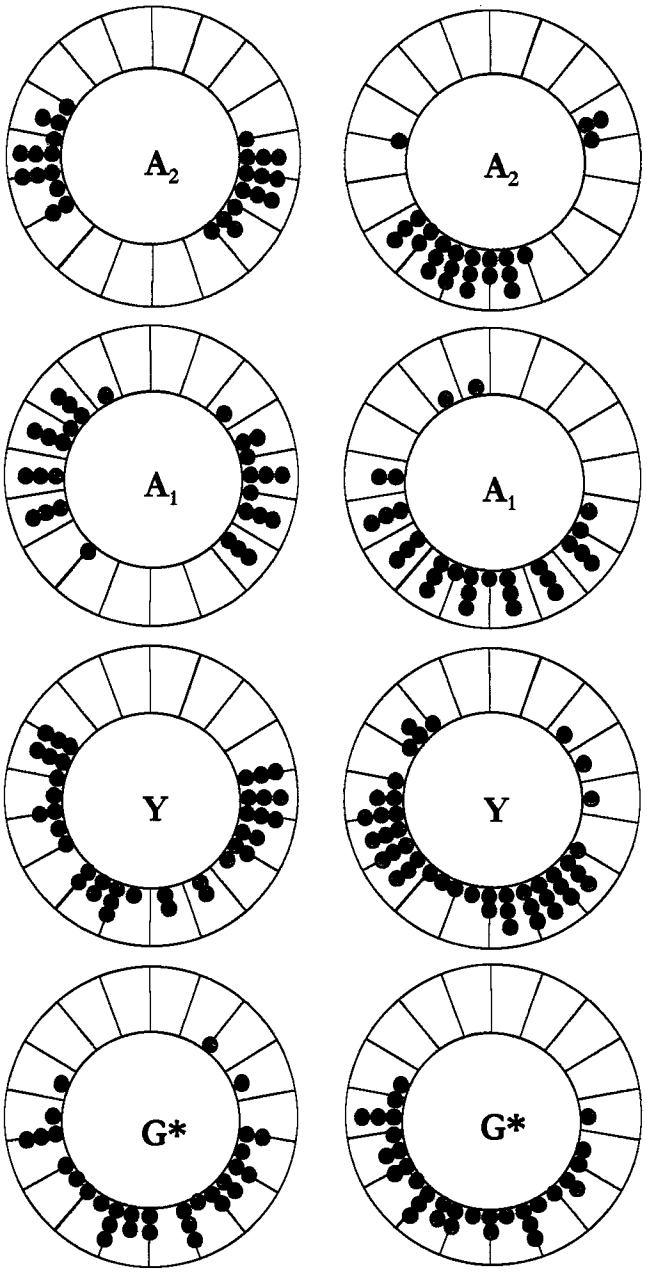

Figure 1-10: Edmundson Wheel Representation of Class A_1, A_2, Y and G* Amphipathic Helices.

The distribution of positively (•) and negatively (•) charged amino-acid side chains for amphipathic α-helices of class A_1, A_2, Y and G* in the exchangable apolipoproteins. The helices are oriented such that the hydrophobic face is directed towards the top of the page.
Adapted from Segrest *et al.* (188)

amphipathic helices do not exhibit any clustering of positive or negative charges on the polar face and the only consensus sequence in this class is a group of Leu residues on the nonpolar face. These helices possess a high hydrophobic moment and a moderately high nonpolar face hydrophobicity. The distribution of class A, Y and G* helices in apoA-I is shown in Fig. 1-11. The class A helices are all of the A_1 variety, A_2 helices are present in apoA-II and apoC- I/II/III.

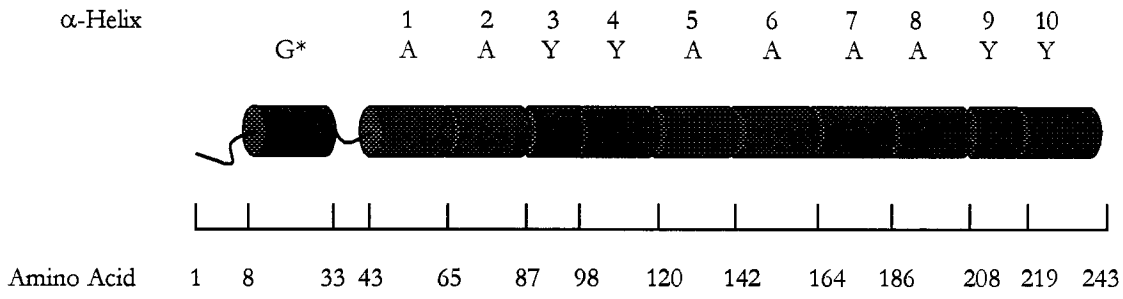

Figure 1-11: Putative Secondary Structural Elements of Human ApoA-I

The putative secondary structure of apoA-I is shown, composed of 1 G* (green), 6 class A (blue) and 4 class Y (red) helices.

1.4.2.3 ApoA-I Tertiary Structure: Lipid-Free and Lipid-Bound Forms

As an exchangeable apolipoprotein, apoA-I exists in equilibrium between lipid-free and lipid-bound forms, the former of which may compose up to 8% of total plasma apoA-I. In the absence of a crystal structure for full-length apoA-I in the presence or absence of lipids, information to date is somewhat indirect. This section discusses the current models of apoA-I tertiary structure in both the lipid-free and lipid-bound forms.

Understanding of the lipid-free structure of apoA-I is so limited that all three major review articles published in the past year on apoA-I structure and functional relationships chose not to address this issue. The most convincing evidence to date includes comparisons

to crystal structures of other exchangeable apolipoproteins, *in vitro* proteolysis, tryptophan fluoresence and analytical centrifugation.

Characterization of exchangable apolipoproteins from human and insects suggests that in the absence of lipids these proteins form compact, helical bundle structures in which the hydrophobic faces are sequestered within the core of the bundle. The amino-terminal domain of human apoE (residues 1-191), at a resolution of 2.5 Å, formed an anti-parallel bundle of four amphipathic helices. The hydrophobic residues formed the core of the bundle while charged amino-acids were positioned on the surface (191). Furthermore, inter- and intrahelical salt bridges are abundant and likely stabilize the helix bundle.

Apolipophorin III (apoLp-III) is an exchangeable apolipoprotein from *Locusta migratoria* (locust). It is a component of low density lipophorin and is involved in the transport of diglyceride from the fat body storage depot to flight muscles where it is the principal energy source (192). The crystal structure of apoLp-III consists of a bundle of five amphipathic helices (193) with proline residues located in inter-helical turns. In addition, the structure of apoLp-III from *Manduca sexta* (sphinx moth) was determined by three-dimensional NMR spectroscopy and is very similar to that of *L. migratoria* (194).

By analogy to the known structures of these apolipoproteins, a helical bundle organization of exchangeable lipoproteins is likely well conserved through evolution, suggesting apoA-I assumes this form as well.

The first evidence of a compact, helical bundle organization in apoA-I was provided by Roberts *et al.* (195). Using chymotrypsin and V_8 protease from *S. aureas* for limited proteolytic digestion, they observed that proteolysis was limited almost exclusively to the C-terminus (residues 187-243) with only limited digestion in the central domain encompassing residues 115-136. The resistance of the N-terminus to enzymatic digestion is consistent with

a compact structure with minimal exposure of the peptide backbone. Interestingly, sulfoxidation of methionines at 112 and 148 rendered sites in helix 1 (44-65), 2 (66-88) and 7 (165-187) accessible to digestion. This suggests that alteration of the amino-acid side chain size and/or charge can affect the stability of the tertiary structure.

Perhaps the most convincing evidence for a helical bundle organization of apoA-I comes from Maiorano *et al.* using tryptophan fluorescence (196). Trp residues in proapoA-I are located at –3, 8, 50, 72 and 108, perfect for analysis of the amino-terminal region. Steady-state fluoresence studies indicated that all Trp residues existed in non-polar environments and were highly protected from solvent exposure. Using time-resolved lifetime and anisotropy, they determined the shape of the monomeric form of proapoA-I is a prolate ellipsoid. These studies suggest that apoA-I adopts a compact, helical bundle tertiary structure in the absence of lipids similar to that described in other exchangeable apolipoproteins. Models of the potential lipid-free forms of apoA-I were proposed by Rogers *et al.* and are shown in Fig. 1-12 (197). ApoA-I may exist in equilibrium between a compact helical bundle organization and an elongated conformer resulting from the reversible unhinging of the bundle located between residues 66-87. The hydrophobic faces of these helices are exposed in the elongated conformer and available for lipid-binding. Therefore, opening of the helix bundle in this manner is thought to represent an intermediate in lipid-binding.

The manner in which apoA-I is oriented around the surface of both native and reconstituted HDL has yet to be resolved and is perhaps the most fundamental aspect of apoA-I and HDL structure still outstanding. Two models have been the focus of much attention during the past several years and are referred to as the 'Picket Fence' and the 'Belt' models of apoA-I (recently reviewed in ref (198)). Due to both the ease and uniformity of

preparation, reconstituted discoidal HDL rather than native HDL have been preferentially used to address these models.

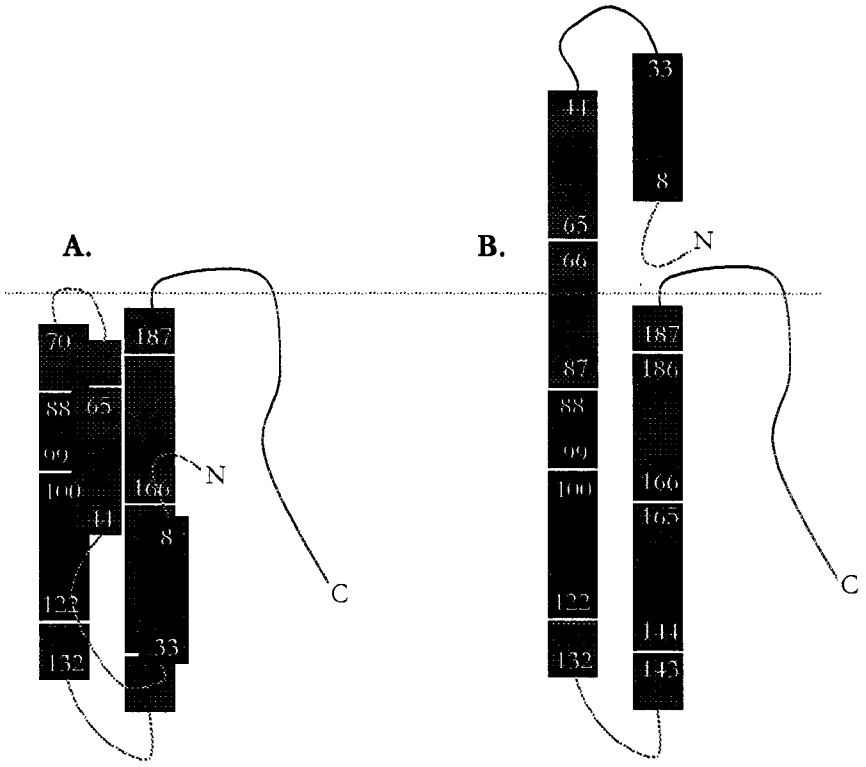

Figure 1-12: Proposed Lipid-Free Conformational Equilibrium of ApoA-I

(A) Folded four helix bundle and (B) elongated, monomeric helical hairpin models are shown. The four helix bundle model was proposed initially by Roberts *et al.* (195), refined by Rogers *et al.* (199) and is similar to the X-ray crystal and NMR structures of other exchangable apolipoproteins. The elongated conformer is derived from experiments using analytical ultracentrifugation and is thought to represent a lipid-free conformer of apoA-I. The dashed line represents the plane of unfolding in which the helical regions N-terminal to residue 70 dissociate from the helical bundle and expose the hydrophobic faces of the bundle for lipid binding.
Adapted from Rogers *et al.* (199)

In the Picket Fence model the amphipathic α-helices of apoA-I surround the periphery of the discoidal phospholipid bilayer and are oriented parallel to the lipid acyl chains (Fig. 1-13). This model was initially widely accepted based upon studies using Fourier Transform Infrared (FTIR) spectroscopy that seemed to provide unequivocal evidence for the Picket Fence orientation of apoA-I in reconstituted lipoprotein films (186).

Subsequently, research interest was directed at elucidating the details of this model rather than testing its validity.

Phillips *et al.* have recently tested this model by computer modeling using a model discoidal lipoprotein containing 2 molecules of apoA-I and 160 molecules of POPC and found that large interhelical distances resulted in the exposure of 20% of the area of the lipid acyl chains to water (200). Presumably the energetics that drive the formation of discoidal lipoproteins depend on the removal of hydrophobic groups from the aqueous environment suggesting this model may not be thermodynamically favoured. Furthermore, they suggest that 2 apoA-I molecules would be unable to shield the entire hydrophobic edge of a discoidal lipoprotein. A surface area corresponding to greater than 25% of the total surface area was found to be solvent-exposed in this model.

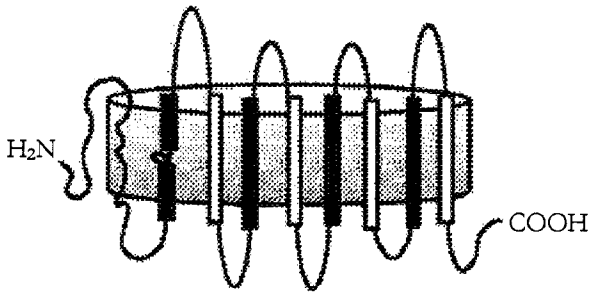

Figure 1-13: Picket Fence Model of ApoA-I in Discoidal HDL

This model illustrates the topology of apoA-I in the context of a discoidal lipoprotein with the amphipathic helices oriented parallel to the lipid acyl chains. The N- and C-termini of each monomer are shown to the left and right of the figure, respectively. The 2 helices that are shown separated from the lipoprotein in panel A represent a potential hinge domain in apoA-I consisting of helices 4 and 5. This region may be important for the plasticity of the protein necessary for accommodating changes in HDL size and composition.
Originally published by Frank et al. (182)

The 'belt' model differs significantly from the Picket fence model because apoA-I wraps around the periphery of the HDL particle perpendicular to the lipid acyl chains. This model was initially proposed based primarily upon the crystal structure of an apoA-I mutant lacking

residues 1-43 in the absence of lipids (189) (refer to Fig. 1-14). This deletion mutant of apoA-I adopts a pseudo-continuous amphipathic α-helix in a crystal structure consisting of an apoA-I dimer oriented in an antiparallel manner with extensive intermolecular interactions. Interestingly, the C-terminal helix (a.a. 227-243) of one monomer forms close contacts with the same helix of the other monomer that forms a closed horseshoe shaped structure which could potentially wrap around a discoidal HDL particle.

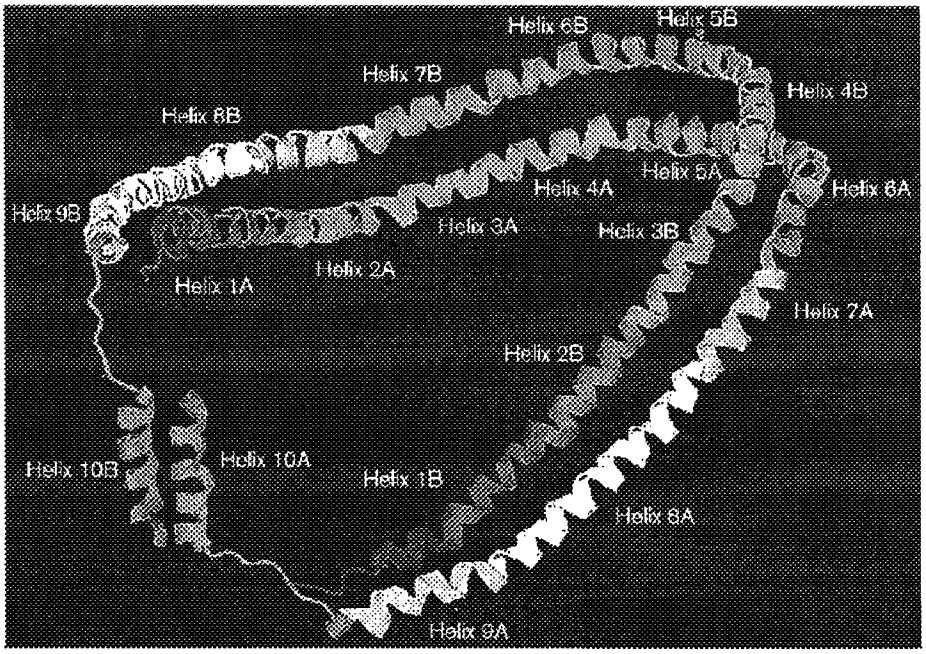

Figure 1-14: Crystal Structure of the Δ1-43 ApoA-I Dimer in the Absence of Lipids
Two apoA-I monomers are shown oriented in an antiparallel manner with helix 10 from each protein forming a close molecular 'handshake'. Intermolecular interactions are located throughout the remainder of the dimer, as well, suggesting this structure may exist on the surface of HDL.
Originally published by Segrest *et al.* (201)

Biochemical evidence suggests this deletion mutant lacks the compact lipid-free tertiary structure of full-length apoA-I but retains most of its native lipid-binding properties (197). Subsequently, it was postulated that the crystal structure of Δ1-43 apoA-I is representative of the lipid-bound structure of wild-type apoA-I in HDL. This model has

recently been supported by several spectroscopic analyses using discoidal reconstituted HDL (196,202,203). Segrest *et al.* have recently constructed a detailed molecular Belt model for discoidal HDL and found that in contrast to the Phillips *et al.* Picket Fence model, their Belt model resulted in the shielding of essentially all of the lipid acyl chains (204) (refer to Fig. 1-15C).

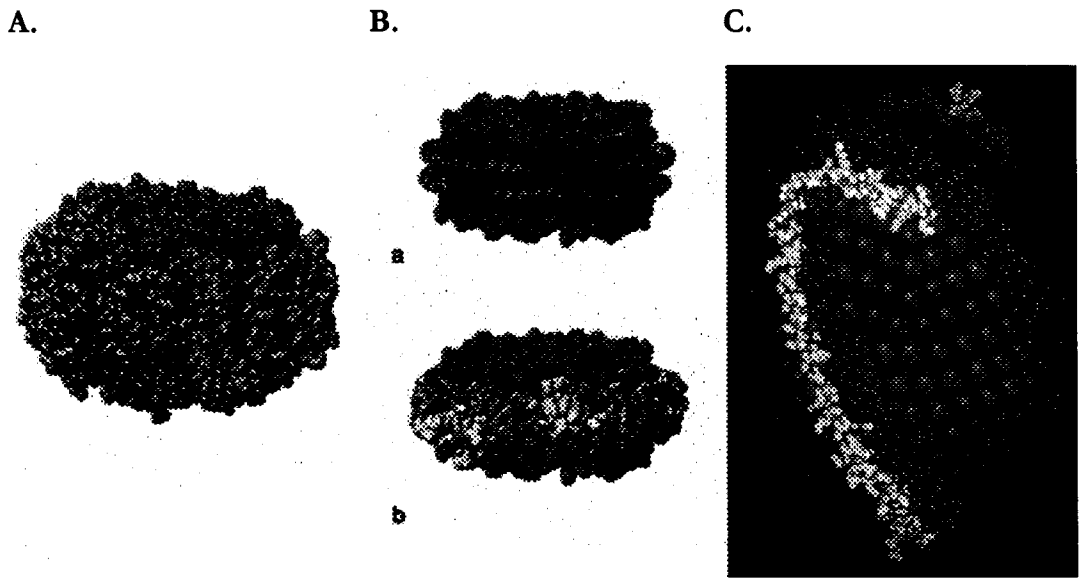

Figure 1-15: Potential Lipid-Bound Structures of ApoA-I

Panel A: This space-filling model illustrates the 'picket-fence' model of a dimer of apoA-I in discoidal lipoproteins. The amphipathic helices are oriented parallel to the phospholipid fatty-acyl chains.
Panel B: These models depict the lipid-bound topology of an apoA-I dimer in the 'belt' model in the context of a discoidal lipoprotien. Monomers are oriented in an anti-parallel fashion, however, in this model the amphipathic helices wrap around the periphery of the lipoprotein particle, perpendicular to the PL fatty-acyl chains. Both ribbon (top) and space filling (bottom) models are shown.
Panel C: This model is adapted from the 'belt' model and illustrates the proposed topology of 2 apoA-I dimers bound to a spherical HDL particle.
Originally published by Brouillette et al. (198)
Reprinted with permission of Elsevier Science

While arguments for both models remain, the Belt model has emerged as the best candidate. However, it is still unclear if the belt orientation of apoA-I reflects its topology in spherical HDL as most direct evidence is derived from discoidal lipoprotein models. One model that has been presented, also based on the crystal structure of Δ1-43 apoA-I, consisted of four molecules of apoA-I on spherical HDL and is referred to as the 'Faberge Egg' (189). Two

dimers were placed on the surface of the HDL particle, passing one another where helices 10 were separated. The conversion of discoidal to spherical HDL is thought to occur via separation of the molecular 'handshake' occurring between apoA-I dimers which could allow for the incorporation of cholesteryl esters in the core of the lipoprotein particle in this manner.

1.4.3 ApoA-I Structure-Function Relationships

The study of apoA-I structure-function relationships is based largely upon the physical and biochemical properties of naturally occurring and engineered apoA-I mutants. The association of specific helical domains of apoA-I with lipid-binding, cholesterol efflux and LCAT activation is addressed.

1.4.3.1 Phospholipid Association

The association of apoA-I with PL is governed by amphipathic α-helices. When combined in the test tube, apoA-I spontaneously clears dimyristoylphosphatidylcholine (DMPC) vesicles at their transition temperature (23.9°C) to form 'disc-shaped' (discoidal) lipoprotein complexes (205-207). Similarly, incubation of apoA-I with POPC and the detergent sodium cholate results in the formation of discoidal lipoproteins (208,209). Incubation of these complexes with LCAT transforms these discs to spheres due to the accumulation of a CE core (210). Using circular dichroism, Segrest and coworkers demonstrated that apoA-I helical content increases upon lipid association from 40-50% to 75% depending upon the lipids used (52,211) suggesting an increase in apoA-I stability in the presence of lipids.

Observations from studies using synthetic peptides modeled after individual or multiple apoA-I helices and deletion mutants suggested apoA-I helices are not equivalent in

lipid affinity. Those helices having greater affinity for PL are proposed to constitute important lipid-binding domains within apoA-I. Palgunachari *et al.* demonstrated that only those peptides analogous to helix 1 (a.a. 44-65) and helix 10 (a.a. 220-243) were able to solubilize DMPC liposomes. This suggests both helix 1 and 10 are important domains which may mediate the initial association of apoA-I with PL (212).

The importance of helix 1 and 10 in lipid association has been confirmed using deletion mutants of apoA-I. Rogers and coworkers compared apoA-I mutants lacking residues 1-43 and 1-65 (referred to as Δ1-43 and Δ1-65 apoA-I) and found that the latter but not the former exhibited significantly reduced lipid-binding affinity relative to wild-type apoA-I (199). The role of helix 10 in binding lipids has been confirmed in various mutagenesis studies. Work in our lab indicates that deletion of residues 187-243 significantly impairs the ability of apoA-I to bind PL vesicles *in vitro* and form lipoprotein particles (213). Animal studies are consistent with *in vitro* findings as apoA-I mutants lacking residues 210-243, 217-243, 226-243 and 190-243 are catabolized more quickly following intravenous infusion in rabbits (214,215). The faster catabolic rate reflects the decreased lipid binding affinity that leads to rapid degradation of the partially lipidated apoA-I.

However, some natural apoA-I mutants in the central domain, $Lys^{107}\rightarrow 0$ and Δ146-160 apoA-I, exhibit impaired lipid-binding (216,217). To address the role of helices in the central domain of apoA-I to lipid-binding, Frank *et al.* constructed deletions of residues 100-143, 122-165 and 144-186 (218). These deletions were found to have little effect on the kinetics of apoA-I association with DMPC, however, they did appear to have a reduced capacity for binding lipids and may not be capable of accommodating varying amounts of HDL PL. Recent work suggests residues 100-121 and 122-143 are important for PL binding *in vivo* (219). ApoA-I deletion mutants lacking these residues were found to associate with

less PL following adenovirus-mediated expression in apoA-I deficient mice. This domain is proposed to constitute a hinge domain in apoA-I that allows apoA-I to accommodate changes in the HDL structure, a hypothesis based upon studies with monoclonal antibodies.

Apart from helix 1, the contribution of the N-terminal domain (residues 1-99) to lipid-binding is poorly understood. Deletion of residues 88-98 reduced the α-helicity of the protein to 34% and significantly compromised the ability of apoA-I to clear DMPC liposome turbidity (199). This helix is one of two putative 11-mers in apoA-I. The deletion of this helix disrupts several structure and functional properties making its contribution to lipid-binding specifically difficult to ascertain.

While G* helices have a reduced affinity for PL as compared to class A and Y, Rogers *et al.* have shown that deletion of residues 1-43 impairs the ability of apoA-I to clarify a solution of DMPC liposomes (220). The potential importance for this region for PL-binding in apoA-I is supported by Mishra and colleagues demonstrating that a synthetic peptide modeled after residues 1-33 of apoA-I exhibits significant lipid-binding affinity relative to other apoA-I peptides (221).

The association of apoA-I with lipids is unlikely the simple sum of the interactions of each helix individually, as the cooperativity of apoA-I helices determines its native lipid-binding properties. Helices at the N- and C-terminus probably play important roles in the initial association of apoA-I with lipids and hence are considered important lipid-binding domains. Other helices may stabilize conformational changes during HDL maturation and remodeling and contribute to lipid association in this manner.

1.4.3.2 Cellular Cholesterol Efflux

As described in Section 1.3.3.2, cholesterol efflux is a process in which cholesterol is transferred from peripheral cells to apolipoprotein and HDL acceptor molecules (reviewed in ref (222)). Diffusional efflux involves desorption of cellular cholesterol by lipoprotein acceptor particles. This movement of cholesterol is passive and dependent upon a concentration gradient between the cell and acceptor particle, the capacity of the lipid surface for cholesterol acquisition and the desorption and adsorption rates of cholesterol (223-225). Glomset also proposed that HDL cholesterol esterification by LCAT may help maintain a concentration gradient driving the net transfer to the lipoprotein acceptor (10). Since the largest free cholesterol pool in the cell is the plasma membrane, this may represent the principal source of cholesterol for diffusional efflux. Phillips, Rothblat and coworkers have demonstrated that there appears to be at least two compartments in the plasma membrane available for cholesterol efflux (226-228). One is readily available for rapid release to a lipoprotein acceptor while the other is slow with respect to efflux out of the cell.

The observation that proteolytic treatment of HDL abolishes a major portion of the transfer of cellular cholesterol to HDL suggests that the apolipoprotein component of the acceptor particle may be important in regulating this form of cholesterol efflux (229). Initial studies using monoclonal antibodies to apoA-I suggested that specific domains in this protein may be directly involved in diffusional efflux of cholesterol as several groups implicated a domain including residues 74 to 150 in this process (230-232). Fielding *et al.* suggested that residues 137-144 are significantly more exposed in preβ-HDL relative to other HDL species making it more accessible for interaction with the cell surface (233). However, monoclonal antibodies to apoA-I can sterically interfere with domains other than the epitope itself (234) and modify secondary structural elements of apoA-I (235).

Studies using various deletion mutants of apoA-I were then conducted to address whether distinct domains in apoA-I are involved in diffusional cholesterol efflux. In these studies, synthetic lipoprotein complexes containing the respective apoA-I deletion mutants, phospholipids and cholesterol were used as the acceptor particles for cholesterol efflux. Work from several groups, including ours, has shown that apoA-I deletion mutants lacking residues 44-126, 139-170, 190-243, 222-243, 210-243, 150-243 and 135-243 were as effective as wild-type apoA-I when lipidated in mediating cholesterol efflux from fibroblasts (236,237). These results indicated that so long as the mutants could associate with PL they were not associated with altered cholesterol efflux and thus a specific domain in apoA-I is not required for diffusional efflux of cholesterol to HDL.

The apolipoprotein-specific or translocation dependent mechanism involves the efflux of cellular phospholipid and cholesterol to lipid-free apolipoproteins, those not associated with a lipoprotein particle. Two distinct phases appear to be involved in this process. Apolipoproteins initially bind to the cell and recruit phospholipids only (238). This binding can be upregulated by various agents that increase the activity of ABCA1 suggesting either that apolipoproteins bind directly to ABCA1 or that ABCA1 activity facilitates the interaction with alternative binding sites. Initial interaction with the cell is thought to result in the formation of apolipoprotein/phospholipid complexes that serve as acceptors for cellular cholesterol. This is corroborated by efflux studies using murine macrophage cell lines in which cholesterol efflux was induced by treatment with cyclic AMP, in parallel with apolipoprotein binding (239,240). Cholesterol for efflux to apolipoproteins is mobilized from an intracellular pool available for esterification by acylCoA:cholesterol acyltransferase (ACAT) and trafficks to the plasma membrane and appears to involve a specific intracellular signal rather than a general decrease of plasma membrane cholesterol (241,242). Caveolin-1

is a component of cholesterol and sphingomyelin-rich cell surface microdomains referred to as caveolae. Caveolin-1 enhances the transport of cholesterol from the intracellular compartment to the plasma membrane (243), forming a complex with chaperone proteins in the cytosol (244), and has been shown to be involved in cholesterol trafficking during apolipoprotein-mediated HDL generation (245).

While apolipoprotein-specific efflux can be elicited by various exchangeable apolipoproteins, apoA-I, apoA-II, apoA-IV, apoE and insect apoIII, and by synthetic amphiphilic peptides (31,104,246,247), some naturally-occurring mutations of apoA-I have a reduced ability to promote apolipoprotein-specific cholesterol efflux. Two of these mutations, $Pro^{165}\rightarrow$Arg and $Arg^{173}\rightarrow$Cys, likely cause significant alterations in the secondary structure of apoA-I and thus indirectly affect efflux. The mutation of $Pro^{165}\rightarrow$Arg may remove a β-turn separating helices 6 and 7, which could affect the native lipid-binding properties of apoA-I and cholesterol efflux in a secondary manner. The substitution $Arg^{173}\rightarrow$Cys results in the dimerization of apoA-I through a disulfide bridge and has been shown to modify the lipid binding properties of both the monomer and dimer. Studies in our lab have indicated that apoA-I mutants with deletions in the central domain had no effect on cholesterol efflux from fibroblasts when considered in the absence of LCAT (213,218).

Characterization of a natural single amino acid deletion, $Glu^{235}\rightarrow 0$, in apoA-I suggested the C-terminus is important in cholesterol efflux as this mutant was associated with a 54% decrease in cholesterol efflux and reduced cell association relative to wild-type apoA-I (248). Efflux from cholesterol-loaded macrophage and association with DMPC was significantly impaired as compared to wild-type apoA-I suggesting functional lipid-binding of

the C-terminus is required for cholesterol efflux. Gillotte *et al.* suggested other helical domains in apoA-I may be important for this form of efflux (249). They demonstrated that synthetic peptides modeled after residues 44-56 and 209-241 of apoA-I were able to efflux cholesterol to a level 50% and 70% of full-length apoA-I, respectively, while peptides modeled after other apoA-I helices were not (249). This further suggested that PL-binding affinity correlates with cholesterol efflux and that the N-terminus of apoA-I (residues 44-65) may be important in this pathway, as well. Concerning the latter, the capacity of apoA-I N-terminal deletion mutants to elicit cholesterol efflux has not been characterized, however this domain has been shown to be important for lipid-binding (199).

1.4.3.3 Activation of LCAT

The physical chemical properties of the LCAT reaction have been intensely studied *in vitro* and demonstrate that LCAT binds not only to HDL but also LDL and PC vesicles. Studies from Jonas *et al.* using surface plasmon resonance have shown that the on-rate constants for LCAT interaction with all of these substrates are virtually equal and that apolipoprotein content does not affect this property (reviewed recently in ref (128)). However, the off-rate constants are dependent upon the apolipoprotein content and the nature of the surface lipids. Replacing apoA-I with apoA-II reduces binding affinity 4-fold, suggesting that LCAT initially binds to the lipid surface followed by a specific interaction and activation by apoA-I, the rate limiting of which appears to be PC binding at the active site (250). The off-rate constants in these studies were very similar to the catalytic turnover rates (0.01 - 0.05s^{-1}), suggesting that LCAT dissociates from HDL after an average of one catalytic cycle. General properties of the apolipoproteins associated with LCAT activation include: an amphipathic α-helix with a non-polar face of approximately 100°, a cluster of

acidic residues opposite the nonpolar face and a distribution of basic residues at the polar-nonpolar interface.

ApoA-I was the first described apolipoprotein activator of LCAT and also the most potent (251), as other apolipoproteins are less than 20% as efficient (252,253). These observations coupled with the fact that apoA-I is the principal protein component of HDL suggested this protein is critical for LCAT mediated CE accumulation in HDL. The observation that numerous apolipoproteins are able to stimulate LCAT activity to some degree suggested that amphipathic α-helices are necessary but not sufficient for this process. Therefore, detailed studies using synthetic peptides modeled after apoA-I helices, CNBr fragmentation and mutagenesis sought to reveal a specific domain(s) responsible for this process. Whereas diffusional cholesterol efflux closely correlated with the PL-binding affinity of apoA-I synthetic peptides, this was shown not to be the case for LCAT activation. Peptides modeled after the C-terminus (a.a. 187-243) of apoA-I could not bind and activate LCAT (254) while residues 148-185 were able to do so. Further studies indicated that peptides with high amphipathic character but no homology to apoA-I could activate LCAT (255,256). Segrest and coworkers found that such peptides gave maximal LCAT activation as a dimer and furthermore only when residue 13 was glutamic acid (257).

More recent work using apoA-I deletion mutants has established that helix 6 (a.a. 144-186) constitutes the principal LCAT activating domain. These studies are corroborated by analysis of naturally occurring apoA-I mutants: $Lys^{107}\rightarrow 0$, $Leu^{141}\rightarrow Arg$, Δ146-160 apoA-I (Seattle), $Arg^{151}\rightarrow Cys$, $Val^{156}\rightarrow Glu$, $Leu^{159}\rightarrow Arg$, $Pro^{165}\rightarrow Arg$ and $Arg^{173}\rightarrow Cys$ which exhibit reduced LCAT activation (reviewed in ref (182)). Two *in vivo* studies support the putative role of this domain in LCAT activation. We have shown that both Δ122-165 and Δ144-186 apoA-I associate with CE poor HDL when expressed in apoA-I deficient mice by

adenovirus-mediated gene transfer (219). In contrast, Δ100-143 was not compromised in CE content. Sorci-Thomas and coworkers have generated a mouse transgenic for an apoA-I mutant lacking helix 6 (258). They observed this apoA-I mutant was associated with CE-poor HDL when crossed into a murine apoA-I deficient background. This is consistent with *in vitro* studies from their lab and ours concerning the role of this helix in LCAT activation (218,259). While the central domain has been implicated in LCAT activation for quite some time, the physical properties responsible have only recently been described. Roosbeek and coworkers proposed that 3 Arg residues at the polar/non-polar interface of helix 6 contribute to a specific region of positive electrostatic potential that may stimulate LCAT activity (260). Site-specific mutagenesis of these Arg residues conferred 11-12-fold reductions in LCAT activation (decrease in V_{max}) without affecting other physical properties of apoA-I. The studies to date clearly identify a central domain, most importantly helix 6, in LCAT activation. This may be due to the presence of a locale of positive surface potential

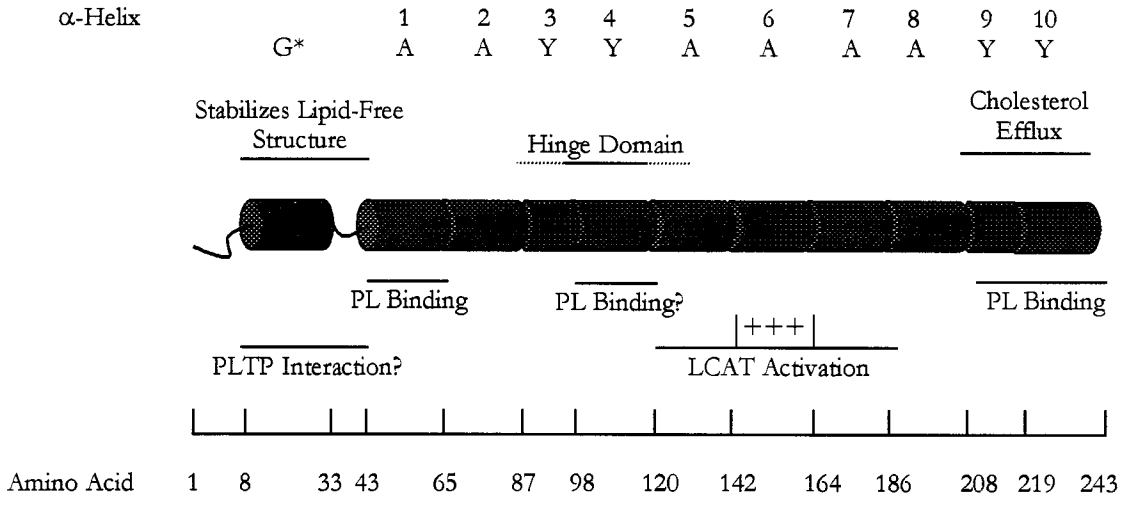

Figure 1-16: Putative Structure-Function Relationships of ApoA-I

involved in LCAT interaction. The secondary structural elements of apoA-I associated with specific functional properties are summarized in Fig. 1-16.

1.4.4 Characterization of ApoA-I and HDL Metabolism in Mouse Models

Genetic manipulation has enabled the development of transgenic and knockout (deficient) animals, which have served to establish the pro- or anti-atherogenic nature of various apolipoproteins, lipolytic enzymes, lipid transfer proteins and cell surface receptors. This section considers various animal models of apoA-I, which demonstrate its potent anti-atherogenic effects and importance in HDL formation.

1.4.4.1 ApoA-I Transgenic Mouse

Transgenic mice expressing high levels of human apoA-I were first described by Walsh *et al.* in 1989 (261). They reported plasma total apoA-I levels of 381 ± 43 mg/dL as compared to 153 ± 17 mg/dL for control mice. Total and HDL cholesterol levels were increased to 125 ± 12 mg/dL and 90 ± 7 mg/dL versus 78 ± 13 mg/dL and 55 ± 11 mg/dL for apoA-I transgenic mice and matched controls, respectively. Non-denaturing gradient gel electrophoresis demonstrated this increase in HDL was due predominantly to smaller HDL_3 type particles, the formation of which could not be attributed to aberrant metabolism of human apoA-I in these mice. In 1991, Rubin *et al.* described human apoA-I transgenic mice in a C57BL/6 background, a mouse strain susceptible to diet-induced atherosclerosis (262). In addition to increases in plasma total apoA-I and cholesterol levels, mouse apoA-I levels were reduced by greater than 4-fold and accounted for only 4% and 13% of total plasma levels in two independent transgenic lines. While wild-type C57BL/6 mice have a single HDL species, the apoA-I transgenic possesses two HDL subclasses comparable to HDL_{2b} and HDL_3 in humans. In support of epidemiological studies demonstrating the incidence of cardiovascular disease is inversely correlated to HDL cholesterol levels, the apoA-I

transgenic C57BL/6 mouse was protected from diet-induced development of fatty streak lesions relative to the wild-type mouse (263).

In 1994, two groups reported that the spontaneous atherosclerosis observed in apoE knockout (apoE-/-) mice could be corrected by introducing a human apoA-I transgene (hapoA-I Tg). ApoE knockout mice are severely hypercholesterolemic and develop atherosclerotic lesions regardless of diet. Paszty *et al.* reported apoE-/-hapoA-I Tg mice had a 2 to 3-fold increase in HDL cholesterol and a six-fold decrease in susceptibility to atherosclerosis (264). Plump *et al.* indicated their apoE-/- hapoA-I Tg had 2-fold increases in HDL cholesterol with reduced atherosclerosis and fibroproliferative lesions by 8 months of age (265).

1.4.4.2 ApoA-I Deficient Mouse

By gene targeting in embryonic stem cells, Williamson *et al.* generated an apoA-I knockout strain 129 mouse in 1992 to determine if mice lacking apoA-I were more susceptible to atherosclerosis (266). Plasma total cholesterol and HDL cholesterol levels were reduced to 26% and 25% of normal levels, respectively, and were deficient in α-migrating HDL particles. Interestingly, Li *et al.* reported apoE levels in these mice were increased 3-fold and constituted 1/3 of HDL protein as compared to wild-type strain 129 mice in which apoE is present at only trace levels in HDL (267). To investigate the effect of apoA-I deficiency on atherosclerotic risk, apoA-I deficient and wild-type strain 129 mice were maintained on an atherogenic diet for 4 weeks. During this period total plasma cholesterol levels increased by 20 mg/dL and 60 mg/dL in apoA-I deficient and normal mice, respectively, however neither group exhibited any early signs of atherogenesis. ApoA-I deficient strain 129 mice were crossed into C57BL/6 mice to study apoA-I deficiency in

mice susceptible to atherosclerotic lesions. These mice with mixed strain 129 and C57BL/6 genetic backgrounds were maintained on a high fat diet for 20 weeks and the aortic surface examined. While some foam cells were identified in these animals, there was no correlation with apoA-I genotype suggesting, while apoA-I may protect against atherogenesis, the lack of apoA-I by itself does not cause atherosclerosis.

1.4.4.3 Expression of Human ApoA-I by Adenovirus-Mediated Gene Transfer in Mice

The potential use of liver directed gene therapy to increase apoA-I and HDL plasma concentrations may prove to be an effective means by which to treat hypercholesterolemic and hypoalphalipoproteinemic patients. Thus, in 1994, Kopfler *et al.* described the first use of recombinant adenovirus to transiently express human apoA-I (hapoA-I Ad5) in BALB/c mice (268). Five days after intravenous infusion of hapoA-I Ad5, human apoA-I serum levels averaged 168 mg/dL while total and HDL cholesterol values increased 47% and 35%, respectively. They reported apoA-I expression declined to <10% of maximal plasma levels (day 4-6 post-injection) after 12 days while hepatic human apoA-I mRNA was undetectable at this time point. Following advances in adenovirus vector technology, Tsukamoto *et al.* reported in 1997 the use of second generation recombinant adenovirus able to mediate prolonged, high expression levels of human apoA-I in mice (269). ApoE deficient mice fed a chow diet, LDL receptor deficient and wild-type C57BL/6 mice fed a Western diet expressed peak apoA-I levels of 235, 324 and 276 mg/dL, respectively, following intravenous injection of this adenovirus. While human apoA-I was barely detectable 6 weeks post-injection in the apoE deficient mouse, the protein was still detectable after 8 months in LDL receptor deficient and wild-type C57BL/6 mice. Benoit *et al.* published in 1999 that injection of a human apoA-I recombinant adenovirus in wild-type C57BL/6 mice resulted in

a 40% increase in plasma HDL cholesterol levels while injection into apoA-I transgenic mice resulted in a 360% increase in plasma HDL cholesterol (270). They suggested this pronounced difference between mouse strains was due to an immune response mounted against human apoA-I in the wild-type C57BL/6 mouse. They subsequently injected this adenovirus into human apoA-I transgenic/apoE deficient mice prone to atherosclerosis. Over a 6 week period, adenovirus mediated expression of apoA-I inhibited the formation of fatty streak lesions by 56% as compared to non-injected controls. Furthermore, Tangirala *et al.* reported in 1999 that injection of a similar apoA-I adenovirus in LDL receptor deficient mice could induce regression of pre-existing fatty streaks (271).

1.5 Rationale and Specific Aims

The goal of this work is to characterize the structure-function relationships associated with the globular domain (residues 1-43) and the first class A helix (residues 44-65) of apoA-I.

Functional properties associated with these regions remain poorly characterized. An apoA-I mutant lacking residues 1-43 (Δ1-43 apoA-I) was described previously (197,199,220) and suggested that the deleted amino-acids stabilized the lipid-free conformation of apoA-I. The X-ray crystal structure of this mutant suggests that apoA-I, when bound to HDL, wraps around the periphery of the particle perpendicular to the PL fatty-acyl chains (189). Previous work also demonstrates that deletion of these residues confers a 2-fold decrease in the ability of apoA-I to activate LCAT suggesting functional properties of this mutant may be moderately affected, as well. The importance of helix 1 (residues 44-65) for association of apoA-I with PL has been shown previously (212). Using synthetic peptides modeled after repeating 22-mer domains of apoA-I, Palgunachari and coworkers demonstrated that only

N- and C-terminal terminal peptides corresponding to a.a. 44-65 and 220-241 of apoA-I were able to clarify DMPC vesicles, implicating both the N- and C-terminus in PL binding. In addition, the characterization of an apoA-I deletion mutant lacking residues 1-65 suggests this protein has significantly less PL binding affinity relative to wild-type and Δ1-43 apoA-I. However, the contributions of this helix to cholesterol efflux, LCAT activation and the *in vivo* maturation of HDL have not been fully characterized.

To investigate structure-function relationships associated with the N-terminus of apoA-I, we have taken a combined *in vitro* and *in vivo* approach. Firstly, histidine-tagged proteins were expressed in and purified from *E. coli*, corresponding to full-length wild-type apoA-I and 2 deletion mutants lacking residues 1-43 and residues 1-65. These recombinant proteins were compared with respect to cholesterol efflux, lipid-binding properties, ability to form reconstituted lipoproteins and activate LCAT. The goal of these studies is to ascertain whether the globular domain and/or the first class A helix contribute to these physical and functional properties of apoA-I. Secondly, recombinant adenoviruses were generated corresponding to wild-type apoA-I and similar N-terminal deletion mutants and injected into apoA-I deficient mice. The mutant proteins were compared to wild-type apoA-I expression levels in plasma, plasma lipid levels and HDL composition, size, electrophoretic migration and morphology. These experiments assess the importance of the globular domain and helix 1 to the *in vivo* maturation of HDL.

CHAPTER 2: IN VITRO STRUCTURE-FUNCTION ANALYSIS OF THE AMINO-TERMINUS OF APOLIPOPROTEIN A-I

2.1 Summary

HDL transport cholesterol from peripheral tissues to the liver for excretion in the bile, a process known as reverse cholesterol transport (10). The primary protein constituent of HDL, apoA-I, is a 243 amino-acid plasma protein composed of 10 class A/Y amphipathic helices (a.a. 44-243) (reviewed in ref (79)) and a globular domain (a.a. 1-43) at the N-terminus containing a G* helix (a.a. 8-33) (188,272). Due to intrinsic differences in their physical properties, individual amphipathic helices are thought to differentially contribute to the physical and functional properties of apoA-I.

In this regard, physical-chemical properties associated with the globular domain and the first class A helix (a.a. 44-65) of apoA-I were studied. Recombinant histidine-tagged wild-type apoA-I (His-Wt apoA-I) and two N-terminal deletion mutants corresponding to the removal of residues 1-43 and 1-65 (referred to as His-Δ1-43 and His-Δ1-65 apoA-I) were expressed in *E. coli* and purified by affinity chromatography.

Cell association and cholesterol efflux from J774 macrophage to His-Wt, His-Δ1-43 and His-Δ1-65 apoA-I were similar while efflux to an apoA-I mutant lacking residues 210-243 was significantly reduced. This suggests the extreme amino-terminus is not crucial for cholesterol efflux mediated by apoA-I. Native lipid-binding properties were disrupted for both His-Δ1-43 and, more markedly, His-Δ1-65 apoA-I relative to His-Wt apoA-I as determined by a reduced rate of clearance of DMPC liposome turbidity. Reconstituted discoidal lipoproteins were prepared in order to compare the stability and functional properties of His-Wt apoA-I to the N-terminal mutants. Reconstituted lipoproteins containing the apoA-I deletion mutants exhibited similar stabilities in the presence of guanidine hydrochloride as compared to those containing His-Wt apoA-I. Therefore,

deletions in the amino-terminus do not appreciably affect the stability of apoA-I in these synthetic lipoprotein particles. Finally, LCAT activation was reduced to 50% and 34% (decrease in V_{max}) for His-Δ1-43 and His-Δ1-65 apoA-I relative to His-Wt apoA-I suggesting the amino-terminus is involved in LCAT activation.

These studies suggest the globular domain (a.a. 1-43) and the first class A helix (a.a. 44-65) are not involved in cholesterol efflux but do affect the native lipid-binding properties of apoA-I. Furthermore, the extreme amino-terminus of apoA-I, encompassing both the globular domain and helix 1 are critical LCAT activating domains.

2.2 *Materials and Methods*

2.2.1 Construction of the cDNA for His-ApoA-I Expression

Histidine (His)-tagged wild-type apoA-I (His-Wt apoA-I) was generated in our laboratory previously (273) and the deletion mutant lacking residues 1-65 (His-Δ1-65 apoA-I) was acquired from Drs. Christie G. Brouillette and Jeffrey A. Engler (199). The apoA-I mutant in which residues 1-43 were deleted (His-Δ1-43 apoA-I) was generated by deletion mutagenesis using the Excite mutagenesis kit from Stratagene and the oligonucleotides: 5'-PCATATGGTGATGGTGATGGTGCG-3' (upstream) and 5'-CTAAAGCTCCTTGACAACTGGGACAGCG-3' (downstream). The apoA-I mutant lacking residues 210-243 (His-Δ210-243 apoA-I) was generated by similar methods using the following oligonucleotides: 5'-GGGCTTGGCCTTCTCGCTGAGCG-3' (upstream) and 5'-PTGAGGCGCCCGCCGCCCCCCTTC-3' (downstream).

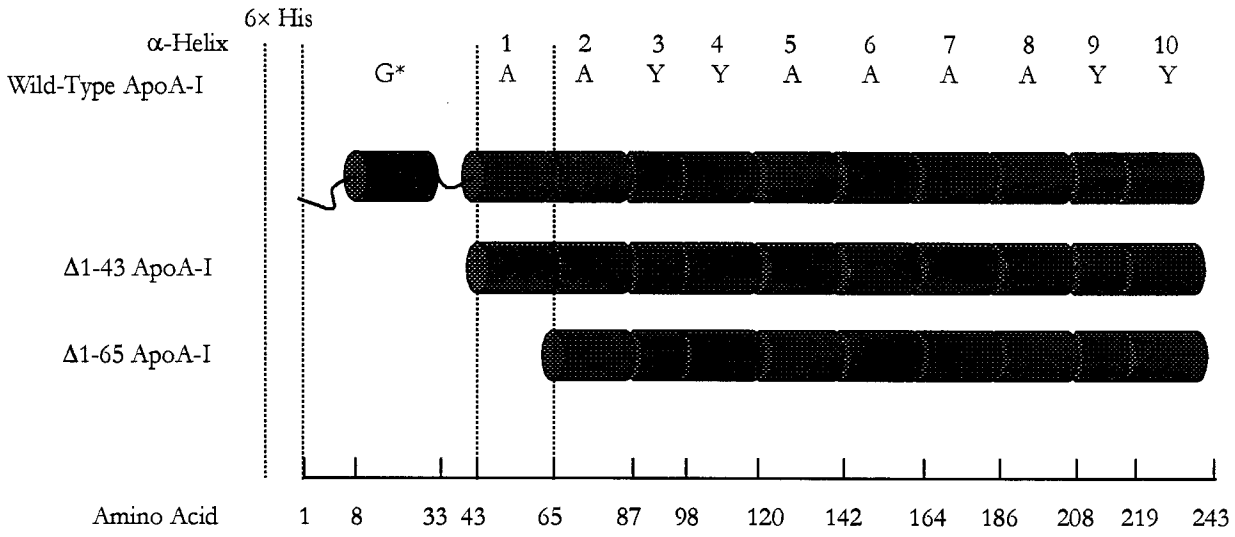

Figure 2-1: Secondary Structural Elements of the Histidine-Tagged ApoA-Is

The positioning of the class A (blue), Y (red) and G* (green) helices in His-Wt apoA-I is shown. Deletion of residues 1-43 removes the globular domain consisting of the G* helix (a.a. 8-33) and the unordered residues 1-7 and 33-44. Deletion of residues 1-65 results in the successive removal of the 1st class A helix (a.a. 44-65).

2.2.2 · *Cell Culture*

J774 mouse peritoneal macrophages were maintained between passages in Dulbecco's modified Eagle's medium (DMEM) supplemented with 10% (vol/vol) fetal bovine serum (FBS), 100 U/mL penicillin, 100 U/mL streptomycin sulfate and 2 mM L-glutamine. Cell culture plasticware and reagents were purchased from Falcon, Gibco BRL and Sigma.

2.2.3 *Purification of Histidine-Tagged ApoA-I*

All recombinant His-apoA-I proteins were expressed under the control of the T_7 promoter and purified in BL21 DE3 *E. coli* as described previously (273) with some minor changes (274). His-Wt and His-Δ1-43 apoA-I were subcloned into the pET 3a expression vector while His-Δ1-65 apoA-I subcloned into the pGEMX expression vector (Invitrogen). For protein expression, *E. coli* were newly transformed with 1 ng of the apoA-I-containing constructs. Overnight LB precultures, grown for 12 h at 37°C in a bacterial shaker at 200 rpm in 100 μg/mL ampicillin, were used to innoculate 1 L flasks of LB growth medium. A 1/100 (v/v) innoculum was used and the cultures grown to an OD_{600} of 0.45. Protein expression was induced by adding 1/100 (v/v) of 0.1 M isopropyl-β-D-thiogalactopyranoside (IPTG), followed by a further 2 h of incubation under the above conditions following. Cells were harvested by centrifugation and frozen at -20°C. The pellet was later resuspended in buffer A (100 mM Na_2HPO_4, 1 mM PMSF and 6 M GdnHCl, pH 8.0). The solution was sonicated on ice and the bacterial debris removed by centrifugation for 1 h at 11 000×g. Nucleic acids were removed by incubation of the supernatant in streptomycin sulfate (10 mL of 10% solution per gram protein) at 4°C for 1 h. Following a

subsequent centrifugation, the supernatant was applied to a nitrilotriacetic acid-agarose (Qiagen) column equilibrated with buffer A. After application, the column was washed with buffer A and then weakly bound proteins were eluted by washing with 100 mM phosphate/citrate, 6 M GdnHCl, pH 6.0. The recombinant, histidine-tagged apoA-I proteins were eluted with the latter buffer adjusted to pH 5.0. Collected fractions were neutralized by addition of 1 M NaOH and supplemented with 0.1 M EDTA and PMSF. The fractions containing the greatest concentration of protein, as determined by 12% SDS-PAGE, were pooled and dialyzed against 5 mM NH_4HCO_3, 1 mM EDTA, 0.02% NaN_3 and lyophilized. Proteins were stored at -20°C. For experiments, the lyophilized protein was solublized in 6 M GdnHCl, pH 8.0 and dialyzed against phosphate-buffered saline (PBS).

2.2.4 Competitive Cell Surface Association

Cholesterol-loaded J774 macrophage were seeded in 12-well plates at a density of 2×10^4 cells/well and grown for 48 h before cholesterol loading. Washed cells were incubated with 1 mL of Dulbecco's minimal essential medium (DMEM) containing 1% FBS and 75 μg of acetylated LDL (AcLDL) for 48 h. Cells were then washed with DMEM containing 0.2% bovine serum albumin (BSA) and incubated in DMEM containing 0.2% BSA with or without 0.3 mM 8-bromoadenosine 3':5'-cyclic monophosphate (cAMP) (Sigma) for 12 h. Washed cells were incubated with 1×10^6 cpm of iodinated His-Wt apoA-I (^{125}I-His-Wt apoA-I) in the presence of nonlabeled His-Wt, His-Δ1-43, His-Δ1-65 and His-Δ210-243 apoA-I in the following molar ratios of labeled to nonlabeled apoA-I: 1:0, 1:1, 1:3, 1:10 and 1:50. After 2 h, the cells were solubilized in 0.5 N NaOH and counted for gamma radioactivity. Radioactivity was normalized to cell protein content assessed by the method of Markwell and Lowry (275).

2.2.5 *Cholesterol Efflux*

Efflux assays were performed with cholesterol loaded J774 macrophage as described by Sakr *et al.* (276) with several modifications. Cells were seeded in 12-well plates at a density of 2×10^4 cells/well and grown for 48 h before cholesterol loading. Cells were cholesterol loaded for 48 h in 1 mL of DMEM containing 1% FBS and [1α, 2α-^{3}H] cholesterol (NEN Life Science Products) (15 μCi/mL final concentration), which had been pre-incubated for 30 min at 37°C with AcLDL (75 μg/mL final concentration). Subsequently, cells were washed 3× in DMEM containing 0.2% BSA and incubated in DMEM containing 0.2% BSA with or without cAMP for 12 h. Cells were then washed 3× in DMEM containing 0.2% BSA. For the efflux assay, cells were incubated for 0, 2, 6 and 24 h in 1 mL of DMEM containing 0.2% BSA with or without 0.3 mM cAMP containing 50 μg His-Wt apoA-I or equivalent moles of each apoA-I deletion mutant. At the appropriate time point, media samples were removed and centrifuged at 1 000×g to remove floating cells. Cells were solubilized in 1 mL of 0.5 N NaOH and assayed for cell protein content by the method of Markwell and Lowry (275). The radioactivity in all samples was determined by liquid scintillation counting. Cholesterol efflux was calculated as the percentage of initial cell radioactivity associated with the media as a function of time. Values were corrected at each time point for the efflux of cholesterol to medium not containing apoA-I. The percentage stimulation of cholesterol efflux in response to cAMP treatment was calculated according to the following equation: (efflux from J774 cells treated with cAMP – efflux from J774 cells in the absence of cAMP)/(efflux from J774 cells in the absence of cAMP)×100% (277).

2.2.6 *DMPC Clearance*

The ability of apoA-I to clear a solution of dimyristoylphosphatidylcholine (DMPC) at its transition temperature (23.9°C) was assessed as initially described by Pownall *et al.* (278) Briefly, DMPC solubilized in chloroform was dried under nitrogen and solubilized above its transition temperature in tris-buffered saline (TBS), pH 8.0. A DMPC to apoA-I ratio of 50:1 was used and the reaction followed at 23.9°C by measuring the absorbance at 325 nm for 30 min. A decrease in absorbance is associated with the solubilization of the liposomes by apoA-I and the formation of discoidal complexes, the rate of which is proportional to the affinity of apoA-I for phospholipid.

2.2.7 *Preparation of Reconstituted Lp2A-I*

Reconstituted discoidal lipoproteins containing 2 molecules of apoA-I (Lp2A-I) were prepared by cholate dispersion/Bio-Bead removal protocol using initial molar ratios of 80:10:1 of 1-palmitoyl-2-oleoyl-phosphatidylcholine (PL) (Avanti Polar Lipids), FC (Sigma) and His-apoA-I, respectively, as described elsewhere (279). Particle size and homogeneity were confirmed by 4-20% non-denaturing gradient gel electrophoresis (PAGGE). Each particle contained 2 molecules of apoA-I as determined by cross-linking with dimethylsuberimidate, according to an established protocol (280). Enzymatic kits were used to determine the final PL (Wako Chemicals) and FC (Roche Diagnostics) concentrations. The apoA-I content was measured according to the method of Markwell and Lowry (275) using a BSA standard. The stability of the Lp2A-Is was assessed by circular dichroism spectroscopy using a Jasco J41A spectropolarimeter and an established protocol (211). The change in molar ellipticity was determined at 222 nm with increasing concentrations of guanidine hydrochloride to calculate the standard free energy of denaturation (ΔG_D°).

2.2.8 LCAT Assay

Human LCAT was purified as described previously (281). Lp2A-Is were prepared containing [^{3}H] cholesterol and His-Wt, His-Δ1-43 or His-Δ1-65 apoA-I. Two distinct types of experiments were performed. The time course assay was performed as described previously (274) by incubating 3.5 U of LCAT with Lp2A-I for 0, 0.5, 1, 2, 3, 4 and 5 h at 37°C at a final apoA-I concentration of 2.14 μM. In the second experiment, the rate constants V_{max} and apparent K_m ($appK_m$) were determined by incubating Lp2A-Is at the concentrations indicated (expressed in μM apoA-I) for 10 min at 37°C. In both cases, the reactions were terminated by the addition of 2 mL of ethanol and minimal substrate conversion was determined (282). The values indicated are the mean (± standard error) of triplicate results and are representative of 2 independent experiments. One unit of LCAT is defined as the amount of enzyme required to convert 1 nmol of FC to CE per hour using a standard His-Wt Lp2A-I at a final concentration of 2.0 μM.

2.2.9 Electrophoresis

SDS-PAGE was performed using 12% acrylamide pre-cast Novex gels (Invitrogen) according to the manufacturer's specifications. Non-denaturing PAGGE was done using 4-20% acrylamide pre-cast Novex gels and samples were separated for 2000V×h. Preβ- and α-HDL were separated by agarose gel electrophoresis (Beckman Lipogel) followed by neutral lipid staining (Beckman) or Western blotting using a biotinylated anti-apoA-I monoclonal antibody (A44). Samples were separated for 30 min at 100V.

2.2.10 Western Blotting

Samples separated by 12% SDS-PAGE were transferred to nitrocellulose at 125 V for 1 h while those separated by 4-20% PAGGE were transferred at 125 V for 2 h. Membranes were probed either with the biotinylated A44 monoclonal antibody directed against the central domain of apoA-I (a.a 149-186), an anti-human apoA-I polyclonal from sheep (Roche Molecular Biochemicals) or an anti-mouse apoE polyclonal from rabbit (Biodesign International). Proteins were visualized by chemiluminescence following incubation with either streptavidin (Amersham Life Science), donkey anti-sheep IgG (Sigma) or donkey anti-rabbit IgG (Amersham Life Science) coupled to HRP.

2.3 Results

2.3.1 *Expression of Histidine-Tagged Wild-Type and Mutant ApoA-I*

In order to address the contribution of the extreme amino-terminus to various physico-chemical properties of apoA-I, His-Wt apoA-I and 2 deletion mutants, corresponding to the removal of residues 1-43 and 1-65, with N-terminal histidine tags were expressed and purified from *E.coli* (Fig. 2-2). All 3 proteins were expressed at high levels and appeared to reach peak expression at similar time-points following the addition of IPTG (2 h). The apparent molecular weight as determined by 12% SDS-PAGE corresponded with the expected size of the histidine-tagged proteins, 29.5 kDa, 24.6 kDa and 22.0 kDa for His-Wt, His-Δ1-43 and His-Δ1-65 apoA-I, respectively. These proteins all efficiently bound the

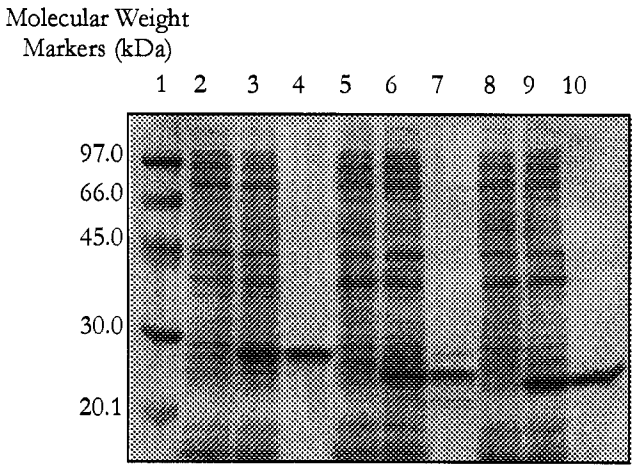

Figure 2-2: *E. coli* Expression of Wild-Type and Mutant Histidine-Tagged ApoA-Is

Overnight precultures of *E. coli* transformed with the His-Wt, His-Δ1-43 and His-Δ1-65 were used to innoculate 1 L flasks of LB growth medium for protein expression. The cultures were grown to an OD_{600} of 0.45 and subsequently induced by the addition of IPTG. Cultures were incubated for a further 2 h at 37°C in a bacterial shaker at 150 rpm and centrifuged to collect a bacterial pellet. *E. coli* cell lysates prior to IPTG induction (lanes 2, 5 and 8), after induction and prior to centrifugation (lanes 3, 6 and 9) and after purification (see *Materials & Methods*) (lanes 4, 7 and 10) are shown for His-Wt (lanes 2, 3 and 4), His-Δ1-43 (lanes 5, 6 and 7) and His-Δ1-65 (lanes 8, 9 and 10) following separation by 12% SDS-PAGE and Coomassie blue staining.

NTA resin and were recovered following elution at pH 5.0 to similar extents. After removal of GdnHCl by dialysis, His-Δ1-43, but not His-Wt or His–Δ1-65 apoA-I, tended to aggregate and precipitate from solution resulting in a lower yield of this protein. The tendency of this mutant to aggregate in solution has been documented previously (272) and may be due to the effect of this particular mutation on the integrity of the lipid-free structure of apoA-I. Inclusion of a small amount of cholic acid in the dialysis buffer significantly increased the yield of this mutant and was subsequently removed by incubation with a hydrophobic, polystyrene absorbent (Bio-Beads).

2.3.2 Effect of Amino-Terminal Deletions on Macrophage Cell Surface Association

We first evaluated the effect of these deletions on the ability of apoA-I to bind macrophage at 37°C. Previous work indicates the binding of apoA-I mutants to macrophage directly correlates with their ability to elicit cellular cholesterol efflux. Thus to emulate the conditions used for cholesterol efflux, J774 macrophages were cholesterol-loaded using AcLDL as described in *Materials & Methods*. In order to compare the relative binding efficiencies of His-Wt, His-Δ1-43 and His-Δ1-65, a competitive cell association assay was used. Iodinated His-Wt apoA-I (1 000 000 cpm) (referred to as ^{125}I-His-Wt apoA-I) was added to the cell culture medium in the absence or presence of non-labeled apoA-I competitor. Non-labelled His-Wt, His-Δ1-43, His-Δ1-65 and His-Δ210-243 were added at molar ratios of 1:0, 1:1, 1:3, 1:10 and 1:50 for ^{125}I-His-Wt apoA-I to competitor, respectively. After 2 h of incubation, the culture medium was removed and the cell-associated radioactivity was determined. In addition, cells were pretreated for 12 h with culture medium containing 0.3 mM cAMP, which increases the expression of ABCA1 (98), and significantly increased the specific association of ^{125}I-His-Wt apoA-I with these cells relative

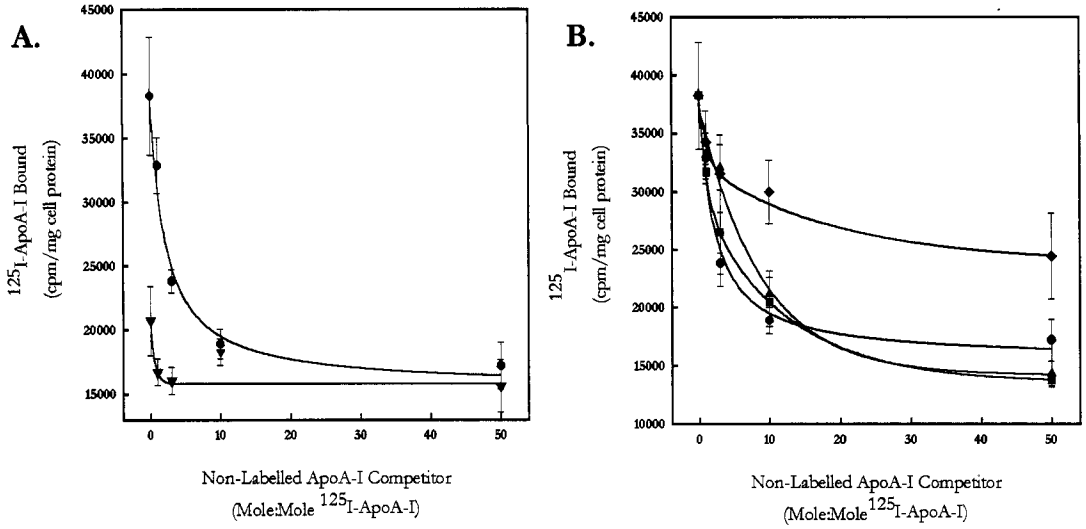

Figure 2-3: Effect of ApoA-I Amino-Terminal Deletions on J774 Macrophage Cell Association

(A) The binding of ^{125}I-His-Wt apoA-I to cholesterol-loaded J774 macrophage, either pretreated (●) or not pretreated (▼) with 0.3 mM cAMP, at 37°C and in the presence of non-labeled His-Wt apoA-I at varying molar ratios is shown.
(B) Cells were pretreated with 0.3 mM cAMP. The abilities of His-Wt (●), His-Δ1-43 (▲), His-Δ1-65 (■) and His-Δ210-243 (♦) apoA-I to compete for the binding of ^{125}I-His-Wt apoA-I are shown.

to cells not pretreated with cAMP (Fig. 2-3A). I found that both His-Δ1-43 and His-Δ1- 65 apoA-I were as effective as His-Wt apoA-I in competing for the binding of ^{125}I-His-Wt apoA-I, while His-Δ210-243 apoA-I poorly competed (Fig. 2-3B). This work suggested that deletion of the globular domain and helix 1 had no effect on the ability of apoA-I to associate with macrophage, which is primarily dependent upon the presence of the carboxy-terminus.

2.3.2 Cholesterol Efflux from J774 Macrophage to His-Wt, His-Δ1-43, His-Δ1-65 and His-Δ210-243 ApoA-I

His-Wt, His- Δ1-43, His- Δ1-65 and His- Δ210-243 apoA-I were used to evaluate the potential contribution of the N-terminus of apoA-I to cellular cholesterol efflux. Cells were

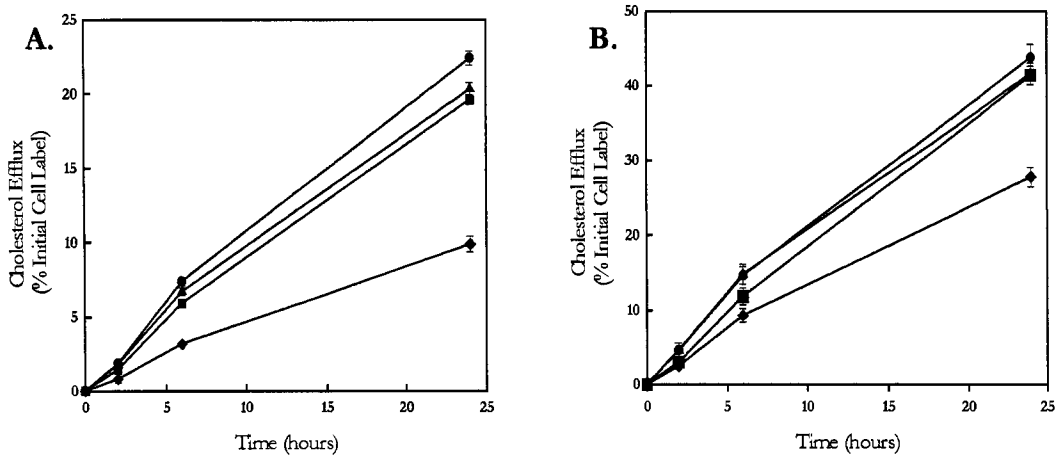

Figure 2-4: Effect of Amino-Terminal Deletions on Cholesterol Efflux to ApoA-I

Cholesterol loaded J774 macrophage were incubated for 12 h in DMEM containing 0.2% BSA with (A) or without (B) 0.3 mM cAMP. This medium was replaced with 1 mL of DMEM containing 0.2% BSA and 50 μg of His-Wt (●) apoA-I or equivalent moles of His-Δ1-43 (▲), His-Δ1-65 (■) and His-Δ210-243 (♦) apoA-I and incubated for 0, 2, 6 and 24 h. At each time point, the medium was removed and radioactivity was determined by liquid scintillation counting.

first cholesterol loaded for 48 h with AcLDL and subsequently equilibrated for 12 h in either the absence or presence of 0.3 mM cAMP. Medium containing 50 μg of His-Wt apoA-I or equivalent moles of His- Δ1-43, His- Δ1-65 and His- Δ210-243 apoA-I were then added and the efflux to each acceptor determined over time. In the absence of cAMP (Fig. 2-4A, Table 2-1), efflux to His-Δ1-43 and His-Δ1-65 apoA-I was slightly, but significantly ($p<0.01$, student's t-test), reduced relative to His-Wt apoA-I while efflux to His- Δ210-243 apoA-I was greatly reduced (2.2-fold) ($p<0.01$, student's t-test) by comparison. In the presence of cAMP (Fig. 2-4B, Table 2-1), efflux to His- Δ1-43 and His- Δ1-65 apoA-I was not statistically different from His-Wt apoA-I. In contrast, efflux in the presence of cAMP for His- Δ210-243 apoA-I was significantly reduced ($p<0.01$, student's t-test) relative to His-Wt apoA-I and the two N-terminal mutants (1.5-fold).

Table 2-1: The Rate of Cholesterol Efflux from J774 Macrophage to His Wt, His-Δ1-43, His-Δ1-65 and His-Δ210-243 ApoA-I

	Slope (% Cell Cholesterol/h)	R^2	Stimulation with cAMP (%)
His-Wt ApoA-I			
-cAMP	0.97 ± 0.02	0.99 ± 0.01	87 ± 5
+cAMP	1.83 ± 0.06	0.99 ± 0.01	
His-Δ1-43 ApoA-I			
-cAMP	0.88 ± 0.02[a]	0.99 ± 0.01	78 ± 3
+cAMP	1.66 ± 0.05	0.99 ± 0.01	
His-Δ1-65 ApoA-I			
-cAMP	0.86 ± 0.02[a]	1.00 ± 0.01	91 ± 1
+cAMP	1.77 ± 0.01	1.00 ± 0.01	
His-Δ210-243 ApoA-I			
-cAMP	0.45 ± 0.03[a]	0.99 ± 0.01	73 ± 1
+cAMP	1.19 ± 0.02[a]	0.99 ± 0.02	

Cholesterol efflux assays using J774 macrophage were performed as described in *Materials & Methods*. After cholesterol loading, cells were equilibrated for 12 h in the absence and in the presence of 0.3 mM cAMP. The slope represents the rate of cholesterol efflux to each apoA-I protein expressed as the percentage of initial cell ^{3}H-cholesterol label effluxed to the media per hour of incubation. Values represent the mean ± SE.
[a]Values statistically different ($p<0.01$) (student's t test) relative to His-Wt apoA-I

2.3.4 Effect of Amino-Terminal Deletions on Phospholipid Binding Affinity

The relative abilities of His-Wt, His-Δ1-43, His-Δ1-65 and His-Δ210-243 apoA-I to clarify a solution of DMPC liposomes was determined to evaluate the effect of these mutations on apoA-I PL binding. In this assay, the various apoA-Is were added to a solution of DMPC, prepared as described in *Materials and Methods*, at a 50:1 molar ratio (DMPC to apoA-I, respectively). ApoA-I solubilizes the DMPC liposomes forming discoidal HDL complexes and concomitantly reduces the turbidity of the solution, a property monitored by the decrease in absorbance at 325 nm. Relative to His-Wt apoA-I, both His-Δ1-43 and, more markedly, His-Δ1-65 exhibited a reduced rate of DMPC clearance suggesting that the initial rate of PL association is significantly affected by both the deletion

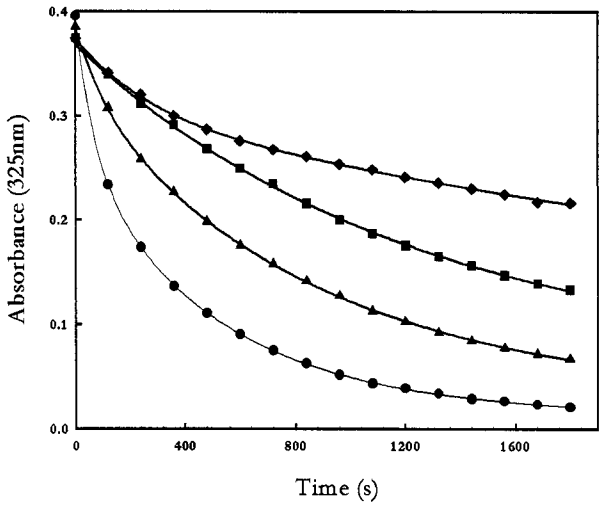

Figure 2-5: Rate of DMPC Clearance Associated Wild-Type and Mutant ApoA-Is

50 μg of His-Wt (●) apoA-I or equivalent moles of His-Δ1-43 (▲), His-Δ1-65 (■) and His-Δ210-243 (♦) apoA-I was added to a solution of DMPC liposomes and the absorbance monitored at 325 nm for 30 min at 23.9°C.

of residues 1-43 and the additional deletion of residues 44-65 (Fig. 2-5). The deletion of residues 1-65 disrupted the rate of DMPC clearance to a degree comparable to that of His-Δ210-243 apoA-I, a mutation which has previously been shown to significantly affect native lipid-binding properties of apoA-I (213).

2.3.5 Preparation of Reconstituted Lipoproteins Containing Wild-Type ApoA-I and the Amino-Terminal Deletion Mutants

Reconstituted, discoidal lipoproteins containing 2 molecules of apoA-I were prepared using the sodium cholate dispersion and Biobead removal method described by Sparks *et al.* (211) using His-Wt, His-Δ1-43 and His-Δ1-65 apoA-I. Initial ratios of 80:10:1 for POPC, FC and His-apoA-I, respectively, were used. The relative compositions, expressed as the number of molecules of PL and FC per molecule of apoA-I, and particle size were then determined (Fig. 2-6). Lp2A-Is reconstituted with His-Δ1-43 apoA-I

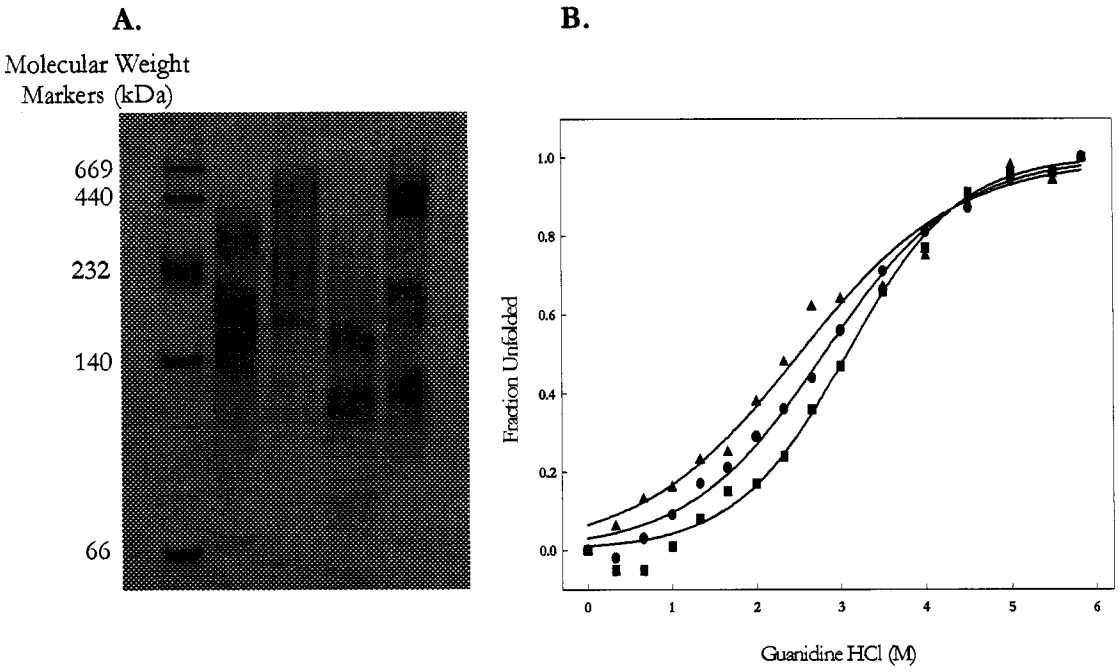

Figure 2-6: Size and Stability of Lp2A-Is Containing His-Wt, His-Δ1-43 and His-Δ1-65 ApoA-I

Lp2A-Is were prepared by cholate dispersion and Biobead removal containing 80:10:1 of PL, FC and His-apoA-I. (A) A non-denaturing 4-20% gradient gel separation of Lp2A-Is containing His-Wt (lane 3), His-Δ1-43 (lane 4) and His-Δ1-65 (lane 5) is shown. Molecular weight markers (lane 1) and human HDL (lane 2) are shown for reference. (B) The thermodynamic stability of the Lp2A-Is were compared by far UV circular dichroism spectroscopy (see *Materials and Methods*). Lp2A-Is containing His-Wt (●), His-Δ1-43 (▲) and His-Δ1-65 (■) were incubated with varying concentrations of the chaotropic agent guanidine hydrochloride for 48 h. Subsequently, the presence of apoA-I secondary structure was ascertained by the absorbance at 222 nm.

contained slightly fewer molecules of PL (58.7 ± 0.9) and FC (7.5 ± 0.2) per molecule of apoA-I as compared to both His-Wt (62.7 ± 5.9 mol PL/mol apoA-I, 8.9 ± 0.3 mol FC/mol apoA-I)) and His-Δ1-65 (64.7 ± 5.8 mol PL/mol apoA-I, 8.7 ± 0.6 mol FC/mol apoA-I) apoA-I. Furthermore, the stability of the reconstituted lipoproteins containing His-Wt, His-Δ1-43 and His-Δ1-65 apoA-I was assessed by far UV circular dichroism spectroscopy. Fig. 2-6B represents the denaturation curve of each lipoprotein expressed as the fraction of apoA-I secondary structure unfolded in the presence of guanidine hydrochloride. The

midpoint of the denaturation curve was used to calculate the standard free energy of denaturation ($\Delta G_D°$) and was very similar for His-Wt (2.81 ± 0.04 M), His-Δ1-43 (2.53 ± 0.06 M) and His-Δ1-65 (3.01 ± 0.09 M) apoA-I containing Lp2A-I.

2.3.6 Effect of ApoA-I Amino-Terminal Deletions on LCAT Activation

Subsequently, we assessed the ability of reconstituted lipoproteins containing His-Wt, His- Δ1-43 and His- Δ1-65 apoA-I to stimulate LCAT mediated cholesterol esterification *in vitro*. Reconstituted, discoidal lipoproteins (Lp2A-I) were prepared with initial molar ratios of 80:10:1 of PL, FC and His-apoA-I, respectively. During a 5 h time course experiment (Fig. 2-7A), the formation of CE was reduced to 50% and 48% for His-

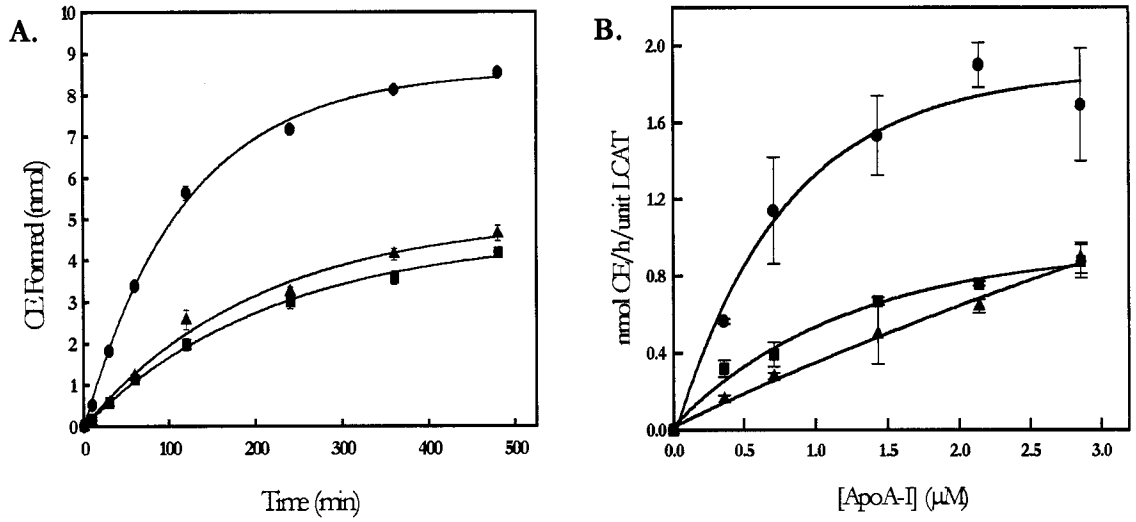

Figure 2-7: Effect of ApoA-I Amino-Terminal Deletions on LCAT Activation

Reconstituted, discoidal Lp2A-Is were prepared as described in the *Materials & Methods* containing ^{3}H-cholesterol. Panel A represents a time-course assay in which these lipoprotein substrates were incubated with 3.5 U of purified human LCAT and the yield of ^{3}H-cholesteryl ester was determined at various time-points after TLC separation and liquid scintillation counting. In Panel B, the substrates were incubated at various concentrations (expressed as μM apoA-I) with 1.25 U of purified human LCAT for 10 min. In both panels the plots representing Lp2A-Is containing His-Wt (●), His-Δ1-43 (▲) and His-Δ1-65 (■) are shown.

Δ1-43 and His- Δ1-65 Lp2A-I, respectively, relative to His-Wt Lp2A-I ($p<0.05$, student's t-test). Analysis of the Michaelis-Menten kinetics (Fig. 2-7B) indicated that the V_{max} for His-Δ1-43 and His- Δ1-65 Lp2A-I was reduced to 50% and 34%, respectively, relative to His-Wt Lp2A-I ($p<0.05$, student's t-test) (Table 2-2).

Table 2-2: LCAT enzyme kinetics associated with His-Wt, His-Δ1-43 and His-Δ1-65 Lp2A-I substrates. V_{max} and apparent K_m values were determined by Lineweaver-Burk analysis.

	V_{max} (nmol CE/h/unit LCAT[a])	AppK_m[b] (μM)
His-Wt ApoA-I	3.14 ± 0.37	1.62 ± 0.20
His-Δ1-43 ApoA-I	1.56 ± 0.20[c]	3.02 ± 0.34[c]
His-Δ1-65 ApoA-I	1.07 ± 0.18[c]	0.90 ± 0.34

LCAT assays were performed as described in *Materials & Methods* using reconstituted Lp2A-I of initial molar ratios 80:10:1 of PL, FC and apoA-I, respectively. V_{max} and apparent K_m (appK_m) were determined by Lineweaver-Burk analysis. Values represent the mean ± SE.

[a]Unit of LCAT activity was defined as the amount of enzyme required to convert 1 nmol of FC to CE using a standard Lp2A-I containing His-Wt apoA-I at 2 μM.

[b]appK_m for apoA-I

[c]Values which are statistically significant to $p<0.05$ (student's t-test) relative to His-Wt apoA-I.

2.4 *Discussion*

Analysis of apoA-I structure-function relationships is important in understanding HDL metabolism and reverse cholesterol transport. Here the extreme amino-terminus composed of the globular domain (a.a. 1-43) and the first class A amphipathic helix (a.a. 44-65) and their contributions to lipid-binding, cholesterol efflux and LCAT activation were addressed.

His-Δ1-43 and His-Δ1-65 apoA-I were expressed at levels comparable to His-Wt apoA-I in *E. coli*. Some apoA-I mutants used in our laboratory previously are expressed at much lower levels but it is not clear why this is the case. The N-terminal deletion mutants might be expected to express at lower levels as these deletions have been shown previously to significantly disrupt the lipid-free structure of apoA-I. This could have rendered these mutants more susceptible to proteolysis in the bacterium, however, there is no indication this was the case. After the removal of GdnHCl, a significant portion of His-Δ1-43 apoA-I was found to aggregate and precipitate from solution, a property of this mutant shown previously, while His-Δ1-65 and His-Wt apoA-I did not. This may be due to the role of the globular domain in maintaining the lipid-free structure of apoA-I. The transition from lipid-free to lipid-bound structure is thought to involve the exposure of the hydrophobic faces of the helices in apoA-I, previously sequestered within the helix bundle for lipid-binding (reviewed in ref (79)). In solution, a disruption of the helix bundle, exposing the hydrophobic faces, may generate hydrophobic pockets where apoA-I self-associates through hydrophobic interactions. The lipid-free structure of His-Δ1-65 apoA-I has been shown previously to be significantly different than His-Δ1-43 apoA-I and may be such that self-association is not significantly altered by this larger deletion. Thus, we can tentatively

conclude that the G* helix (a.a 8-33) serves to mask the hydrophobic face of helix 1 (a.a. 44-65) in the lipid-free form of apoA-I.

The importance of the C-terminus (a.a. 187-243) of apoA-I in both PL binding and cholesterol efflux has been shown previously (213,237,283), suggesting these 2 properties may be related. In order to determine if either the N-terminal globular domain or helix 1 are involved in cell binding or cellular cholesterol efflux, I compared these properties using cholesterol loaded J774 macrophages and lipid-free His-Wt, His-Δ1-43, His-Δ1-65 and His-Δ210-243 apoA-I. Deletion of the globular domain and helix 1 did not impair the ability of apoA-I to associate with macrophage at 37°C (Fig. 2-3B) or elicit cholesterol efflux (Fig. 2-4, Table 2-1) to an appreciable extent. Interestingly, these observations are inconsistent with studies addressing the ability of individual apoA-I synthetic peptides to elicit cholesterol efflux from human skin fibroblasts (249). From a panel of synthetic peptides modeled after apoA-I helices, only those corresponding to a.a. 44-65, 44-87 and 209-241 were shown to stimulate cholesterol efflux, suggesting a.a. 44-65 are important for this property. However, it is difficult to compare individual helical peptides to apoA-I mutants containing many more amphipathic α-helices. Furthermore, comparison of efflux to apoA-I mutants from macrophage and fibroblast cell lines has yielded conflicting results previously (213,249), suggesting that extrapolation from one cell type to another is not necessarily warranted. Nonetheless, the results here show that the C-terminus of apoA-I is more important than the N-terminus in promoting cholesterol efflux from macrophage.

The amino-terminal deletions were then compared to His-Wt apoA-I with respect to their ability to bind to DMPC liposomes and form reconstituted, discoidal lipoproteins. Both the deletion of the globular domain and the subsequent deletion of helix 1 were associated with significant reductions in the ability of apoA-I to bind PL (Fig. 2-5). The

importance of residues 44-65 was suggested initially by Palgunachari *et al* (212). They demonstrated that from a panel of synthetic peptides modeled after the exon 4 encoded 22-mers of apoA-I (residues 44-243) that only those corresponding to residues 44-65 and 220-241 had significant lipid binding affinity. While initial studies by Segrest *et al.* suggested little PL binding could be attributed to the globular domain of apoA-I (reviewed in ref (188)), Mishra *et al.* showed that a synthetic peptide modeled after residues 1-33 of apoA-I had significant affinity for PL (221). This suggests the globular domain may be an important region for lipid-binding., as the removal of residues 1-43 significantly reduced the rate at which apoA-I binds to DMPC liposomes.

While the initial rate of PL binding was reduced by deletion of the amino-terminus of apoA-I, the structure and stability of reconstituted lipoproteins were minimally affected. The His-Δ1-43 apoA-I mutant was associated with slightly less PL and FC and correlated with a smaller particle size relative to both His-Wt and His-Δ1-65 apoA-I (Fig. 2-6A). This may have been due to the self-aggregation observed for this mutant in solution, which could have altered the association with PL and FC to form discoidal lipoproteins. This did not appear to have a significant effect on the stability of the reconstituted lipoprotein, which exhibited a similar ΔG_D° to Lp2A-Is containing His-Wt and His-Δ1-65 apoA-I (Fig. 2-6B).

Subsequently, we used these reconstituted lipoproteins to address the contribution of the N-terminus to LCAT activation. Deletion of the globular domain of apoA-I has been shown previously to confer a 2-fold reduction in the capacity of apoA-I to activate LCAT (197), however, the role of helix 1 was previously unclear. The effect conferred by the deletion of residues 1-65 of apoA-I was assayed previously using an egg PC vesicular assay (199), however, this study could not differentiate between decreased PL binding and a direct effect of this mutation on LCAT activation. Here, we prepared reconstituted Lp2A-Is with

His-Wt, His-Δ1-43, and His-Δ1-65 apoA-I that were of similar composition and stability, properties that have been shown to affect LCAT activation independently (284). We observed that His-Δ1-43 and His-Δ1-65 apoA-I were associated with 50% and 34% decreases in LCAT activation, respectively, relative to His-Wt apoA-I (Fig. 2-7, Table 2-2). The observation that these deletions affected LCAT activation is intriguing since this property is generally associated with class A helices of the central domain, in particular helix 6 (219,258,259). Recent work suggests that a cluster of 3 Arg residues at the interface of the hydrophilic and hydrophobic faces in helix 6 contributes to a specific locale of positive surface potential that may stimulate LCAT activity (260). Site-specific mutagenesis of these residues conferred 11-12-fold reductions (decrease in V_{max}) in LCAT activation without affecting other physical properties of apoA-I. The current study supports previous work implicating the globular domain of apoA-I in LCAT activation and further suggests that helix 1 may be an important domain for this property, as well.

In summary, this work suggests that although the amino-terminus of apoA-I does contribute to the native lipid-binding properties of apoA-I, it is not involved in cholesterol efflux from macrophage. However, the N-terminus of apoA-I does appear to act as a critical LCAT activating domain.

CHAPTER 3: CONTRIBUTION OF THE AMINO-TERMINUS OF APOLIPOPROTEIN A-I TO THE IN VIVO MATURATION OF HDL

3.1 Summary

Nascent HDL are secreted by hepatocytes, liberated from chylomicrons during TG lipolysis, and are derived from HDL remodeling by hepatic lipase and CETP (reviewed in Section 1.3.3.1). The importance of PLTP in the lipidation of this nascent HDL pool has recently emerged since PLTP deficient mice exhibit defective PL transfer from TG-rich lipoproteins to HDL, reduced HDL levels and increased HDL catabolism (285). Efflux of cholesterol and PL from cells provide nascent HDL with lipid constituents. This step is important for steady-state concentrations of HDL and may be rate-limiting as heterozygous mutations in ABCA1 can cause familial HDL deficiency (118). The combined actions of PLTP and ABCA1 generate larger, discoidal preβ_2 and preβ_3-HDL from the nascent HDL pool. These are converted to spherical α-migrating HDL by the actions of LCAT as newly synthesized CE partitions to the HDL core.

To further define the role of the amino-terminus of apoA-I in HDL maturation, we constructed recombinant adenoviruses containing Wt apoA-I and two similar mutants with deletions of residues 7-43 and 7-65 (referred to as Δ7-43 and Δ7-65 apoA-I). Residues 1-6 were not removed in these mutants to allow proper cleavage of the pro-sequence *in vivo*. Following injection of these adenoviruses into apoA-I deficient mice, both Δ7-43 and Δ7-65 apoA-I were expressed at approximately 4-fold lower levels than Wt apoA-I. A 4-fold greater adenovirus dose for both Δ7-43 and Δ7-65 apoA-I Ad5 resulted in plasma levels 4 days post-injection of these mutants similar to Wt apoA-I. HDL associated with each of these mutants accumulated less CE than Wt apoA-I HDL. Wt and Δ7-43 apoA-I formed predominantly α-migrating and spherical HDL whereas only Δ7-65 apoA-I formed preβ-

HDL of discoidal morphology. This demonstrates that the N-terminus of apoA-I, in particular the first class A helix (a.a. 44-65), is important for the *in vivo* maturation of HDL.

3.2 *Materials and Methods*

3.2.1 Production of 1st Generation Recombinant Adenoviruses

The cDNAs for apoA-I deletion mutants lacking residues 7-43 (Δ7-43 apoA-I) and residues 7-65 (Δ7-65 apoA-I) were subcloned into the pCA13 vector (Microbix Biosystems Inc.). Wt apoA-I Ad5 was generated in our laboratory previously (219). Recombinant adenoviruses (Δ7-43 apoA-I Ad5 and Δ7-65 apoA-I Ad5) were prepared as previously described for the wild-type apoA-I (Wt apoA-I) adenovirus (Wt apoA-I Ad5) (219). Briefly, low passage human embryonic kidney (HEK) 293 cells were co-transfected at 40-60% confluency with 5 μg of the pCA13 + apoA-I constructs and 6.5 μg of pJM17, the plasmid containing the adenovirus genome. Homologous recombination upstream and downstream of the multiple cloning site generated a replication deficient (E1 deleted) adenovirus genome

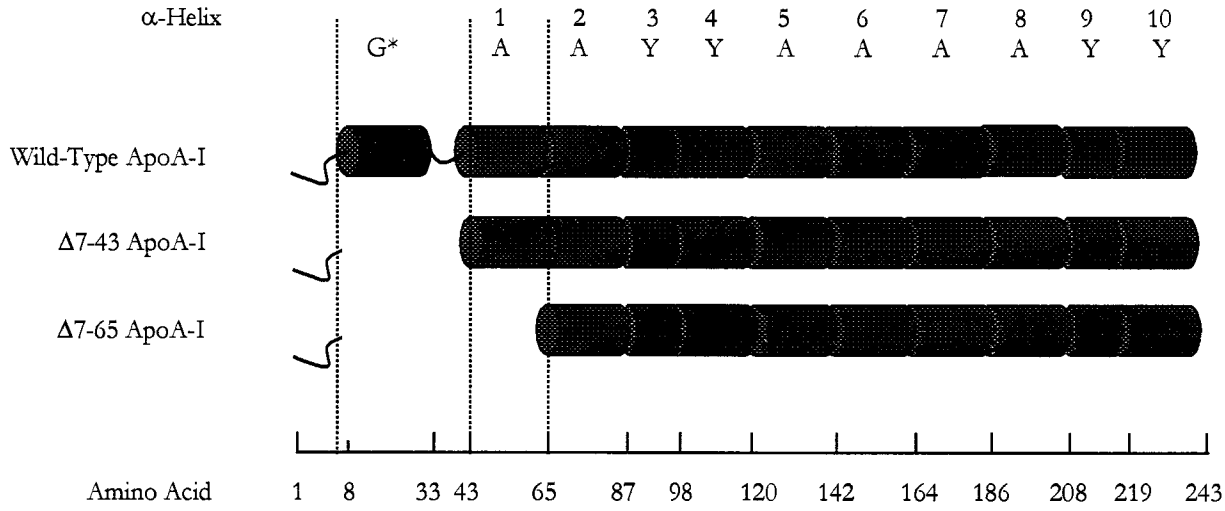

Figure 3-1: Structural Elements of the Mutant ApoA-Is Expressed in ApoA-I Deficient Mice

Deletion of residues 7-43 removes the majority of the globular domain with the exception of residues 1-6, which are thought to adopt an unordered structure (272). The removal of residues 7-65 results in the deletion of the globular domain and of the 1st class A helix (a.a. 44-65).

containing the apoA-I cDNA. Following transfection, cells were overlayed with Eagles's minimal essential medium containing 0.65% SeaPlaque GTG agarose (FMC BioProducts) to isolate individual viral plaques. Post-transfection (6-14 days) viral plaques were isolated and screened by PCR amplification of the apoA-I cDNA. To do this, infected 293 cells were treated with 0.05% pronase (in 10 mM Tris-HCl, pH 7.5, 10 mM EDTA and 0.5% (w/v) SDS) at 37°C for 12 hours. Cell lysates were extracted once with phenol:chloroform:isoamylalcohol (25:24:1, v/v/v) and DNA precipitated from the aqueous phase using 96% ethanol. This was used as a template for PCR amplification of the apoA-I cDNA using upstream and downstream primers annealing to the CMV promoter and non-translated apoA-I sequence, respectively. Positive plaques were scaled-up and purified by CsCl gradient ultracentrifugation. Purified virus was titered by UV absorbance at 260 nm. Purified virus was diluted 1:1 with 0.1% SDS, 10 mM Tris-HCl (pH 7.4) and 1 mM EDTA and incubated at 56°C for 10 min and the concentration of viral particles determined according to the following equation:

Concentration of Viral Stock (Viral Particles/mL) = $(OD_{260}) \times$ (viral dilution) $\times 1.1\times10^{12}$

Simultaneous plaque assays indicated approximately 18 viral particles per pfu, consistent with previous reports.

3.2.2 Animals

ApoA-I deficient ($ApoA1^{tmlUnc}$) mice were obtained from Jackson Laboratories. Mice were maintained on a 12 h light/12 h dark schedule and were fed a normal chow diet (Charles River rodent diet 5075 – 18% protein and 4.5% fat). All experiments were performed in accordance with protocols approved by the University of Ottawa Animal Care Committee. Mice used for these studies were all 4-12 month old males.

3.2.3 Quantification of ApoA-I in Plasma

Following adenovirus injections, plasma apoA-I levels were determined by quantitative Western blotting. Equivalent volumes of plasma were separated by 12% SDS-PAGE and analyzed by Western blot using a polyclonal anti-human apoA-I antibody raised in sheep. The concentrations of Wt apoA-I and the two N-terminal deletion mutants in mouse plasma samples were determined by densitometry and comparison to apoA-I standards of known concentrations using Quantity One software (BioRad). To eliminate the possibility that differential immunoreactivity may under or overestimate the plasma levels of the mutant apoA-Is expressed in the mouse, we compared the immunoreactivity of His-Wt apoA-I with the 2 N-terminal deletion mutants, His-Δ1-43 and His-Δ1-65 apoA-I. Equivalent amounts of the purified histidine-tagged apoA-Is (determined by Markwell and Lowry method (275)) were separated by SDS-PAGE and analyzed by Western blot. A mass range of 0.2-5 μg was used, covering the range in apoA-I mass detected in plasma by this method. The relative intensity was then plotted versus the mass of apoA-I used for His-Wt, His-Δ1-43 and His-Δ1-65 apoA-I (data not shown). The plots were virtually identical indicating that differential immunoreactivity is not a concern in this assay.

3.2.4 Size Exclusion Chromatography

Separation of mouse plasma by size exclusion chromatography (FPLC) was performed as described previously (219). Briefly, 500 μL of mouse plasma was passed through 2 Superdex 200 (analytical grade – Amersham Pharmacia Biotech) columns connected in series. Separation was achieved at a flow rate of 0.1 mL/min and 5 mL fractions were collected. Each fraction was assayed for TC Roche Diagnostics Corp.), FC

and PL content using standard enzymatic kits. Each fraction (100 μL aliquot) was analyzed for apoA-I content by slot blot (BioRad Bio-Dot SF unit) followed by Western blot analysis using a biotinylated A44 monoclonal antibody.

3.2.5 Discontinuous Gradient Ultracentrifugation

ApoA-I deficient mouse plasma samples were separated by discontinuous gradient ultracentrifugation as described previously (219). Samples were centrifuged for 18 h and 210 000×g at 8°C. Fractions (1 mL) were collected from top to bottom and densities were determined by refractometer (Fisher Scientific) analysis. Aliquots of each fraction were dialyzed against PBS (0.025 μm filter disks – Millipore Corp.) and analyzed by SDS-PAGE. Western blot analysis was performed using a polyclonal anti-human apoA-I antibody from sheep.

3.2.6 Electron Microscopy

Negative stain electron microscopy was performed as described by others (50). Briefly, discontinuous gradient samples were dialyzed against 0.125 M ammonium acetate, 2.6 mM ammonium carbonate and 0.26 mM EDTA, pH 7.4 and concentrated to 100-200 μg/mL total protein. Samples were mixed 1:1 with sodium phosphotungstate, pH 7.4 before applying to carbon-coated Formvar grids (200 mesh) and visualized using a Hitachi H-7100 electron microscope at 50 000 and 70 000× magnification.

3.2.7 Electrophoresis and Western Blotting

Please refer to these protocols as outlined in the *Materials and Methods* section of Chapter 2.

3.3 Results

3.3.1 Generation of ApoA-I Recombinant Adenoviruses

The cDNAs for Δ7-43 and Δ7-65 apoA-I were constructed and subcloned into the pCA13 shuttle vector, as previously described for the cDNA encoding Wt apoA-I (219). Sequencing in both in the 5'→ 3' and 3'→5' orientations indicated that both deletions were correct and that no other mutations were present.

Following cotransfection of 293 cells, viral plaques were screened by PCR using primers that annealed in the CMV promoter and distal to the apoA-I stop codon, upstream and downstream of the apoA-I cDNA, respectively. The recombination step confers a reduction in Ad5 genome size, relative to pJM17, which is able to package into the viral capsid.

Potential viral plaques were screened by PCR amplification of the apoA-I cDNA. Electrophoretic separation of the amplified products in 1% agarose revealed the presence and expected size of Wt, Δ7-43 and Δ7-65 apoA-I following ethidium bromide staining (Fig. 3-2). The plaques were scaled-up by repeated infections of 293 cells and purified by cesium chloride ultracentrifugation. The titers of the purified stocks of adenovirus were on the order of $0.5\text{-}2\times10^{11}$ p.f.u./mL.

3.3.2 ApoA-I and Lipid Levels Following Injection of Recombinant Adenoviruses

To explore the role of the N-terminus of apoA-I *in vivo*, we used recombinant adenovirus constructs to transiently express similar concentrations of Wt apoA-I and two N-terminal mutants (Δ7-43 and Δ7-65 apoA-I Ad5) in apoA-I deficient mice. Residues 1-6

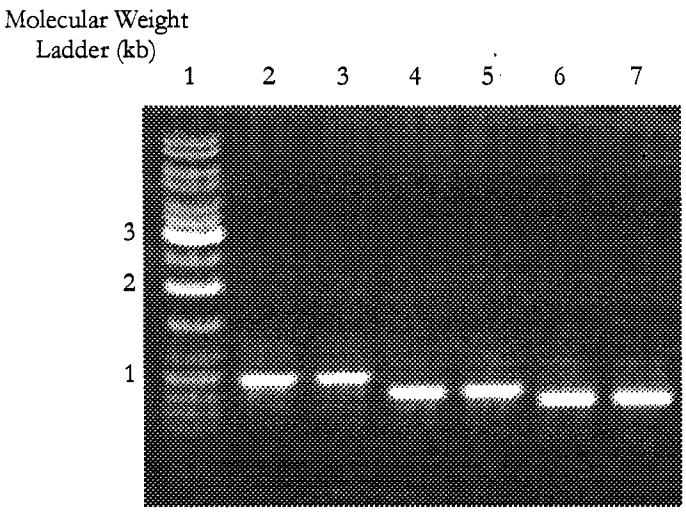

Figure 3-2: PCR Amplification of ApoA-I cDNAs from 293 Cells Infected with Potential Wt, Δ7-43 and Δ7-65 ApoA-I Adenoviruses

HEK 293 cells infected with potential Wt, Δ7-43 and Δ7-65 apoA-I recombinant adenoviruses were lysed by treatment with 0.05% pronase. Cell lysates were treated with phenol:chloroform:isoamylalcohol and DNA in the aqueous phase subject to ethanol precipitation. PCR amplification of the apoA-I transgene indicated that cDNAs of the expected size for Wt (lanes 2 and 3), Δ7-43 (lanes 4 and 5) and Δ7-65 (lanes 6 and 7) were cloned into their respective recombinant adenoviruses.

were maintained to allow proper cleavage of the hexapeptide pro-sequence *in vivo* (see discussion). We have previously shown that apoA-I deficient mice express high levels of human apoA-I following tail vein administration of 2×10^9 p.f.u. of the recombinant adenovirus (219). To determine the expression levels of Δ7-43 and Δ7-65 apoA-I relative to Wt apoA-I, sex and age matched mice were injected with 2×10^9 p.f.u. of each respective adenovirus. Analysis of plasma lipid levels at various time points post-injection indicated that injection of this adenovirus dose was not associated with increases in plasma lipid levels above background for Δ7-43 and Δ7-65 apoA-I (Fig. 3-3). Analysis of fasting plasma samples 4 days post-injection indicated that Δ7-43 (Fig.3-4, lane 4) and Δ7-65 (Fig. 3-4, lane 6) apoA-I were expressed at approximately 4-fold lower levels than Wt apoA-I (Fig. 3-4, lane 3). In order to attain plasma levels of Δ7-43 and Δ7-65 apoA-I comparable to Wt apoA-I, a

4-fold greater dose (8×10^9 p.f.u.) of the Δ7-43 and Δ7-65 apoA-I Ad5 was used. We have shown previously that injection of up to 1×10^{10} p.f.u. of a luciferase Ad5 is not itself

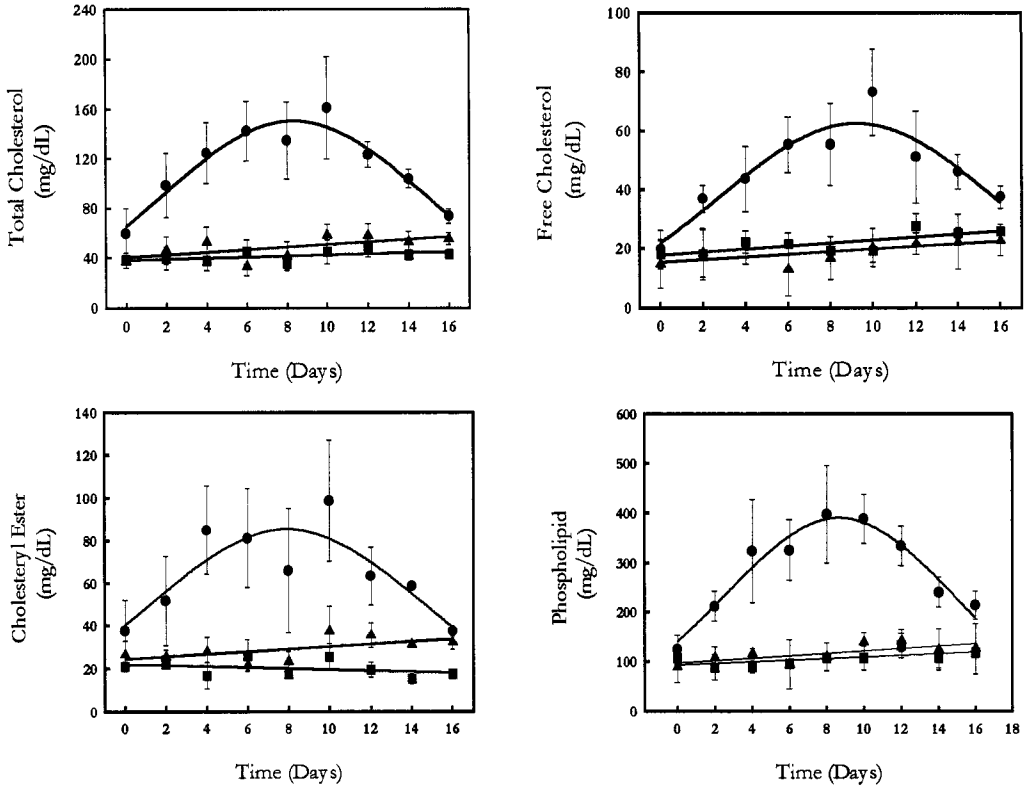

Figure 3-3: Plasma Lipid Levels in ApoA-I Deficient Mice Post-Injection with Wt, Δ7-43 and Δ7-65 ApoA-I Adenoviruses

ApoA-I deficient mice were injected with 2×10^9 p.f.u. of Wt (●), Δ7-43 (▲) and Δ7-65 (■) apoA-I Ad5 and the plasma total cholesterol, FC, CE and PL levels determined using standard enzymatic kits.

associated with short- term changes in plasma lipid levels relative to non-injected mice (219). This is corroborated by others using similar adenovirus control vectors (286,287). Injecting 8×10^9 p.f.u. of the Δ7-43 (Fig. 3-4, lane 5) and Δ7-65 (Fig. 3-4, lane 7) apoA-I Ad5 resulted in plasma apoA-I levels comparable to Wt apoA-I and this dose was used for all subsequent experiments. Analysis of plasma lipid levels (Table 3-1) indicated that TC, FC and PL concentrations were increased significantly ($p<0.05$, student's t-test) for Wt, Δ7-43 and Δ7-65 apoA-I above those of non-injected controls. CE levels were increased ($p<0.05$,

student's t-test) above background for Wt and Δ7-43 apoA-I but not for Δ7-65 apoA-I. The plasma CE/TC ratios in mice expressing Δ7-43 (0.49 ± 0.12) and Δ7-65 (0.25 ± 0.20) apoA-I

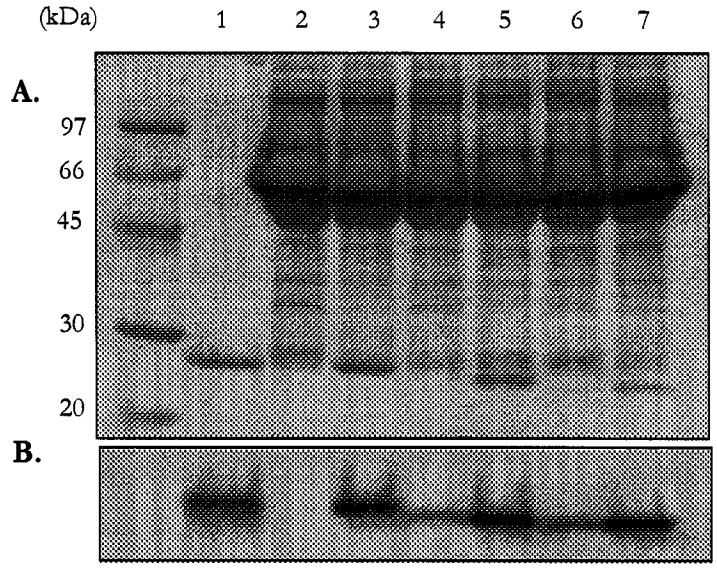

Figure 3-4: Relative Expression of Wt, Δ7-43 and Δ7-65 ApoA-I in ApoA-I Deficient Mouse Plasma Following Adenovirus Injection.

ApoA-I deficient mice were injected with 2×10^9 pfu of Wt apoA-I Ad5 (lane 3), 2×10^9 and 8×10^9 pfu of Δ7-43 apoA-I Ad5 (lanes 4 and 5, respectively) and 2×10^9 and 8×10^9 pfu of Δ7-65 apoA-I Ad5 (lanes 6 and 7, respectively). Equal volumes of plasma were separated by 12% SDS-PAGE and visualized by Coomassie blue staining (A) and anti-human apoA-I Western blotting using a polyclonal antibody from sheep (B). A human apoA-I standard and non-injected apoA-I deficient mouse plasma are shown in lanes 1 and 2, respectively.

significantly reduced relative to those expressing Wt apoA-I.

3.3.3 FPLC Analysis of Wt, Δ7-43 and Δ7-65 apoA-I containing HDL

Fasting plasma samples from apoA-I deficient mice 4 days post-injection with 2×10^9 p.f.u. of Wt apoA-I Ad5 or 8×10^9 p.f.u. of Δ7-43 and Δ7-65 apoA-I Ad5 were separated by size exclusion chromatography. Individual fractions were assayed for TC content (Fig. 3-5A) and relative apoA-I distribution by slot blot analysis (Fig. 3-5B). This indicates that Wt, Δ7-

43 and Δ7-65 apoA-I associate with lipoproteins of HDL size. In each case, the plasma lipoprotein size distribution is shifted to a similar extent for each of these apoA-I proteins

Table 3-1: ApoA-I, cholesterol (total, free and esterified) and phospholipid levels were determined 4 days post-injection with apoA-I recombinant adenoviruses.

	ApoA-I	TC	FC	CE	PL	CE/TC
			mg/dL			
None (n=3)	-	42 ± 6[b]	25 ± 5[b]	16 ± 3[b]	106 ± 40[b]	0.39 ± 0.07[b]
Wt ApoA-I† (n=5)	294 ± 40	125 ± 24[a]	44 ± 9[a]	81 ± 22[a]	226 ± 38[a]	0.64 ± 0.07[a]
Δ7-43 ApoA-I‡ (n=5)	287 ± 63	102 ± 25[a]	53 ± 19[a]	50 ± 16[a,b]	201 ± 49[a]	0.49 ± 0.12[b]
Δ7-65 ApoA-I‡ (n=3)	278 ± 41	83 ± 4[a,b]	62 ± 13[a]	21 ± 17[b]	211 ± 18[a]	0.25 ± 0.20[b]

2×10^9 pfu (†) or 8×10^9 pfu (‡) of recombinant adenovirus was injected and the mouse plasma sampled 4 days post-injection following a 10 h fast. All mice were male apoA-I deficient mice 6-10 months of age. ApoA-I, TC, FC and PL levels were determined as described in *Materials & Methods*. Plasma CE concentrations were taken as the difference between TC and FC levels. Values represent the mean ± SE.

[a]Values significantly different ($p<0.05$, student's t-test) than non-injected mice.

[b]Values significantly different ($p<0.05$, student's t-test) than Wt apoA-I Ad5 injected mice.

relative to that of the non-injected apoA-I deficient mouse (Fig. 3-5A). The shift in HDL size relative to the non-injected mouse was due to the replacement of apoE with apoA-I on these HDL. We have shown previously that *de novo* expression of Wt apoA-I reduces plasma concentrations of apoE in the apoA-I deficient mouse following adenovirus administration (219) and appears to occur to similar extents for Wt, Δ7-43 and Δ7-65 apoA-I (Fig. 3-5A, inset). Despite lower plasma cholesterol levels associated with Δ7-43 and Δ7-65 apoA-I,

HDL and apoA-I distributions were not significantly altered as compared to Wt apoA-I. In addition, Wt, Δ7-43 and Δ7-65 apoA-I did not associate with a lipid-free/poor pool (fractions 26-28) as all detectable apoA-I co-localized with the HDL cholesterol peak.

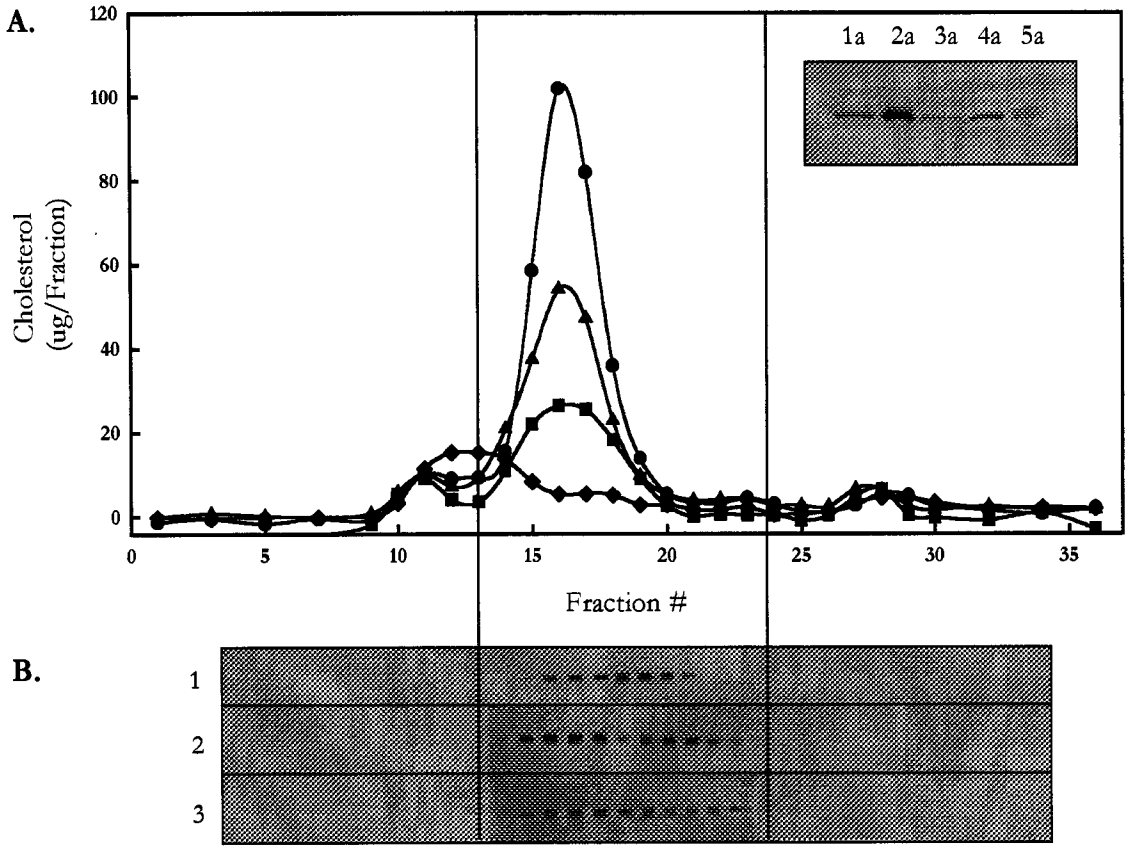

Figure 3-5: Analysis of Wt, Δ7-43 and Δ7-65 ApoA-I Containing HDL by Size Exclusion Chromatography.

ApoA-I deficient mouse plasma 4 days post-injection with 2×10^9 pfu of Wt apoA-I Ad5 (● and 1), 8×10^9 pfu of Δ7-43 apoA-I Ad5 (▲ and 2) and 8×10^9 pfu of Δ7-65 apoA-I Ad5 (■ and 3) was separated by size exclusion chromatography (see *Materials and Methods*). Individual fractions were sampled for TC content (A) and apoA-I distribution by slot blot analysis followed by anti-human apoA-I Western blotting using the A44 monoclonal antibody (B). In addition, the FPLC cholesterol profile of non-injected apoA-I deficient mouse plasma is shown (♦). The inset shows a Western blot of mouse plasma apoE before (lane 2a) and 4 days post-injection with Wt (lane 3a), Δ7-43 (lane 4a) and Δ7-65 (lane 5a) apoA-I Ad5. Relative expression of apoE in wild-type C57BL/6J mice not injected with adenovirus is shown for reference (lane 1a).

Subsequently, the TC, FC, CE and PL content in FPLC fractions corresponding to HDL size were normalized to the respective apoA-I concentrations. As compared to Wt apoA-I

HDL, Δ7-43 and, more markedly, Δ7-65 apoA-I HDL contained less TC, on average, per HDL particle (Fig. 3-6A). This is predominantly due to a reduced CE content for Δ7-43

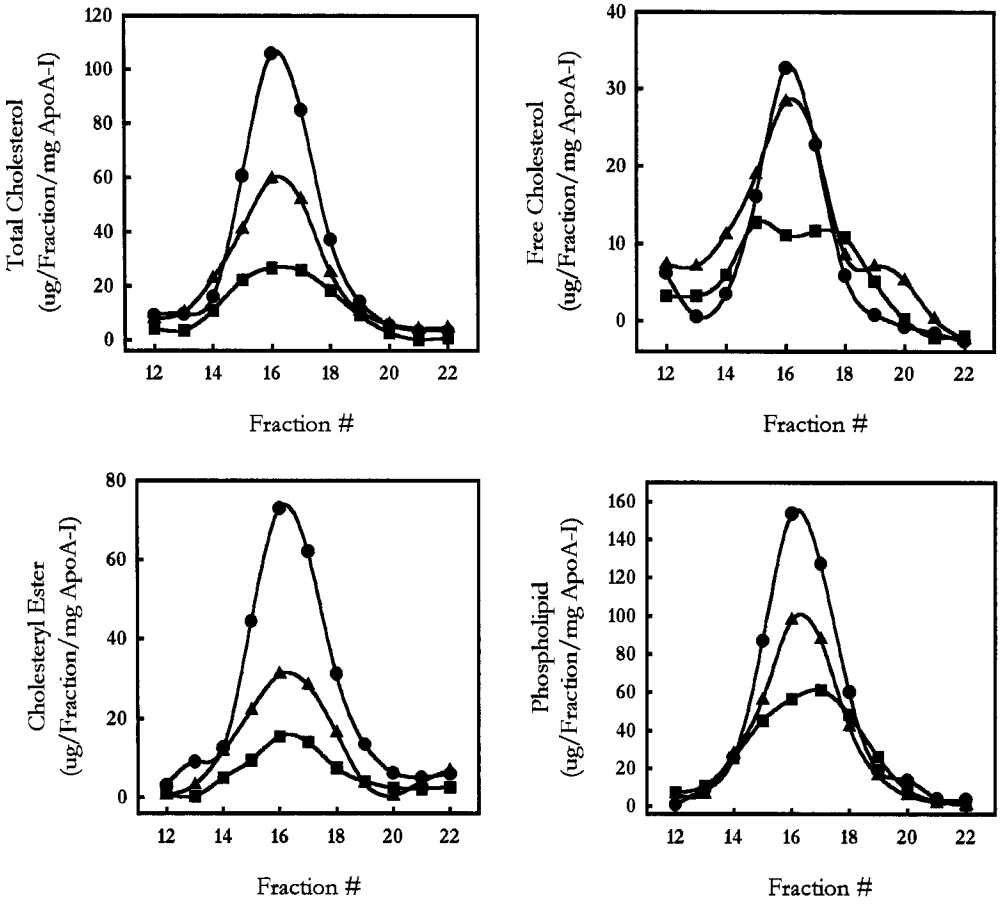

Figure 3-6: Relative Lipid Composition of Wt, Δ7-43 and Δ7-65 ApoA-I HDL

TC (A), FC (B), CE (C) and PL (D) levels in FPLC fractions corresponding to HDL size were normalized to the respective apoA-I protein mass. The resultant profiles represent the relative lipid content of HDL containing Wt (●), Δ7-43 (▲) and Δ7-65 (■) apoA-I. The lipid measurements were done using enzymatic kits (see *Materials and Methods*).

and, more markedly, Δ7-65 apoA-I HDL as compared to Wt apoA-I HDL (Fig. 3-6C). Furthermore, Wt apoA-I HDL contained more PL than Δ7-43 or Δ7-65 apoA-I HDL (Fig. 3-6D), however, this reduction was proportionately less than that observed for CE.

3.3.4 Agarose and PAGGE Separation of Wt, Δ7-43 and Δ7-65 ApoA-I HDL

Mouse plasma samples were isolated 4 days following injection of either the Wt, Δ7-43 or Δ7-65 apoA-I Ad5. The relative amounts of preβ- and α-HDL associated with each of the apoA-I proteins were evaluated by agarose gel electrophoresis. HDL were visualized either by neutral lipid staining (Fig. 3-7A) or Western blot analysis with an anti-human apoA-I monoclonal antibody (Fig. 3-7B). Two independent apoA-I Ad5 injections are shown in each panel and are representative of 4 separate injections. Expression of Wt apoA-I was associated with high levels of α-migrating neutral lipid staining (Fig. 3-7A, lanes 3, 4) and was consistent with the position of Wt apoA-I by Western blot (Fig. 3-7B, lanes 3, 4). Δ7-43 apoA-I associated HDL migrated predominantly to the α-position (Fig. 3-7B, lanes 5, 6) and accumulated significant levels of neutral lipid (Fig. 3-7A, lanes 5, 6), although less than observed for Wt apoA-I. In addition, Δ7-43 apoA-I formed more preβ-HDL than was observed for Wt apoA-I. Strikingly, Δ7-65 apoA-I formed only preβ-HDL as demonstrated by Western blot analysis (Fig. 3-7B, lanes 7, 8) and neutral lipid staining (Fig. 3-7A, lanes 7, 8) (no α-migrating HDL detected).

Non-denaturing PAGGE was next used to determine the size of HDL formed with Wt, Δ7-43 and Δ7-65 apoA-I. Wt (Fig. 3-7C, lanes 3, 4) and Δ7-43 (Fig. 3-7C, lanes 5, 6) apoA-I formed 2 distinct HDL pools (10.1 – 10.7 nm and 8.8 – 9.9 nm) similar in size to each other and to a human HDL standard (10.3 – 11.0 nm and 8.8 – 9.9 nm) (Fig. 3-7C, lanes 1). In contrast, Δ7-65 (Fig. 3-7C, lanes 7, 8) apoA-I formed a more heterogeneous HDL population. The predominant species was of similar size to Wt and Δ7-43 apoA-I HDL (10.3 nm) but included additional species of 11.6 nm, 11.1 nm, 9.4 nm and 8.8 nm in diameter.

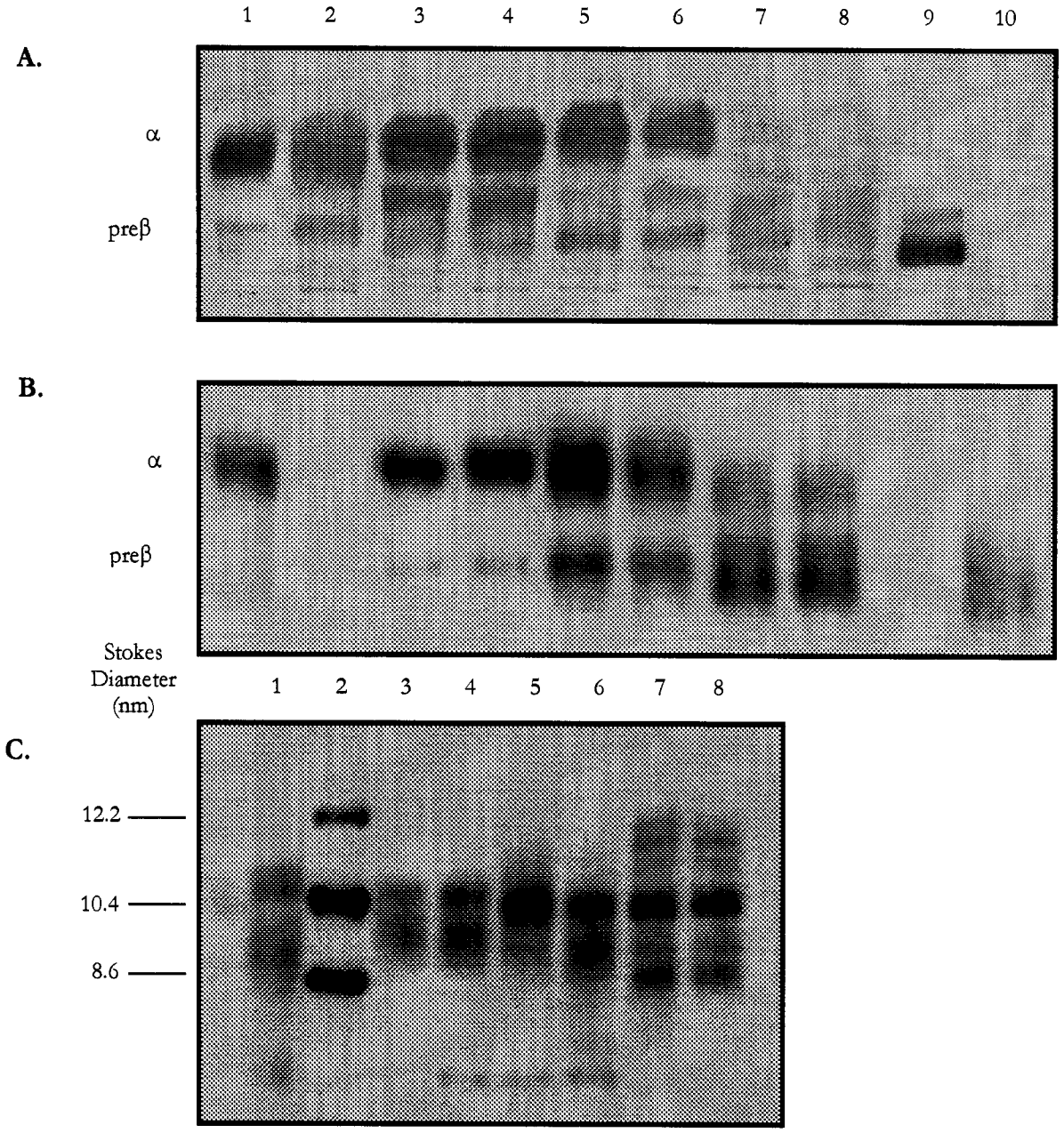

Figure 3-7: Characterization of Wt, Δ7-43 and Δ7-65 ApoA-I HDL by Agarose and Non-Denaturing PAGGE

(A, B) Mouse plasma 4 days post-injection with Wt (lanes 3, 4), Δ7-43 (lanes 5, 6) and Δ7-65 (lanes 7, 8) apoA-I Ad5 were separated by agarose electrophoresis and visualized by neutral lipid staining (A) and anti-apoA-I Western blotting (B) using the biot-A44 mAb. Human HDL (lane 1), non-injected apoA-I deficient mouse plasma (lane 2), human LDL (lane 9) and wild-type apoA-I (lane 10) are shown for reference.

3.3.5 Effect of Apo-I N-Terminal Deletions on HDL Morphology

ApoA-I deficient mouse plasma 4 days post-injection with 2×10^9 p.f.u. of Wt apoA-I Ad5 and 8×10^9 p.f.u of Δ7-43 and Δ7-65 apoA-I Ad5 was separated by discontinuous density gradient ultracentrifugation (Fig. 3-8). The density distributions of Wt, Δ7-43 and Δ7-65 apoA-I HDL were very similar with Δ7-65 apoA-I HDL shifted to a peak density of 1.12 g/mL relative to Wt and Δ7-43 apoA-I HDL at 1.06-1.09 g/mL. The morphology of these HDL particles was determined by negative stain electron microscopy. Wt apoA-I HDL (Fig. 3-9B) exhibited a typical hexagonal packing array characteristic of spherical HDL.

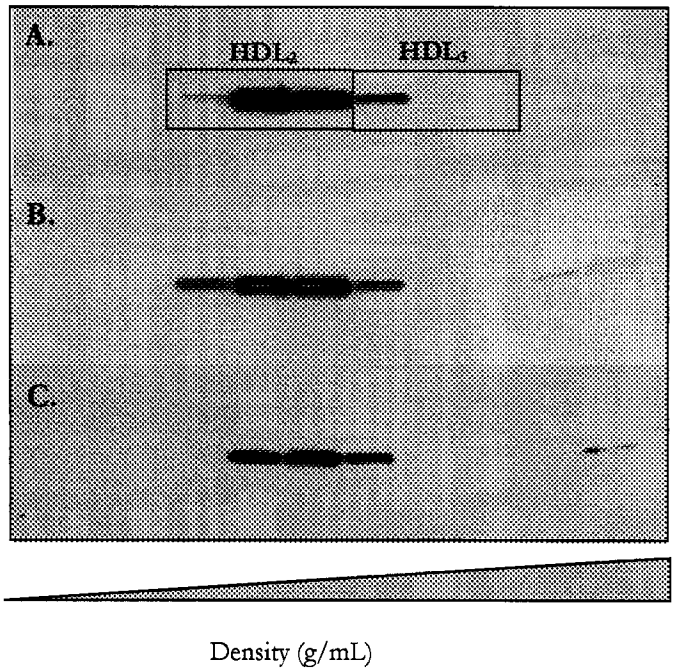

Figure 3-8: Density Separation of ApoA-I Deficient Mouse Plasma 4 Days Post-Injection with Wt, Δ7-43 and Δ7-65 ApoA-I Ad5.

ApoA-I deficient mice were injected with either 2×10^9 p.f.u. of Wt (A) apoA-I Ad5 or 8×10^9 p.f.u. of Δ7-43 (B) and Δ7-65 (C) apoA-I Ad5 and the plasma collected 4 days post-injection in the fasted state. Plasma samples were separated by gradient ultracentrifugation and individual gradient samples were further subject to 12% SDS-PAGE. A Western blot using a sheep polyclonal anti-human apoA-I antibody of the electrophoretic separation is shown.

HDL associated with Δ7-43 (Fig. 3-9C, D) apoA-I were predominantly spherical and comparable in size to Wt apoA-I HDL, although some discoidal HDL were present. In contrast, expression of Δ7-65 (Fig. 3-9E, F) apoA-I was consistently associated with abnormal HDL morphology. These lipoproteins presented as 'rouleaux' of stacked structures characteristic of discoidal HDL. These discoidal particles were absent in non-injected (not shown) and luc-Ad5 apoA-I deficient mice (Fig. 3-9A), which demonstrates that these HDL formed as a consequence of expressing this mutant apoA-I.

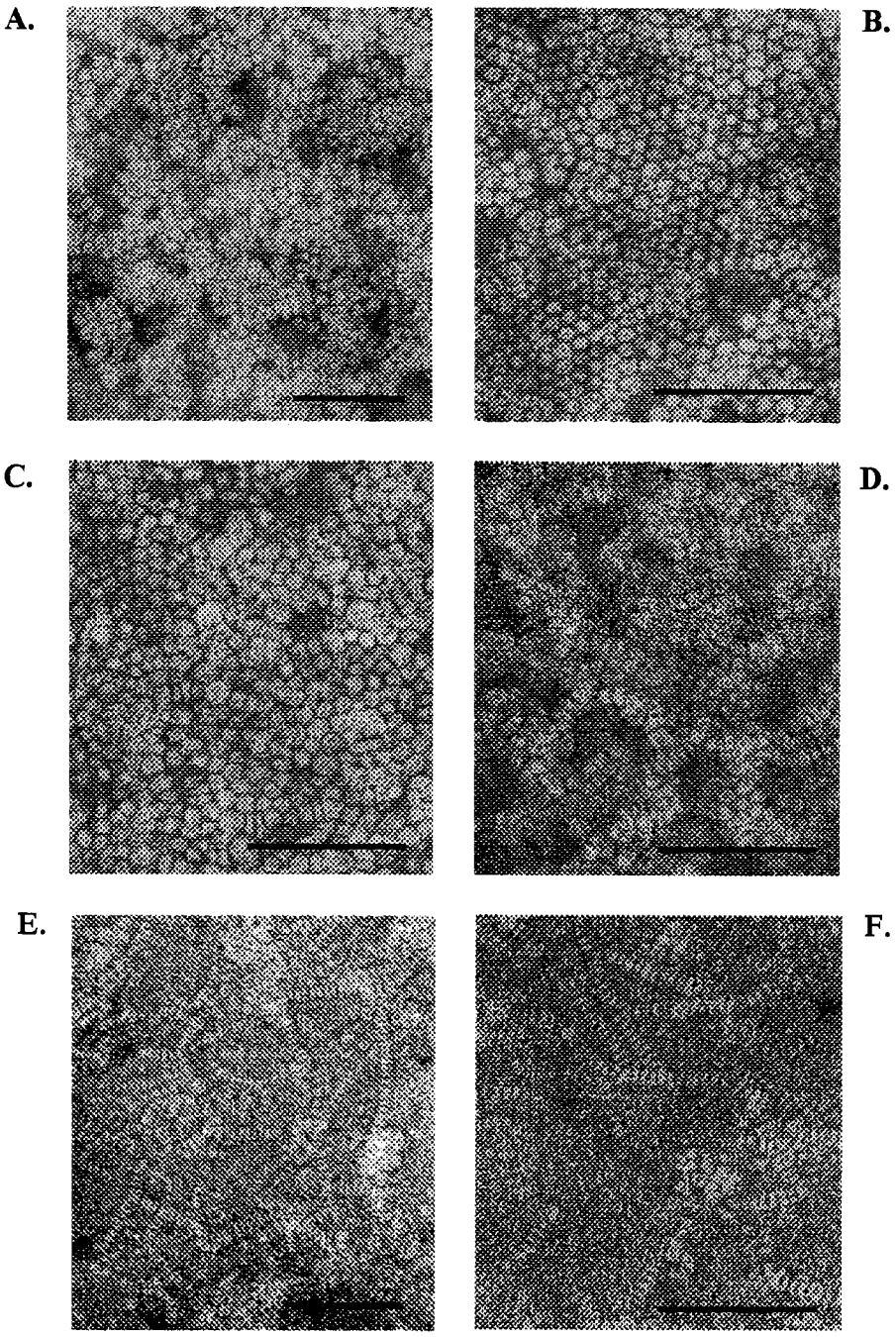

Figure 3-9: Effect of ApoA-I N-terminal Deletions on HDL Morphology

ApoA-I deficient mouse plasma HDL formed 4 days post-injection with luc- (panel A, ρ=1.09g/mL), Wt (panel B, ρ=1.06 g/mL), Δ7-43 (panel C, ρ=1.06 g/mL) (panel D, ρ=1.09 g/mL) and Δ7-65 (panel E and F, ρ=1.12g/mL) apoA-I Ad5 were isolated by discontinuous gradient ultracentrifugation and visualized by negative stain electron microscopy as described in *Materials and Methods*. The bar in each panel represents 100 nm. Electron micrographs were taken at 50 000X magnification in panels A and E whereas panels B, C, D and F were taken at 70 000X magnification.

3.4 Discussion

The use of animal models to corroborate apoA-I structure-function relationships observed *in vitro* has been described previously. To further address the contribution of the globular domain and helix 1 of apoA-I in HDL metabolism, we expressed Wt, Δ7-43 and Δ7-65 apoA-I in apoA-I deficient mice by adenovirus-mediated gene transfer. ApoA-I is secreted as a proprotein containing 6 additional residues at the N-terminus that are removed by a putative metalloprotease which recognizes residues -2 to +4 and cleaves the pro-sequence thereby generating the mature protein (167). Therefore, residues 1-6 were not removed when constructing the cDNAs for *in vivo* expression to enable proper processing of these mutants. Plasma concentrations of Δ7-43 and Δ7-65 apoA-I were decreased 4-fold relative to Wt apoA-I when compared 4 days post-injection with 2×10^9 p.f.u. of recombinant adenovirus (Fig. 3-4). We have previously shown that deletions of residues 100-143, 122-165, 144-186 (219) and 210-243 (unpublished observations) also result in significantly lower levels of these apoA-I mutants in plasma following adenovirus-mediated expression. In the current study, this was not due to impaired secretion as pulse-chase analysis indicated that both mutants were secreted as efficiently as Wt apoA-I from primary apoA-I deficient hepatocytes (data not shown). The lower expression of Δ7-43 and Δ7-65 apoA-I may result from decreased stability of these proteins in the lipid-free form as similar deletions have been shown to significantly alter the conformation of apoA-I in solution (199). Alternatively, reduced PL binding affinity may account for this observation as this property associates with a greater fractional catabolic rate amongst some apoA-I mutants (214). Injection of a 4-fold greater dose of the Δ7-43 and Δ7-65 apoA-I Ad5 resulted in plasma levels of these proteins similar to Wt apoA-I (Fig. 3-4, Table 3-1). Analysis of plasma lipid

concentrations indicated that the CE/TC ratio for both the Δ7-43 and, more markedly, Δ7-65 apoA-I Ad5 injected mice was significantly reduced relative to Wt apoA-I Ad5. This observation corroborates our *in vitro* observations as the deletion of these residues decreases LCAT activation. The size distribution of the lipoproteins formed by these mutants was analyzed by size exclusion chromatography (Fig. 3-5) and demonstrated that Wt, Δ7-43 and Δ7-65 apoA-I were associated exclusively with lipoproteins of HDL size. This indicates the plasma CE/TC ratios discussed previously are representative of HDL composition.

Analysis of HDL by agarose gel electrophoresis (Fig. 3-7A, B) indicated both Δ7-43 and Δ7-65 apoA-I formed progressively more preβ-HDL as compared to Wt apoA-I. However, unexpectedly based on our *in vitro* observations addressed in Chapter 2, Δ7-65 apoA-I was unable to form α-migrating HDL. Davidson and coworkers characterized the molecular basis governing the surface charge of preβ- and α-migrating HDL (29). They found the greatest contributors were phosphatidylinositol content and the presence of a neutral lipid ester core. While the lipid core does not directly contribute to the lipoprotein charge, conformational changes in the surface apolipoproteins are believed to confer this effect. The increases in preβ-HDL and reductions in α-migrating HDL associated with Δ7-43 and Δ7-65 apoA-I HDL might be linked to a gradual impairment in LCAT activation with progressive deletion of the N-terminus. This postulate is supported by the progressive loss of HDL-CE content associated with these apoA-I deletions.

Analysis of HDL size by non-denaturing PAGGE indicated that Δ7-65 apoA-I HDL were significantly more heterogeneous in size than either Wt or Δ7-43 apoA-I HDL (Fig. 3-7C). In human plasma, preβ-HDL constitutes 4–14% of total HDL and consists of $preβ_1$, $preβ_2$ and $preβ_3$ subtypes (reviewed in ref (15)). $Preβ_1$-HDL are on average 5.6 nm in

diameter and are considered the initial acceptors of cellular FC. Preβ_2 and preβ_3 -HDL have greater FC and PL contents and are significantly larger, in the range of 10-14 nm in diameter. Furthermore, preβ-HDL contains little, if any, CE, which associates with α-migrating $HDL_{2/3}$. Δ7-65 apoA-I HDL corresponded to preβ_2/preβ_3 in size and suggests that HDL maturation may be impaired at the level of conversion of these subtypes to α-migrating HDL.

Electron microscopic analysis of HDL formed by these mutants (Fig. 3-9) indicated Δ7-65 apoA-I formed exclusively stacked 'rouleaux' of discoidal HDL while Δ7-43 and Wt apoA-I formed predominantly spherical HDL with typical hexagonal packing arrays. The appearance of discoidal HDL associated with Δ7-65 apoA-I was anticipated based upon a drastically reduced CE/TC ratio in the plasma and predominant preβ- migration on agarose gels.

In summary, this work demonstrates that the N-terminus of apoA-I is important for the *in vivo* maturation of HDL. Deletion of the globular domain alone reduces plasma apoA-I levels and reduces the CE content of HDL. The additional deletion of residues 44-65 further reduces the CE content of HDL and impairs the ability of apoA-I to form spherical HDL.

CHAPTER 4: CONCLUSIONS

The use of naturally-occurring and engineered mutations, synthetic peptides, monoclonal antibodies, proteolytic digestion and chemical modification have been employed to delineate apoA-I structure-function relationships. However, to date most studies have addressed the role(s) of helices in the central (residues 100-186) and C-terminal (residues 187-243) domains while the involvement of the N-terminus remains poorly understood.

The globular domain (residues 1-43) is encoded in exon 3 while the remainder of apoA-I is derived from exon 4, providing rationale at the genomic level for considering this region independently from the rest of the protein structure. This region contains an amphipathic α-helix (residues 8-33) of the G* class and differs from the helices in the rest of apoA-I, which are of class A and Y (188). While G* helices have reduced lipid-binding affinity relative to class A or Y, analysis of a synthetic peptide analogous to residues 1-33 of apoA-I indicates these residues have moderate affinity for phospholipid relative to other apoA-I peptides (221). G* helices are present within 5 of the 7 exchangeable apolipoproteins: apoA-I, apoA-IV, apoC-II, apoC-III and apoE. A Δ1-43 apoA-I has been described previously (189,197,199,220). These studies suggest that the globular domain is involved in the maintainance of the lipid-free conformation of apoA-I, which has been proposed to constitute a helical bundle encompassing residues 1-187 in tryptophan fluorescence (288) and limited proteolysis (195) experiments. Proposing this mutant may adopt a conformation in solution analogous to the lipid-bound form, it was subsequently crystallized by Borhani *et al.* to determine the lipid-bound topology of apoA-I (189). The X-ray crystal structure suggests that apoA-I wraps around the periphery of the HDL particle perpendicular to the phospholipid fatty-acyl chains, an orientation referred to as the 'belt' model. However, deletion of these residues also confers a 2-fold reduction in the ability of

apoA-I to activate LCAT suggesting functional properties of this mutant may be affected as well.

The importance of helix 1 (residues 44-65) for PL association has been shown previously (212,220). Using synthetic peptides modeled after repeating 22-mer domains of apoA-I, Palgunachari *et al.* demonstrated that only N- and C- terminal peptides corresponding to residues 44-65 and 220-241 were able to clarify DMPC liposomes implicating both the N-and C-terminus in PL binding (212). Characterization of a Δ1-65 apoA-I deletion mutant using POPC vesicular binding assay suggested this protein had significantly less lipid affinity relative to Wt and Δ1-43 apoA-I. However, the contribution of this helix to cholesterol efflux, LCAT activation and the *in vivo* maturation of HDL has not been determined.

Several naturally-occurring mutations in the N-terminus of apoA-I have been described (reviewed in refs (78)), however, their effects on HDL metabolism have not been well characterized. ApoA-I Iowa ($Gly^{26}\rightarrow Arg$) is associated with hereditary systemic amyloidosis (289), low plasma levels of HDL and apoA-I and has been shown to have enhanced catabolism when infused into normal subjects (290). This mutation lies within the G* helix in the globular domain, suggesting that disruption of this helix alters structural and/or functional properties of apoA-I. Point-mutations in helix 1 have also been identified (291-293). Unfortunately, it appears that the effects of these mutations on apoA-I and HDL levels have not been fully reported. As amyloidogenic mutations are proposed to perturb structural properties of apoA-I, a detailed analysis of these mutants may clarify the role(s) of these helical domains in HDL metabolism. Furthermore, Booth and coworkers reported a novel apoA-I deletion/insertion where residues 60 to 71 were deleted and replaced by single

valine and threonine residues, disrupting a portion of helix 1 (294). This mutant was associated with significantly lower apoA-I and HDL levels.

Therefore, limited analysis of naturally occurring mutations in the N-terminus of apoA-I suggests more detailed studies are warranted to delineate functional properties associated with this region. We have evaluated the contribution of the globular domain (a.a. 1-43) and the first class A amphipathic α-helix (a.a. 44-65) in HDL maturation both *in vitro* and *in vivo*.

In Chapter 2 we demonstrated that deletion of the amino-terminus greatly reduced the ability of apoA-I to bind PL and to activate LCAT without affecting cholesterol efflux. The contribution of the globular domain and helix 1 to the native-lipid binding properties of apoA-I is consistent with previous studies using synthetic apoA-I peptides. In particular, the involvement of residues 44-65 in the initial phases of PL binding is well established, in which the two end helices of apoA-I are thought to mediate this interaction. Gillotte *et al.* have also suggested that the association of apoA-I with cell membranes may also be mediated by these helices and may facilitate the acquisition of membrane PL and cholesterol (249). This hypothesis is not supported by our work, which indicates that cell association and cholesterol efflux is not dependent upon the presence of residues 44-65. A potential importance of the G* domain in PL binding is not well established but is suggested by this work. The reduced rate of DMPC clearance may be due to the affect of this deletion on apoA-I conformation and an effect of PL binding may be secondary. Okon *et al.* have suggested the G* helix, because of its moderate lipid affinity and the fact that it is separated from the rest of the protein by 11 residues of unordered structure, may be capable of dissociating from the HDL surface for interaction with cell surface receptors, lipid transfer protein or lipolytic enzymes (272). This hypothesis has yet to be corroborated by any

functional data. Clearly the deletion of the extreme N-terminus of apoA-I reduced the capacity of apoA-I to activate LCAT. This effect was conferred by both the deletion of residues 1-43 and the subsequent removal of residues 44-65. Rogers *et al.* have also demonstrated that the globular domain of apoA-I is involved in LCAT activation and observed a similar reduction of approximately 2-fold in the V_{max} (197). The observation that deletion of helix 1 affects LCAT activation is novel as previous work by Rogers *et al.* was unable to differentiate between lipid-binding affinity and LCAT activation (197). Our work suggests that the extreme amino-terminus of apoA-I differs significantly from both the central (a.a. 100-186) and C-terminal (a.a. 187-243) domains because only the deletion of the N-terminus affects both phospholipid binding and LCAT activation.

In order to evalutate the importance of the amino-terminus of apoA-I for the *in vivo* maturation of HDL, we generated recombinant adenovirus vectors for the transient expression of Wt, Δ7-43 and Δ7-65 apoA-I in apoA-I deficient mice. We observed that these deletions did not affect the secretion rate of apoA-I from primary apoA-I deficient hepatocytes (data not shown) but did result in a 4-fold reduction in plasma apoA-I levels 4 days post-injection relative to Wt apoA-I. Injection of a 4-fold greater adenovirus dose for the 2 mutants resulted in similar plasma levels of apoA-I, however, the plasma CE/TC ratio was greatly reduced for Δ7-43 and, more markedly, Δ7-65 apoA-I injected mice. Δ7-65 apoA-I associated HDL were found to be predominantly preβ- migrating while Δ7-43 and Wt apoA-I HDL were mostly α- migrating. This was corroborated by electron microscopic examination, which revealed that Δ7-65 apoA-I HDL were of discoidal morphology whereas Δ7-43 and Wt apoA-I HDL were spherical. As opposed to the *in vitro* studies of Chapter 2, the *in vivo* model suggests that the further deletion of residues 44-65 significantly disrupted

physical and/or functional properties of apoA-I resulting in the inability to form mature α-HDL.

The *in vitro* studies suggest that the reduced CE content of HDL containing Δ7-43 or Δ7-65 apoA-I HDL observed *in vivo* can be attributed to a reduced capacity of these mutants to activate LCAT. Furthermore, the effect conferred by the deletion of residues 7-65 on HDL morphology seems far greater than might be predicted based solely on a reduced capacity to activate LCAT. It is conceivable that the first class A helix, based on its high lipid-binding affinity, may also indirectly contribute to the CE enrichment of HDL, such as stabilizing apoA-I during the conversion of $pre\beta_{2,3}$-HDL to spherical, α-migrating HDL.

In summary, we have shown that the globular domain (a.a. 1-43) and helix 1 (a.a. 44-65) of apoA-I are important for HDL maturation *in vivo*. Removal of the globular domain alone decreases plasma apoA-I levels and significantly reduces the cholesterol content of HDL (and lowers the CE/TC ratio). This supports current and previous *in vitro* findings that the globular domain is involved in LCAT activation and suggests this domain contributes to steady-state concentrations of HDL. The subsequent deletion of residues 44-65 further reduces the ability of apoA-I to activate LCAT *in vitro*. A reduced capacity to activate LCAT directly may account for the inability of Δ7-65 apoA-I to form spherical α-migrating HDL. Alternatively, in addition to a direct effect of this deletion on LCAT activation, helix 1 may contribute to the accumulation or stabilization of core neutral lipids and transformation of preβ- into α-migrating HDL. This latter effect could involve the high affinity of this specific helix for PL. This is the first demonstration that the globular domain and helix 1 of apoA-I are essential for the formation of mature HDL in a physiologically relevant animal model.

REFERENCE LIST

1. Ross R, Glomset JA. Atherosclerosis and the arterial smooth muscle cell: Proliferation of smooth muscle is a key event in the genesis of the lesions of atherosclerosis. Science 1973;180:1332-9.

2. Gimbrone MA, Jr. Vascular endothelium, hemodynamic forces, and atherogenesis. Am J Pathol 1999;155:1-5.

3. Boren J, Olin K, Lee I, Chait A, Wight TN, Innerarity TL. Identification of the principal proteoglycan-binding site in LDL. A single-point mutation in apo-B100 severely affects proteoglycan interaction without affecting LDL receptor binding. J Clin Invest 1998;101:2658-64.

4. Watson AD, Leitinger N, Navab M, Faull KF, Horkko S, Witztum JL, Palinski W, Schwenke D, Salomon RG, Sha W, Subbanagounder G, Fogelman AM, Berliner JA. Structural identification by mass spectrometry of oxidized phospholipids in minimally oxidized low density lipoprotein that induce monocyte/endothelial interactions and evidence for their presence in vivo. J Biol Chem 1997;272:13597-607.

5. Suzuki H, Kurihara Y, Takeya M, Kamada N, Kataoka M, Jishage K, Ueda O, Sakaguchi H, Higashi T, Suzuki T, Takashima Y, Kawabe Y, Cynshi O, Wada Y, Honda M, Kurihara H, Aburatani H, Doi T, Matsumoto A, Azuma S, Noda T, Toyoda Y, Itakura H, Yazaki Y, Kodama T. A role for macrophage scavenger receptors in atherosclerosis and susceptibility to infection. Nature 1997;386:292-6.

6. Febbraio M, Podrez EA, Smith JD, Hajjar DP, Hazen SL, Hoff HF, Sharma K, Silverstein RL. Targeted disruption of the class B scavenger receptor CD36 protects against atherosclerotic lesion development in mice. J Clin Invest 2000;105:1049-56.

7. Libby P. Changing concepts of atherogenesis. J Intern Med 2000;247:349-58.

8. Albers JJ, Segrest JP. Plasma lipoproteins. Part A: Preparation, structure, and molecular biology. Methods Enzymol 1986;128:1-992.

9. Vance DE, Vance, J. Biochemistry of Lipids, Lipoproteins and Membranes. Elsevier Science Publishers, Amsterdam. 1996;44-69.

10. Glomset JA. The plasma lecithins:cholesterol acyltransferase reaction. J Lipid Res 1968;9:155-67.

11. Eisenberg S. High density lipoprotein metabolism. J Lipid Res 1984;25:1017-58.

12. Patsch JR, Gotto AM, Jr. The high density lipoproteins. Expos Annu Biochim Med 1982;35:1-12.:1-12.

13. Gofman JW, de Lalla O, Glazier F, Freeman NK, Lindgren FT, Nichols AV, Strisower EH, Tamplin AR. The serum lipoprotein transport system in health,

metabolic disorders, atherosclerosis and coronary artery disease. Plasma 1954;2:413-84.

14. Eisenberg S. Plasma lipoprotein conversions: the origins of low-density and high-density lipoproteins. Ann N Y Acad Sci 1980;348:30-47.

15. Barrans A, Jaspard B, Barbaras R, Chap H, Perret B, Collet X. Pre-beta HDL: structure and metabolism. Biochim Biophys Acta 1996;1300:73-85.

16. Nikkila EA, Taskinen MR, Kekki M. Relation of plasma high-density lipoprotein cholesterol to lipoprotein-lipase activity in adipose tissue and skeletal muscle of man. Atherosclerosis 1978;29:497-501.

17. Nikkila EA. Metabolic regulation of plasma high density lipoprotein concentrations. Eur J Clin Invest 1978;8:111-3.

18. Kekki M. Lipoprotein-lipase action determining plasma high density lipoprotein cholesterol level in adult normolipaemics. Atherosclerosis 1980;37:143-50.

19. Lusk LT, Walker LF, DuBien LH, Getz GS. Isolation and partial characterization of high-density lipoprotein HDL1 from rat plasma by gradient centrifugation. Biochem J 1979;183:83-90.

20. Patsch W, Kim K, Wiest W, Schonfeld G. Effects of sex hormones on rat lipoproteins. Endocrinology 1980;107:1085-94.

21. Oschry Y, Eisenberg S. Rat plasma lipoproteins: re-evaluation of a lipoprotein system in an animal devoid of cholesteryl ester transfer activity. J Lipid Res 1982;23:1099-106.

22. Marcel YL, Vezina C, Emond D, Suzue G. Heterogeneity of human high density lipoprotein: presence of lipoproteins with and without apoE and their roles as substrates for lecithin:cholesterol acyltransferase reaction. Proc Natl Acad Sci U S A 1980;77:2969-73.

23. Schmitz G, Assmann G. Isolation of human serum HDL1 by zonal ultracentrifugation. J Lipid Res 1982;23:903-10.

24. Mahley RW. Atherogenic hyperlipoproteinemia. The cellular and molecular biology of plasma lipoproteins altered by dietary fat and cholesterol. Med Clin North Am 1982;66:375-402.

25. Kunitake ST, La Sala KJ, Kane JP. Apolipoprotein A-I-containing lipoproteins with pre-beta electrophoretic mobility. J Lipid Res 1985;26:549-55.

26. Castro GR, Fielding CJ. Early incorporation of cell-derived cholesterol into pre-beta-migrating high-density lipoprotein. Biochemistry 1988;27:25-9.

27. Ishida BY, Frolich J, Fielding CJ. Prebeta-migrating high density lipoprotein: quantitation in normal and hyperlipidemic plasma by solid phase radioimmunoassay following electrophoretic transfer. J Lipid Res 1987;28:778-86.

28. Huang Y, von Eckardstein A, Assmann G. Cell-derived unesterified cholesterol cycles between different HDLs and LDL for its effective esterification in plasma. Arterioscler Thromb 1993;13:445-58.

29. Davidson WS, Sparks DL, Lund-Katz S, Phillips MC. The molecular basis for the difference in charge between pre-beta- and alpha-migrating high density lipoproteins. J Biol Chem 1994;269:8959-65.

30. Phillips MC, Johnson WJ, Rothblat GH. Mechanisms and consequences of cellular cholesterol exchange and transfer. Biochim Biophys Acta 1987;906:223-76.

31. Yancey PG, Bielicki JK, Johnson WJ, Lund-Katz S, Palgunachari MN, Anantharamaiah GM, Segrest JP, Phillips MC, Rothblat GH. Efflux of cellular cholesterol and phospholipid to lipid-free apolipoproteins and class A amphipathic peptides. Biochemistry 1995;34:7955-65.

32. Miida T, Kawano M, Fielding CJ, Fielding PE. Regulation of the concentration of pre beta high-density lipoprotein in normal plasma by cell membranes and lecithin-cholesterol acyltransferase activity. Biochemistry 1992;31:11112-7.

33. Cheung MC, Albers JJ. Characterization of lipoprotein particles isolated by immunoaffinity chromatography. Particles containing A-I and A-II and particles containing A-I but no A-II. J Biol Chem 1984;259:12201-9.

34. Puchois P, Kandoussi A, Fievet P, Fourrier JL, Bertrand M, Koren E, Fruchart JC. Apolipoprotein A-I containing lipoproteins in coronary artery disease. Atherosclerosis 1987;68:35-40.

35. Ohta T, Hattori S, Nishiyama S, Higashi A, Matsuda I. Quantitative and qualitative changes of apolipoprotein AI-containing lipoproteins in patients on continuous ambulatory peritoneal dialysis. Metabolism 1989;38:843-9.

36. Duverger N, Rader D, Brewer HB, Jr. Distribution of subclasses of HDL containing apoA-I without apoA-II (LpA-I) in normolipidemic men and women. Arterioscler Thromb 1994;14:1594-9.

37. Labeur C, Lambert G, Van Cauteren T, Duverger N, Vanloo B, Chambaz J, Vandekerckhove J, Castro G, Rosseneu M. Displacement of apo A-I from HDL by apo A-II or its C-terminal helix promotes the formation of pre-beta1 migrating particles and decreases LCAT activation. Atherosclerosis 1998;139:351-62.

38. Durbin DM, Jonas A. The effect of apolipoprotein A-II on the structure and function of apolipoprotein A-I in a homogeneous reconstituted high density lipoprotein particle. J Biol Chem 1997;272:31333-9.

39. Jonas A. Reconstitution of high-density lipoproteins. Methods Enzymol 1986;128:553-82.

40. Johnson WJ, Kilsdonk EP, Van Tol A, Phillips MC, Rothblat GH. Cholesterol efflux from cells to immunopurified subfractions of human high density lipoprotein: LP-AI and LP-AI/AII. J Lipid Res 1991;32:1993-2000.

41. Oikawa S, Mendez AJ, Oram JF, Bierman EL, Cheung MC. Effects of high-density lipoprotein particles containing apo A-I, with or without apo A-II, on intracellular cholesterol efflux. Biochim Biophys Acta 1993;1165:327-34.

42. Barbaras R, Puchois P, Fruchart JC, Ailhaud G. Cholesterol efflux from cultured adipose cells is mediated by LpAI particles but not by LpAI:AII particles. Biochem Biophys Res Commun 1987;142:63-9.

43. Huang Y, von Eckardstein A, Wu S, Assmann G. Cholesterol efflux, cholesterol esterification, and cholesteryl ester transfer by LpA-I and LpA-I/A-II in native plasma. Arterioscler Thromb Vasc Biol 1995;15:1412-8.

44. Lagrost L, Dengremont C, Athias A, de Geitere C, Fruchart JC, Lallemant C, Gambert P, Castro G. Modulation of cholesterol efflux from Fu5AH hepatoma cells by the apolipoprotein content of high density lipoprotein particles. Particles containing various proportions of apolipoproteins A-I and A-II. J Biol Chem 1995;270:13004-9.

45. Boisfer E, Lambert G, Atger V, Tran NQ, Pastier D, Benetollo C, Trottier JF, Beaucamps I, Antonucci M, Laplaud M, Griglio S, Chambaz J, Kalopissis AD. Overexpression of human apolipoprotein A-II in mice induces hypertriglyceridemia due to defective very low density lipoprotein hydrolysis. J Biol Chem 1999;274:11564-72.

46. Zhong S, Goldberg IJ, Bruce C, Rubin E, Breslow JL, Tall A. Human ApoA-II inhibits the hydrolysis of HDL triglyceride and the decrease of HDL size induced by hypertriglyceridemia and cholesteryl ester transfer protein in transgenic mice. J Clin Invest 1994;94:2457-67.

47. Weng W, Brandenburg NA, Zhong S, Halkias J, Wu L, Jiang XC, Tall A, Breslow JL. ApoA-II maintains HDL levels in part by inhibition of hepatic lipase. Studies In apoA-II and hepatic lipase double knockout mice. J Lipid Res 1999;40:1064-70.

48. Jahn CE, Osborne JC, Jr., Schaefer EJ, Brewer HB, Jr. In vitro activation of the enzymic activity of hepatic lipase by apoA-II. FEBS Lett 1981;131:366-8.

49. Kubo M, Matsuzawa Y, Yokoyama S, Tajima S, Ishikawa K, Yamamoto A, Tarui S. Mechanism of inhibition of hepatic triglyceride lipase from human postheparin plasma by apolipoproteins A-I and A-II. J Biochem (Tokyo) 1982;92:865-70.

50. Forte TM, Nordhausen RW. Electron microscopy of negatively stained lipoproteins. Methods Enzymol 1986;128:442-57.

51. Dory L, Boquet LM, Hamilton RL, Sloop CH, Roheim PS. Heterogeneity of dog interstitial fluid (peripheral lymph) high density lipoproteins: implications for a role in reverse cholesterol transport. J Lipid Res 1985;26:519-27.

52. Jonas A, Kezdy KE, Wald JH. Defined apolipoprotein A-I conformations in reconstituted high density lipoprotein discs. J Biol Chem 1989;264:4818-24.

53. Sparks DL, Davidson WS, Lund-Katz S, Phillips MC. Effect of cholesterol on the charge and structure of apolipoprotein A-I in recombinant high density lipoprotein particles. J Biol Chem 1993;268:23250-7.

54. Clay MA, Pyle DH, Rye KA, Barter PJ. Formation of spherical, reconstituted high density lipoproteins containing both apolipoproteins A-I and A-II is mediated by lecithin:cholesterol acyltransferase. J Biol Chem 2000;275:9019-25.

55. Liang HQ, Rye KA, Barter PJ. Remodelling of reconstituted high density lipoproteins by lecithin: cholesterol acyltransferase. J Lipid Res 1996;37:1962-70.

56. Miller NE. Associations of high-density lipoprotein subclasses and apolipoproteins with ischemic heart disease and coronary atherosclerosis. Am Heart J 1987;113:589-97.

57. Miller NE, Thelle DS, Forde OH, Mjos OD. The Tromso heart-study. High-density lipoprotein and coronary heart-disease: a prospective case-control study. Lancet 1977;1:965-8.

58. Gordon T, Castelli WP, Hjortland MC, Kannel WB, Dawber TR. High density lipoprotein as a protective factor against coronary heart disease. The Framingham Study. Am J Med 1977;62:707-14.

59. Gordon DJ, Probstfield JL, Garrison RJ, Neaton JD, Castelli WP, Knoke JD, Jacobs DR, Jr., Bangdiwala S, Tyroler HA. High-density lipoprotein cholesterol and cardiovascular disease. Four prospective American studies. Circulation 1989;79:8-15.

60. Gordon DJ, Rifkind BM. High-density lipoprotein--the clinical implications of recent studies. N Engl J Med 1989;321:1311-6.

61. Calabresi L, Franceschini G. High density lipoprotein and coronary heart disease: insights from mutations leading to low high density lipoprotein. Curr Opin Lipidol 1997;8:219-24.

62. Barter PJ, Rye KA. High density lipoproteins and coronary heart disease. Atherosclerosis 1996;121:1-12.

63. Klimov AN, Gurevich VS, Nikiforova AA, Shatilina LV, Kuzmin AA, Plavinsky SL, Teryukova NP. Antioxidative activity of high density lipoproteins in vivo. Atherosclerosis 1993;100:13-8.

64. Parthasarathy S, Santanam N. Mechanisms of oxidation, antioxidants, and atherosclerosis. Curr Opin Lipidol 1994;5:371-5.

65. Epand RM, Stafford A, Leon B, Lock PE, Tytler EM, Segrest JP, Anantharamaiah GM. HDL and apolipoprotein A-I protect erythrocytes against the generation of procoagulant activity. Arterioscler Thromb 1994;14:1775-83.

66. Cockerill GW, Rye KA, Gamble JR, Vadas MA, Barter PJ. High-density lipoproteins inhibit cytokine-induced expression of endothelial cell adhesion molecules. Arterioscler Thromb Vasc Biol 1995;15:1987-94.

67. Blackburn WD, Jr., Dohlman JG, Venkatachalapathi YV, Pillion DJ, Koopman WJ, Segrest JP, Anantharamaiah GM. Apolipoprotein A-I decreases neutrophil degranulation and superoxide production. J Lipid Res 1991;32:1911-8.

68. Rosenfeld SI, Packman CH, Leddy JP. Inhibition of the lytic action of cell-bound terminal complement components by human high density lipoproteins and apoproteins. J Clin Invest 1983;71:795-808.

69. Naqvi TZ, Shah PK, Ivey PA, Molloy MD, Thomas AM, Panicker S, Ahmed A, Cercek B, Kaul S. Evidence that high-density lipoprotein cholesterol is an independent predictor of acute platelet-dependent thrombus formation. Am J Cardiol 1999;84:1011-7.

70. Levine DM, Parker TS, Donnelly TM, Walsh A, Rubin AL. In vivo protection against endotoxin by plasma high density lipoprotein. Proc Natl Acad Sci U S A 1993;90:12040-4.

71. Tytler EM, Moore DR, Pierce MA, Hager KM, Esko JD, Hajduk SL. Reconstitution of the trypanolytic factor from components of a subspecies of human high-density lipoproteins. Mol Biochem Parasitol 1995;69:9-17.

72. Hager KM, Pierce MA, Moore DR, Tytler EM, Esko JD, Hajduk SL. Endocytosis of a cytotoxic human high density lipoprotein results in disruption of acidic intracellular vesicles and subsequent killing of African trypanosomes. J Cell Biol 1994;126:155-67.

73. Hajduk SL, Hager KM, Esko JD. Human high density lipoprotein killing of African trypanosomes. Annu Rev Microbiol 1994;48:139-62.

74. Wang Y, Agerberth B, Lothgren A, Almstedt A, Johansson J. Apolipoprotein A-I binds and inhibits the human antibacterial/cytotoxic peptide LL-37. J Biol Chem 1998;273:33115-8.

75. Jorgensen EV, Anantharamaiah GM, Segrest JP, Gwynne JT, Handwerger S. Synthetic amphipathic peptides resembling apolipoproteins stimulate the release of human placental lactogen. J Biol Chem 1989;264:9215-9.

76. Yui Y, Aoyama T, Morishita H, Takahashi M, Takatsu Y, Kawai C. Serum prostacyclin stabilizing factor is identical to apolipoprotein A-I (Apo A-I). A novel function of Apo A-I. J Clin Invest 1988;82:803-7.

77. Rees D, Sloane T, Jessup W, Dean RT, Kritharides L. Apolipoprotein A-I stimulates secretion of apolipoprotein E by foam cell macrophages. J Biol Chem 1999;274:27925-33.

78. Genschel J, Haas R, Propsting MJ, Schmidt HH. Apolipoprotein A-I induced amyloidosis. FEBS Lett 1998;430:145-9.

79. Brouillette CG, Anantharamaiah GM. Structural models of human apolipoprotein A-I. Biochim Biophys Acta 1995;1256:103-29.

80. Hamilton RL, Williams MC, Fielding CJ, Havel RJ. Discoidal bilayer structure of nascent high density lipoproteins from perfused rat liver. J Clin Invest 1976;58:667-80.

81. Dory L, Sloop CH, Boquet LM, Hamilton RL, Roheim PS. Lecithin:cholesterol acyltransferase-mediated modification of discoidal peripheral lymph high density lipoproteins: possible mechanism of formation of cholesterol-induced high density lipoproteins (HDLc) in cholesterol-fed dogs. Proc Natl Acad Sci U S A 1983;80:3489-93.

82. Green PH, Glickman RM. Intestinal lipoprotein metabolism. J Lipid Res 1981;22:1153-73.

83. Sorci-Thomas M, Prack MM, Dashti N, Johnson F, Rudel LL, Williams DL. Differential effects of dietary fat on the tissue-specific expression of the apolipoprotein A-I gene: relationship to plasma concentration of high density lipoproteins. J Lipid Res 1989;30:1397-403.

84. Sorci-Thomas M, Prack MM, Dashti N, Johnson F, Rudel LL, Williams DL. Apolipoprotein (apo) A-I production and mRNA abundance explain plasma apoA-I and high density lipoprotein differences between two nonhuman primate species with high and low susceptibilities to diet-induced hypercholesterolemia. J Biol Chem 1988;263:5183-9.

85. Davis RC, Wong H, Nikazy J, Wang K, Han Q, Schotz MC. Chimeras of hepatic lipase and lipoprotein lipase. Domain localization of enzyme-specific properties. J Biol Chem 1992;267:21499-504.

86. Patsch JR, Prasad S, Gotto AM, Jr., Patsch W. High density lipoprotein2. Relationship of the plasma levels of this lipoprotein species to its composition, to the magnitude of postprandial lipemia, and to the activities of lipoprotein lipase and hepatic lipase. J Clin Invest 1987;80:341-7.

87. Tall AR, Small DM. Plasma high-density lipoproteins. N Engl J Med 1978;299:1232-6.

88. Day JR, Albers JJ, Lofton-Day CE, Gilbert TL, Ching AF, Grant FJ, O'Hara PJ, Marcovina SM, Adolphson JL. Complete cDNA encoding human phospholipid transfer protein from human endothelial cells. J Biol Chem 1994;269:9388-91.

89. Albers JJ, Tu AY, Wolfbauer G, Cheung MC, Marcovina SM. Molecular biology of phospholipid transfer protein. Curr Opin Lipidol 1996;7:88-93.

90. Albers JJ, Tollefson JH, Chen CH, Steinmetz A. Isolation and characterization of human plasma lipid transfer proteins. Arteriosclerosis 1984;4:49-58.

91. Kostner GM, Oettl K, Jauhiainen M, Ehnholm C, Esterbauer H, Dieplinger H. Human plasma phospholipid transfer protein accelerates exchange/transfer of alpha-tocopherol between lipoproteins and cells. Biochem J 1995;305:659-67.

92. Hailman E, Albers JJ, Wolfbauer G, Tu AY, Wright SD. Neutralization and transfer of lipopolysaccharide by phospholipid transfer protein. J Biol Chem 1996;271:12172-8.

93. Nishida HI, Nishida T. Phospholipid transfer protein mediates transfer of not only phosphatidylcholine but also cholesterol from phosphatidylcholine-cholesterol vesicles to high density lipoproteins. J Biol Chem 1997;272:6959-64.

94. Jiang XC, Bruce C, Mar J, Lin M, Ji Y, Francone OL, Tall AR. Targeted mutation of plasma phospholipid transfer protein gene markedly reduces high-density lipoprotein levels. J Clin Invest 1999;103:907-14.

95. Tu AY, Paigen B, Wolfbauer G, Cheung MC, Kennedy H, Chen H, Albers JJ. Introduction of the human PLTP transgene suppresses the atherogenic diet-induced increase in plasma phospholipid transfer activity in C57BL/6 mice. Int J Clin Lab Res 1999;29:14-21.

96. van Haperen R, Van Tol A, Vermeulen P, Jauhiainen M, van Gent T, van den BP, Ehnholm S, Grosveld F, van der KA, de Crom R. Human plasma phospholipid transfer protein increases the antiatherogenic potential of high density lipoproteins in transgenic mice. Arterioscler Thromb Vasc Biol 2000;20:1082-8.

97. Jaari S, van Dijk KW, Olkkonen VM, van der ZA, Metso J, Havekes L, Jauhiainen M, Ehnholm C. Dynamic changes in mouse lipoproteins induced by transiently expressed human phospholipid transfer protein (PLTP): importance of PLTP in prebeta-HDL generation. Comp Biochem Physiol B Biochem Mol Biol 2001;128:781-92.

98. Oram JF, Vaughan AM. ABCA1-mediated transport of cellular cholesterol and phospholipids to HDL apolipoproteins. Curr Opin Lipidol 2000;11:253-60.

99. Nichols JW, Pagano RE. Use of resonance energy transfer to study the kinetics of amphiphile transfer between vesicles. Biochemistry 1982;21:1720-6.

100. Backer JM, Dawidowicz EA. Mechanism of cholesterol exchange between phospholipid vesicles. Biochemistry 1981;20:3805-10.

101. McLean LR, Phillips MC. Mechanism of cholesterol and phosphatidylcholine exchange or transfer between unilamellar vesicles. Biochemistry 1981;20:2893-900.

102. Rothblat GH, Bamberger M, Phillips MC. Reverse cholesterol transport. Methods Enzymol 1986;129:628-44.:628-44.

103. Mahlberg FH, Rothblat GH. Cellular cholesterol efflux. Role of cell membrane kinetic pools and interaction with apolipoproteins AI, AII, and Cs. J Biol Chem 1992;267:4541-50.

104. Hara H, Yokoyama S. Interaction of free apolipoproteins with macrophages. Formation of high density lipoprotein-like lipoproteins and reduction of cellular cholesterol. J Biol Chem 1991;266:3080-6.

105. Forte TM, Bielicki JK, Goth-Goldstein R, Selmek J, McCall MR. Recruitment of cell phospholipids and cholesterol by apolipoproteins A-II and A-I: formation of nascent apolipoprotein-specific HDL that differ in size, phospholipid composition, and reactivity with LCAT. J Lipid Res 1995;36:148-57.

106. Eisenberg S. High density lipoprotein metabolism. J Lipid Res 1984;25:1017-58.

107. Oram JF. Tangier disease and ABCA1. Biochim Biophys Acta 2000;1529:321-30.

108. Assmann G, Smootz E, Adler K, Capurso A, Oette K. The lipoprotein abnormality in Tangier disease: quantitation of A apoproteins. J Clin Invest 1977;59:565-75.

109. Makrides SC, Ruiz-Opazo N, Hayden M, Nussbaum AL, Breslow JL, Zannis VI. Sequence and expression of Tangier apoA-I gene. Eur J Biochem 1988;173:465-71.

110. Walter M, Gerdes U, Seedorf U, Assmann G. The high density lipoprotein- and apolipoprotein A-I-induced mobilization of cellular cholesterol is impaired in fibroblasts from Tangier disease subjects. Biochem Biophys Res Commun 1994;205:850-6.

111. Francis GA, Knopp RH, Oram JF. Defective removal of cellular cholesterol and phospholipids by apolipoprotein A-I in Tangier Disease. J Clin Invest 1995;96:78-87.

112. Rogler G, Trumbach B, Klima B, Lackner KJ, Schmitz G. HDL-mediated efflux of intracellular cholesterol is impaired in fibroblasts from Tangier disease patients. Arterioscler Thromb Vasc Biol 1995;15:683-90.

113. Oram JF, Yokoyama S. Apolipoprotein-mediated removal of cellular cholesterol and phospholipids. J Lipid Res 1996;37:2473-91.

114. Bodzioch M, Orso E, Klucken J, Langmann T, Bottcher A, Diederich W, Drobnik W, Barlage S, Buchler C, Porsch-Ozcurumez M, Kaminski WE, Hahmann HW,

Oette K, Rothe G, Aslanidis C, Lackner KJ, Schmitz G. The gene encoding ATP-binding cassette transporter 1 is mutated in Tangier disease. Nat Genet 1999;22:347-51.

115. Brooks-Wilson A, Marcil M, Clee SM, Zhang LH, Roomp K, van Dam M, Yu L, Brewer C, Collins JA, Molhuizen HO, Loubser O, Ouelette BF, Fichter K, Ashbourne-Excoffon KJ, Sensen CW, Scherer S, Mott S, Denis M, Martindale D, Frohlich J, Morgan K, Koop B, Pimstone S, Kastelein JJ, Hayden MR, . Mutations in ABC1 in Tangier disease and familial high-density lipoprotein deficiency. Nat Genet 1999;22:336-45.

116. Rust S, Rosier M, Funke H, Real J, Amoura Z, Piette JC, Deleuze JF, Brewer HB, Duverger N, Denefle P, Assmann G. Tangier disease is caused by mutations in the gene encoding ATP-binding cassette transporter 1. Nat Genet 1999;22:352-5.

117. Schmitz G, Kaminski WE, Orso E. ABC transporters in cellular lipid trafficking. Curr Opin Lipidol 2000;11:493-501.

118. Marcil M, Brooks-Wilson A, Clee SM, Roomp K, Zhang LH, Yu L, Collins JA, van Dam M, Molhuizen HO, Loubster O, Ouellette BF, Sensen CW, Fichter K, Mott S, Denis M, Boucher B, Pimstone S, Genest J, Kastelein JJ, Hayden MR. Mutations in the ABC1 gene in familial HDL deficiency with defective cholesterol efflux. Lancet 1999;354:1341-6.

119. Hayden MR, Clee SM, Brooks-Wilson A, Genest J, Jr., Attie A, Kastelein JJ. Cholesterol efflux regulatory protein, Tangier disease and familial high-density lipoprotein deficiency. Curr Opin Lipidol 2000;11:117-22.

120. Walker JE, Saraste M, Runswick MJ, Gay NJ. EMBO J 1982;8:945-51.

121. Lawn RM, Wade DP, Garvin MR, Wang X, Schwartz K, Porter JG, Seilhamer JJ, Vaughan AM, Oram JF. The Tangier disease gene product ABC1 controls the cellular apolipoprotein-mediated lipid removal pathway. J Clin Invest 1999;104:R25-R31.

122. Hamon Y, Broccardo C, Chambenoit O, Luciani MF, Toti F, Chaslin S, Freyssinet JM, Devaux PF, McNeish J, Marguet D, Chimini G. ABC1 promotes engulfment of apoptotic cells and transbilayer redistribution of phosphatidylserine. Nat Cell Biol 2000;2:399-406.

123. Qu Q, Sharom FJ. FRET analysis indicates that the two ATPase active sites of the P-glycoprotein multidrug transporter are closely associated. Biochemistry 2001;40:1413-22.

124. Wang N, Silver DL, Costet P, Tall AR. Specific binding of ApoA-I, enhanced cholesterol efflux, and altered plasma membrane morphology in cells expressing ABC1. J Biol Chem 2000;275:33053-8.

125. Oram JF, Lawn RM, Garvin MR, Wade DP. ABCA1 is the cAMP-inducible apolipoprotein receptor that mediates cholesterol secretion from macrophages. J Biol Chem 2000;275:34508-11.

126. Chambenoit O, Hamon Y, Marguet D, Rigneault H, Rosseneu M, Chimini G. Specific docking of apolipoprotein A-I at the cell surface requires a functional ABCA1 transporter. J Biol Chem 2001;276:9955-60.

127. Glomset JA. Physiological role of lecithin-cholesterol acyltransferase. Am J Clin Nutr 1970;23:1129-36.

128. Jonas A. Lecithin cholesterol acyltransferase. Biochim Biophys Acta 2000;1529:245-56.

129. Ollis DL, Cheah E, Cygler M, Dijkstra B, Frolow F, Franken SM, Harel M, Remington SJ, Silman I, Schrag J, . The alpha/beta hydrolase fold. Protein Eng 1992;5:197-211.

130. Kuivenhoven JA, Pritchard H, Hill J, Frohlich J, Assmann G, Kastelein J. The molecular pathology of lecithin:cholesterol acyltransferase (LCAT) deficiency syndromes. J Lipid Res 1997;38:191-205.

131. Hoeg JM, Vaisman BL, Demosky SJ, Jr., Meyn SM, Talley GD, Hoyt RF, Jr., Feldman S, Berard AM, Sakai N, Wood D, Brousseau ME, Marcovina S, Brewer HB, Jr., Santamarina-Fojo S. Lecithin:cholesterol acyltransferase overexpression generates hyperalpha-lipoproteinemia and a nonatherogenic lipoprotein pattern in transgenic rabbits. J Biol Chem 1996;271:4396-402.

132. Mehlum A, Muri M, Hagve TA, Solberg LA, Prydz H. Mice overexpressing human lecithin: cholesterol acyltransferase are not protected against diet-induced atherosclerosis. APMIS 1997;105:861-8.

133. Francone OL, Gong EL, Ng DS, Fielding CJ, Rubin EM. Expression of human lecithin-cholesterol acyltransferase in transgenic mice. Effect of human apolipoprotein AI and human apolipoprotein all on plasma lipoprotein cholesterol metabolism. J Clin Invest 1995;96:1440-8.

134. Holvoet P, De Geest B, Van Linthout S, Lox M, Danloy S, Raes K, Collen D. The Arg123-Tyr166 central domain of human ApoAI is critical for lecithin:cholesterol acyltransferase-induced hyperalphalipoproteinemia and HDL remodeling in transgenic mice. Arterioscler Thromb Vasc Biol 2000;20:459-66.

135. Brousseau ME, Santamarina-Fojo S, Vaisman BL, Applebaum-Bowden D, Berard AM, Talley GD, Brewer HB, Jr., Hoeg JM. Overexpression of human lecithin:cholesterol acyltransferase in cholesterol-fed rabbits: LDL metabolism and HDL metabolism are affected in a gene dose-dependent manner. J Lipid Res 1997;38:2537-47.

136. Forte TM, Oda MN, Knoff L, Frei B, Suh J, Harmony JA, Stuart WD, Rubin EM, Ng DS. Targeted disruption of the murine lecithin:cholesterol acyltransferase gene is associated with reductions in plasma paraoxonase and platelet-activating factor acetylhydrolase activities but not in apolipoprotein J concentration. J Lipid Res 1999;40:1276-83.

137. Berard AM, Foger B, Remaley A, Shamburek R, Vaisman BL, Talley G, Paigen B, Hoyt RF, Jr., Marcovina S, Brewer HB, Jr., Santamarina-Fojo S. High plasma HDL concentrations associated with enhanced atherosclerosis in transgenic mice overexpressing lecithin-cholesteryl acyltransferase. Nat Med 1997;3:744-9.

138. Bruce C, Chouinard RA, Jr., Tall AR. Plasma lipid transfer proteins, high-density lipoproteins, and reverse cholesterol transport. Annu Rev Nutr 1998;18:297-330.

139. Lagrost L. Regulation of cholesteryl ester transfer protein (CETP) activity: review of in vitro and in vivo studies. Biochim Biophys Acta 1994;1215:209-36.

140. Ha YC, Barter PJ. Differences in plasma cholesteryl ester transfer activity in sixteen vertebrate species. Comp Biochem Physiol B 1982;71:265-9.

141. Stahnke G, Sprengel R, Augustin J, Will H. Human hepatic triglyceride lipase: cDNA cloning, amino acid sequence and expression in a cultured cell line. Differentiation 1987;35:45-52.

142. Sanan DA, Fan J, Bensadoun A, Taylor JM. Hepatic lipase is abundant on both hepatocyte and endothelial cell surfaces in the liver. J Lipid Res 1997;38:1002-13.

143. Greaves DR, Gough PJ, Gordon S. Recent progress in defining the role of scavenger receptors in lipid transport, atherosclerosis and host defence. Curr Opin Lipidol 1998;9:425-32.

144. Glass C, Pittman RC, Weinstein DB, Steinberg D. Dissociation of tissue uptake of cholesterol ester from that of apoprotein A-I of rat plasma high density lipoprotein: selective delivery of cholesterol ester to liver, adrenal, and gonad. Proc Natl Acad Sci U S A 1983;80:5435-9.

145. Acton SL, Scherer PE, Lodish HF, Krieger M. Expression cloning of SR-BI, a CD36-related class B scavenger receptor. J Biol Chem 1999;269:21003-9.

146. Acton S, Rigotti A, Landschulz KT, Xu S, Hobbs HH, Krieger M. Identification of scavenger receptor SR-BI as a high density lipoprotein receptor. Science 1996;271:518-20.

147. Swarnakar S, Temel RE, Connelly MA, Azhar S, Williams DL. Scavenger receptor class B, type I, mediates selective uptake of low density lipoprotein cholesteryl ester. J Biol Chem 1999;274:29733-9.

148. Kozarsky KF, Donahee MH, Rigotti A, Iqbal SN, Edelman ER, Krieger M. Overexpression of the HDL receptor SR-BI alters plasma HDL and bile cholesterol levels. Nature 1997;387:414-7.

149. Wang N, Arai T, Ji Y, Rinninger F, Tall AR. Liver-specific overexpression of scavenger receptor BI decreases levels of very low density lipoprotein ApoB, low density lipoprotein ApoB, and high density lipoprotein in transgenic mice. J Biol Chem 1998;273:32920-6.

150. Rigotti A, Trigatti BL, Penman M, Rayburn H, Herz J, Krieger M. A targeted mutation in the murine gene encoding the high density lipoprotein (HDL) receptor scavenger receptor class B type I reveals its key role in HDL metabolism. Proc Natl Acad Sci U S A 1997;94:12610-5.

151. Blum CB, Levy RI, Eisenberg S, Hall M, III, Goebel RH, Berman M. High density lipoprotein metabolism in man. J Clin Invest 1977;60:795-807.

152. Shepherd J, Patsch JR, Packard CJ, Gotto AM, Jr., Taunton OD. Dynamic properties of human high density lipoprotein apoproteins. J Lipid Res 1978;19:383-9.

153. Goldberg IJ, Vanni TM, Ramakrishnan R. Effects of intralipid-induced hypertriglyceridemia on plasma high-density lipoprotein metabolism in the cynomolgus monkey. Metabolism 1992;41:1176-84.

154. Newnham HH, Barter PJ. Synergistic effects of lipid transfers and hepatic lipase in the formation of very small high-density lipoproteins during incubation of human plasma. Biochim Biophys Acta 1990;1044:57-64.

155. Peterson DR, Hjelle JT, Carone FA, Moore PA. Renal handling of plasma high density lipoprotein. Kidney Int 1984;26:411-21.

156. Saku K, Gartside PS, Hynd BA, Mendoza SG, Kashyap ML. Apolipoprotein AI and AII metabolism in patients with primary high-density lipoprotein deficiency associated with familial hypertriglyceridemia. Metabolism 1985;34:754-64.

157. Horowitz BS, Goldberg IJ, Merab J, Vanni TM, Ramakrishnan R, Ginsberg HN. Increased plasma and renal clearance of an exchangeable pool of apolipoprotein A-I in subjects with low levels of high density lipoprotein cholesterol. J Clin Invest 1993;91:1743-52.

158. Clay MA, Newnham HH, Barter PJ. Hepatic lipase promotes a loss of apolipoprotein A-I from triglyceride-enriched human high density lipoproteins during incubation in vitro. Arterioscler Thromb 1991;11:415-22.

159. Braschi S, Neville TA, Vohl MC, Sparks DL. Apolipoprotein A-I charge and conformation regulate the clearance of reconstituted high density lipoprotein in vivo. J Lipid Res 1999;40:522-32.

160. Lamon-Fava S, Sastry R, Ferrari S, Rajavashisth TB, Lusis AJ, Karathanasis SK. Evolutionary distinct mechanisms regulate apolipoprotein A-I gene expression: differences between avian and mammalian apoA-I gene transcription control regions. J Lipid Res 1992;33:831-42.

161. Karathanasis SK. Apolipoprotein multigene family: tandem organization of human apolipoprotein AI, CIII, and AIV genes. Proc Natl Acad Sci U S A 1985;82:6374-8.

162. Li WH, Tanimura M, Luo CC, Datta S, Chan L. The apolipoprotein multigene family: biosynthesis, structure, structure-function relationships, and evolution. J Lipid Res 1988;29:245-71.

163. Luo CC, Li WH, Moore MN, Chan L. Structure and evolution of the apolipoprotein multigene family. J Mol Biol 1986;187:325-40.

164. Mahley RW, Innerarity TL, Rall SC, Jr., Weisgraber KH. Plasma lipoproteins: apolipoprotein structure and function. J Lipid Res 1984;25:1277-94.

165. Wu AL, Windmueller HG. Relative contributions by liver and intestine to individual plasma apolipoproteins in the rat. J Biol Chem 1979;254:7316-22.

166. Stoffel W. Synthesis, transport, and processing of apolipoproteins of high density lipoproteins. J Lipid Res 1984;25:1586-92.

167. Pyle LE, Sviridov D, Fidge NH. Characterization of the maturation of human pro-apolipoprotein A-I in an in vitro model. Biochemistry 2001;40:3101-8.

168. Sparrow DA, Lee BR, Laplaud PM, Auboiron S, Bauchart D, Chapman MJ, Gotto AM, Jr., Yang CY, Sparrow JT. Plasma lipid transport in the preruminant calf, Bos spp: primary structure of bovine apolipoprotein A-I. Biochim Biophys Acta 1992;1123:145-50.

169. Collet X, Marcel YL, Tremblay N, Lazure C, Milne RW, Perret B, Weech PK. Evolution of mammalian apolipoprotein A-I and conservation of antigenicity: correlation with primary and secondary structure. J Lipid Res 1997;38:634-44.

170. Segrest JP, Jackson RL, Morrisett JD, Gotto AM, Jr. A molecular theory of lipid-protein interactions in the plasma lipoproteins. FEBS Lett 1974;38:247-58.

171. Breslow JL, Ross D, McPherson J, Williams H, Kurnit D, Nussbaum AL, Karathanasis SK, Zannis VI. Isolation and characterization of cDNA clones for human apolipoprotein A-I. Proc Natl Acad Sci U S A 1982;79:6861-5.

172. Polites HG, Melchior GW, Castle CK, Marotti KR. The primary structure of cynomolgus monkey apolipoprotein A-1 deduced from the cDNA sequence: comparison to the human sequence. Gene 1986;49:103-10.

173. Chung H, Randolph A, Reardon I, Heinrikson RL. The covalent structure of apolipoprotein A-I from canine high density lipoproteins. J Biol Chem 1982;257:2961-7.

174. Birchbauer A, Knipping G, Juritsch B, Aschauer H, Zechner R. Characterization of the apolipoprotein AI and CIII genes in the domestic pig. Genomics 1993;15:643-52.

175. Pan TC, Hao QL, Yamin TT, Dai PH, Chen BS, Chen SL, Kroon PA, Chao YS. Rabbit apolipoprotein A-I mRNA and gene. Evidence that rabbit apolipoprotein A-I is synthesized in the intestine but not in the liver. Eur J Biochem 1987;170:99-104.

176. O'hUigin C, Chan L, Li WH. Cloning and sequencing of bovine apolipoprotein A-I cDNA and molecular evolution of apolipoproteins A-I and B-100. Mol Biol Evol 1990;7:327-39.

177. Sparrow DA, Laplaud PM, Saboureau M, Zhou G, Dolphin PJ, Gotto AM, Jr., Sparrow JT. Plasma lipid transport in the hedgehog: partial characterization of structure and function of apolipoprotein A-I. J Lipid Res 1995;36:485-95.

178. Stoffel W, Muller R, Binczek E, Hofmann K. Mouse apolipoprotein AI. cDNA-derived primary structure, gene organisation and complete nucleotide sequence. Biol Chem Hoppe Seyler 1992;373:187-93.

179. Poncin JE, Martial JA, Gielen JE. Cloning and structure analysis of the rat apolipoprotein A-I cDNA. Eur J Biochem 1984;140:493-8.

180. Byrnes L, Luo CC, Li WH, Yang CY, Chan L. Chicken apolipoprotein A-I: cDNA sequence, tissue expression and evolution. Biochem Biophys Res Commun 1987;148:485-92.

181. Powell R, Higgins DG, Wolff J, Byrnes L, Stack M, Sharp PM, Gannon F. The salmon gene encoding apolipoprotein A-I: cDNA sequence, tissue expression and evolution. Gene 1991;104:155-61.

182. Frank PG, Marcel YL. Apolipoprotein A-I: structure-function relationships. J Lipid Res 2000;41:853-72.

183. Chou PY, Fasman GD. Prediction of the secondary structure of proteins from their amino acid sequence. Adv Enzymol Relat Areas Mol Biol 1978;47:45-148.

184. Fitch WM. Phylogenies constrained by the crossover process as illustrated by human hemoglobins and a thirteen-cycle, eleven-amino-acid repeat in human apolipoprotein A-I. Genetics 1977;86:623-44.

185. McLachlan AD. Repeated helical pattern in apolipoprotein-A-I. Nature 1977;267:465-6.

186. Brasseur R, De Meutter J, Vanloo B, Goormaghtigh E, Ruysschaert JM, Rosseneu M. Mode of assembly of amphipathic helical segments in model high-density lipoproteins. Biochim Biophys Acta 1990;1043:245-52.

187. Sparks DL, Phillips MC, Lund-Katz S. The conformation of apolipoprotein A-I in discoidal and spherical recombinant high density lipoprotein particles. 13C NMR studies of lysine ionization behavior. J Biol Chem 1992;267:25830-8.

188. Segrest JP, Jones MK, De Loof H, Brouillette CG, Venkatachalapathi YV, Anantharamaiah GM. The amphipathic helix in the exchangeable apolipoproteins: a review of secondary structure and function. J Lipid Res 1992;33:141-66.

189. Borhani DW, Rogers DP, Engler JA, Brouillette CG. Crystal structure of truncated human apolipoprotein A-I suggests a lipid-bound conformation. Proc Natl Acad Sci U S A 1997;94:12291-6.

190. Segrest JP, De Loof H, Dohlman JG, Brouillette CG, Anantharamaiah GM. Amphipathic helix motif: classes and properties. Proteins 1990;8:103-17.

191. Wilson C, Wardell MR, Weisgraber KH, Mahley RW, Agard DA. Three-dimensional structure of the LDL receptor-binding domain of human apolipoprotein E. Science 1991;252:1817-22.

192. Narayanaswami V, Ryan RO. Molecular basis of exchangeable apolipoprotein function. Biochim Biophys Acta 2000;1483:15-36.

193. Breiter DR, Kanost MR, Benning MM, Wesenberg G, Law JH, Wells MA, Rayment I, Holden HM. Molecular structure of an apolipoprotein determined at 2.5-A resolution. Biochemistry 1991;30:603-8.

194. Wang J, Gagne SM, Sykes BD, Ryan RO. Insight into lipid surface recognition and reversible conformational adaptations of an exchangeable apolipoprotein by multidimensional heteronuclear NMR techniques. J Biol Chem 1997;272:17912-20.

195. Roberts LM, Ray MJ, Shih TW, Hayden E, Reader MM, Brouillette CG. Structural analysis of apolipoprotein A-I: limited proteolysis of methionine-reduced and -oxidized lipid-free and lipid-bound human apo A-I. Biochemistry 1997;36:7615-24.

196. Maiorano JN, Davidson WS. The orientation of helix 4 in apolipoprotein A-I-containing reconstituted high density lipoproteins. J Biol Chem 2000;275:17374-80.

197. Rogers DP, Brouillette CG, Engler JA, Tendian SW, Roberts L, Mishra VK, Anantharamaiah GM, Lund-Katz S, Phillips MC, Ray MJ. Truncation of the amino terminus of human apolipoprotein A-I substantially alters only the lipid-free conformation. Biochemistry 1997;36:288-300.

198. Brouillette CG, Anantharamaiah GM, Engler JA, Borhani DW. Structural models of human apolipoprotein A-I: a critical analysis and review. Biochim Biophys Acta 2001;1531:4-46.

199. Rogers DP, Roberts LM, Lebowitz J, Datta G, Anantharamaiah GM, Engler JA, Brouillette CG. The lipid-free structure of apolipoprotein A-I: effects of amino-terminal deletions. Biochemistry 1998;37:11714-25.

200. Phillips JC, Wriggers W, Li Z, Jonas A, Schulten K. Predicting the structure of apolipoprotein A-I in reconstituted high-density lipoprotein disks. Biophys J 1997;73:2337-46.

201. Segrest JP, Li L, Anantharamaiah GM, Harvey SC, Liadaki KN, Zannis V. Structure and function of apolipoprotein A-I and high-density lipoprotein. Curr Opin Lipidol 2000;11:105-15.

202. Koppaka V, Silvestro L, Engler JA, Brouillette CG, Axelsen PH. The structure of human lipoprotein A-I. Evidence for the "belt" model. J Biol Chem 1999;274:14541-4.

203. Li H, Lyles DS, Thomas MJ, Pan W, Sorci-Thomas MG. Structural determination of lipid-bound ApoA-I using fluorescence resonance energy transfer. J Biol Chem 2000;275:37048-54.

204. Segrest JP, Jones MK, Klon AE, Sheldahl CJ, Hellinger M, De Loof H, Harvey SC. A detailed molecular belt model for apolipoprotein A-I in discoidal high density lipoprotein. J Biol Chem 1999;274:31755-8.

205. Tall AR, Small DM, Deckelbaum RJ, Shipley GG. Structure and thermodynamic properties of high density lipoprotein recombinants. J Biol Chem 1977;252:4701-11.

206. Pownall HJ, Massey JB, Kusserow SK, Gotto AM, Jr. Kinetics of lipid--protein interactions: interaction of apolipoprotein A-I from human plasma high density lipoproteins with phosphatidylcholines. Biochemistry 1978;17:1183-8.

207. Jonas A, Drengler SM. Kinetics and mechanism of apolipoprotein A-I interaction with L-alpha-dimyristoylphosphatidylcholine vesicles. J Biol Chem 1980;255:2190-4.

208. Matz CE, Jonas A. Micellar complexes of human apolipoprotein A-I with phosphatidylcholines and cholesterol prepared from cholate-lipid dispersions. J Biol Chem 1982;257:4535-40.

209. Nichols AV, Blanche PJ, Gong EL, Shore VG, Forte TM. Molecular pathways in the transformation of model discoidal lipoprotein complexes induced by lecithin:cholesterol acyltransferase. Biochim Biophys Acta 1985;834:285-300.

210. Jonas A, Wald JH, Toohill KL, Krul ES, Kezdy KE. Apolipoprotein A-I structure and lipid properties in homogeneous, reconstituted spherical and discoidal high density lipoproteins. J Biol Chem 1990;265:22123-9.

211. Sparks DL, Lund-Katz S, Phillips MC. The charge and structural stability of apolipoprotein A-I in discoidal and spherical recombinant high density lipoprotein particles. J Biol Chem 1992;267:25839-47.

212. Palgunachari MN, Mishra VK, Lund-Katz S, Phillips MC, Adeyeye SO, Alluri S, Anantharamaiah GM, Segrest JP. Only the two end helixes of eight tandem amphipathic helical domains of human apo A-I have significant lipid affinity. Implications for HDL assembly. Arterioscler Thromb Vasc Biol 1996;16:328-38.

213. Burgess JW, Frank PG, Franklin V, Liang P, McManus DC, Desforges M, Rassart E, Marcel YL. Deletion of the C-terminal domain of apolipoprotein A-I impairs cell surface binding and lipid efflux in macrophage. Biochemistry 1999;38:14524-33.

214. Schmidt HH, Remaley AT, Stonik JA, Ronan R, Wellmann A, Thomas F, Zech LA, Brewer HB, Jr., Hoeg JM. Carboxyl-terminal domain truncation alters apolipoprotein A-I in vivo catabolism. J Biol Chem 1995;270:5469-75.

215. Holvoet P, Danloy S, Collen D. Role of the carboxy-terminal domain of human apolipoprotein AI in high-density-lipoprotein metabolism--a study based on deletion and substitution variants in transgenic mice. Eur J Biochem 1997;245:642-7.

216. Jonas A, von Eckardstein A, Kezdy KE, Steinmetz A, Assmann G. Structural and functional properties of reconstituted high density lipoprotein discs prepared with six apolipoprotein A-I variants. J Lipid Res 1991;32:97-106.

217. Lindholm EM, Bielicki JK, Curtiss LK, Rubin EM, Forte TM. Deletion of amino acids Glu146-->Arg160 in human apolipoprotein A-I (ApoA-ISeattle) alters lecithin:cholesterol acyltransferase activity and recruitment of cell phospholipid. Biochemistry 1998;37:4863-8.

218. Frank PG, N'Guyen D, Franklin V, Neville T, Desforges M, Rassart E, Sparks DL, Marcel YL. Importance of central alpha-helices of human apolipoprotein A-I in the maturation of high-density lipoproteins. Biochemistry 1998;37:13902-9.

219. McManus DC, Scott BR, Frank PG, Franklin V, Schultz JR, Marcel YL. Distinct central amphipathic alpha-helices in apolipoprotein A-I contribute to the in vivo maturation of high density lipoprotein by either activating lecithin-cholesterol acyltransferase or binding lipids. J Biol Chem 2000;275:5043-51.

220. Rogers DP, Roberts LM, Lebowitz J, Engler JA, Brouillette CG. Structural analysis of apolipoprotein A-I: effects of amino- and carboxy-terminal deletions on the lipid-free structure. Biochemistry 1998;37:945-55.

221. Mishra VK, Palgunachari MN, Datta G, Phillips MC, Lund-Katz S, Adeyeye SO, Segrest JP, Anantharamaiah GM. Studies of synthetic peptides of human apolipoprotein A-I containing tandem amphipathic alpha-helixes. Biochemistry 1998;37:10313-24.

222. Yokoyama S. Release of cellular cholesterol: molecular mechanism for cholesterol homeostasis in cells and in the body. Biochim Biophys Acta 2000;1529:231-44.

223. Rothblat GH, Phillips MC. Mechanism of cholesterol efflux from cells. Effects of acceptor structure and concentration. J Biol Chem 1982;257:4775-82.

224. Johnson WJ, Mahlberg FH, Chacko GK, Phillips MC, Rothblat GH. The influence of cellular and lipoprotein cholesterol contents on the flux of cholesterol between fibroblasts and high density lipoprotein. J Biol Chem 1988;263:14099-106.

225. Johnson WJ, Bamberger MJ, Latta RA, Rapp PE, Phillips MC, Rothblat GH. The bidirectional flux of cholesterol between cells and lipoproteins. Effects of phospholipid depletion of high density lipoprotein. J Biol Chem 1986;261:5766-76.

226. Yancey PG, Rodrigueza WV, Kilsdonk EP, Stoudt GW, Johnson WJ, Phillips MC, Rothblat GH. Cellular cholesterol efflux mediated by cyclodextrins. Demonstration Of kinetic pools and mechanism of efflux. J Biol Chem 1996;271:16026-34.

227. Rothblat GH, Mahlberg FH, Johnson WJ, Phillips MC. Apolipoproteins, membrane cholesterol domains, and the regulation of cholesterol efflux. J Lipid Res 1992;33:1091-7.

228. Haynes MP, Phillips MC, Rothblat GH. Efflux of cholesterol from different cellular pools. Biochemistry 2000;39:4508-17.

229. Mendez AJ, Oram JF. Limited proteolysis of high density lipoprotein abolishes its interaction with cell-surface binding sites that promote cholesterol efflux. Biochim Biophys Acta 1997;1346:285-99.

230. Banka CL, Black AS, Curtiss LK. Localization of an apolipoprotein A-I epitope critical for lipoprotein-mediated cholesterol efflux from monocytic cells. J Biol Chem 1994;269:10288-97.

231. Luchoomun J, Theret N, Clavey V, Duchateau P, Rosseneu M, Brasseur R, Denefle P, Fruchart JC, Castro GR. Structural domain of apolipoprotein A-I involved in its interaction with cells. Biochim Biophys Acta 1994;1212:319-26.

232. Sviridov D, Pyle L, Fidge N. Identification of a sequence of apolipoprotein A-I associated with the efflux of intracellular cholesterol to human serum and apolipoprotein A-I containing particles. Biochemistry 1996;35:189-96.

233. Fielding PE, Kawano M, Catapano AL, Zoppo A, Marcovina S, Fielding CJ. Unique epitope of apolipoprotein A-I expressed in pre-beta-1 high-density lipoprotein and its role in the catalyzed efflux of cellular cholesterol. Biochemistry 1994;33:6981-5.

234. Bergeron J, Frank PG, Scales D, Meng QH, Castro G, Marcel YL. Apolipoprotein A-I conformation in reconstituted discoidal lipoproteins varying in phospholipid and cholesterol content. J Biol Chem 1995;270:27429-38.

235. Meng QH, Bergeron J, Sparks DL, Marcel YL. Role of apolipoprotein A-I in cholesterol transfer between lipoproteins. Evidence for involvement of specific apoA-I domains. J Biol Chem 1995;270:8588-96.

236. Gillotte KL, Davidson WS, Lund-Katz S, Rothblat GH, Phillips MC. Apolipoprotein A-I structural modification and the functionality of reconstituted high density lipoprotein particles in cellular cholesterol efflux. J Biol Chem 1996;271:23792-8.

237. Sviridov D, Pyle LE, Fidge N. Efflux of cellular cholesterol and phospholipid to apolipoprotein A-I mutants. J Biol Chem 1996;271:33277-83.

238. Li Q, Komaba A, Yokoyama S. Cholesterol is poorly available for free apolipoprotein-mediated cellular lipid efflux from smooth muscle cells. Biochemistry 1993;32:4597-603.

239. Smith JD, Miyata M, Ginsberg M, Grigaux C, Shmookler E, Plump AS. Cyclic AMP induces apolipoprotein E binding activity and promotes cholesterol efflux from a macrophage cell line to apolipoprotein acceptors. J Biol Chem 1996;271:30647-55.

240. Takahashi Y, Smith JD. Cholesterol efflux to apolipoprotein AI involves endocytosis and resecretion in a calcium-dependent pathway. Proc Natl Acad Sci U S A 1999;96:11358-63.

241. Li Q, Yokoyama S. Independent regulation of cholesterol incorporation into free apolipoprotein-mediated cellular lipid efflux in rat vascular smooth muscle cells. J Biol Chem 1995;270:26216-23.

242. Li Q, Tsujita M, Yokoyama S. Selective down-regulation by protein kinase C inhibitors of apolipoprotein-mediated cellular cholesterol efflux in macrophages. Biochemistry 1997;36:12045-52.

243. Smart EJ, Ying Y, Donzell WC, Anderson RG. A role for caveolin in transport of cholesterol from endoplasmic reticulum to plasma membrane. J Biol Chem 1996;271:29427-35.

244. Uittenbogaard A, Ying Y, Smart EJ. Characterization of a cytosolic heat-shock protein-caveolin chaperone complex. Involvement in cholesterol trafficking. J Biol Chem 1998;273:6525-32.

245. Arakawa R, Abe-Dohmae S, Asai M, Ito JI, Yokoyama S. Involvement of caveolin-1 in cholesterol enrichment of high density lipoprotein during its assembly by apolipoprotein and THP-1 cells. J Lipid Res 2000;41:1952-62.

246. Hara H, Hara H, Komaba A, Yokoyama S. Alpha-helical requirements for free apolipoproteins to generate HDL and to induce cellular lipid efflux. Lipids 1992;27:302-4.

247. Mendez AJ, Anantharamaiah GM, Segrest JP, Oram JF. Synthetic amphipathic helical peptides that mimic apolipoprotein A-I in clearing cellular cholesterol. J Clin Invest 1994;94:1698-705.

248. Han H, Sasaki J, Matsunaga A, Hakamata H, Huang W, Ageta M, Taguchi T, Koga T, Kugi M, Horiuchi S, Arakawa K. A novel mutant, ApoA-I nichinan (Glu235-->0),

is associated with low HDL cholesterol levels and decreased cholesterol efflux from cells. Arterioscler Thromb Vasc Biol 1999;19:1447-55.

249. Gillotte KL, Zaiou M, Lund-Katz S, Anantharamaiah GM, Holvoet P, Dhoest A, Palgunachari MN, Segrest JP, Weisgraber KH, Rothblat GH, Phillips MC. Apolipoprotein-mediated plasma membrane microsolubilization. Role of lipid affinity and membrane penetration in the efflux of cellular cholesterol and phospholipid. J Biol Chem 1999;274:2021-8.

250. Parks JS, Gebre AK. Long-chain polyunsaturated fatty acids in the sn-2 position of phosphatidylcholine decrease the stability of recombinant high density lipoprotein apolipoprotein A-I and the activation energy of the lecithin:cholesterol acyltransferase reaction. J Lipid Res 1997;38:266-75.

251. Fielding CJ, Shore VG, Fielding PE. A protein cofactor of lecithin:cholesterol acyltransferase. Biochem Biophys Res Commun 1972;46:1493-8.

252. Steinmetz A, Utermann G. Activation of lecithin: cholesterol acyltransferase by human apolipoprotein A-IV. J Biol Chem 1985;260:2258-64.

253. Chen CH, Albers JJ. Activation of lecithin: cholesterol acyltransferase by apolipoproteins E-2, E-3, and A-IV isolated from human plasma. Biochim Biophys Acta 1985;836:279-85.

254. Sparrow JT, Gotto AM, Jr. Phospholipid binding studies with synthetic apolipoprotein fragments. Ann N Y Acad Sci 1980;348:187-211.

255. Yokoyama S, Fukushima D, Kupferberg JP, Kezdy FJ, Kaiser ET. The mechanism of activation of lecithin:cholesterol acyltransferase by apolipoprotein A-I and an amphiphilic peptide. J Biol Chem 1980;255:7333-9.

256. Ponsin G, Hester L, Gotto AM, Jr., Pownall HJ, Sparrow JT. Lipid-peptide association and activation of lecithin:cholesterol acyltransferase. Effect of alpha-helicity. J Biol Chem 1986;261:9202-5.

257. Anantharamaiah GM, Venkatachalapathi YV, Brouillette CG, Segrest JP. Use of synthetic peptide analogues to localize lecithin:cholesterol acyltransferase activating domain in apolipoprotein A-I. Arteriosclerosis 1990;10:95-105.

258. Sorci-Thomas MG, Thomas M, Curtiss L, Landrum M. Single repeat deletion in ApoA-I blocks cholesterol esterification and results in rapid catabolism of delta6 and wild-type ApoA-I in transgenic mice. J Biol Chem 2000;275:12156-63.

259. Sorci-Thomas MG, Curtiss L, Parks JS, Thomas MJ, Kearns MW, Landrum M. The hydrophobic face orientation of apolipoprotein A-I amphipathic helix domain 143-164 regulates lecithin:cholesterol acyltransferase activation. J Biol Chem 1998;273:11776-82.

260. Roosbeek S, Vanloo B, Duverger N, Caster H, Breyne J, De B, I, Patel H, Vandekerckhove J, Shoulders C, Rosseneu M, Peelman F. Three arginine residues in apolipoprotein A-I are critical for activation of lecithin:cholesterol acyltransferase. J Lipid Res 2001;42:31-40.

261. Walsh A, Ito Y, Breslow JL. High levels of human apolipoprotein A-I in transgenic mice result in increased plasma levels of small high density lipoprotein (HDL) particles comparable to human HDL3. J Biol Chem 1989;264:6488-94.

262. Rubin EM, Ishida BY, Clift SM, Krauss RM. Expression of human apolipoprotein A-I in transgenic mice results in reduced plasma levels of murine apolipoprotein A-I and the appearance of two new high density lipoprotein size subclasses. Proc Natl Acad Sci U S A 1991;88:434-8.

263. Rubin EM, Krauss RM, Spangler EA, Verstuyft JG, Clift SM. Inhibition of early atherogenesis in transgenic mice by human apolipoprotein AI. Nature 1991;353:265-7.

264. Paszty C, Maeda N, Verstuyft J, Rubin EM. Apolipoprotein AI transgene corrects apolipoprotein E deficiency-induced atherosclerosis in mice. J Clin Invest 1994;94:899-903.

265. Plump AS, Scott CJ, Breslow JL. Human apolipoprotein A-I gene expression increases high density lipoprotein and suppresses atherosclerosis in the apolipoprotein E-deficient mouse. Proc Natl Acad Sci U S A 1994;91:9607-11.

266. Williamson R, Lee D, Hagaman J, Maeda N. Marked reduction of high density lipoprotein cholesterol in mice genetically modified to lack apolipoprotein A-I. Proc Natl Acad Sci U S A 1992;89:7134-8.

267. Li H, Reddick RL, Maeda N. Lack of apoA-I is not associated with increased susceptibility to atherosclerosis in mice. Arterioscler Thromb 1993;13:1814-21.

268. Kopfler WP, Willard M, Betz T, Willard JE, Gerard RD, Meidell RS. Adenovirus-mediated transfer of a gene encoding human apolipoprotein A-I into normal mice increases circulating high-density lipoprotein cholesterol. Circulation 1994;90:1319-27.

269. Tsukamoto K, Hiester KG, Smith P, Usher DC, Glick JM, Rader DJ. Comparison of human apoA-I expression in mouse models of atherosclerosis after gene transfer using a second generation adenovirus. J Lipid Res 1997;38:1869-76.

270. Benoit P, Emmanuel F, Caillaud JM, Bassinet L, Castro G, Gallix P, Fruchart JC, Branellec D, Denefle P, Duverger N. Somatic gene transfer of human ApoA-I inhibits atherosclerosis progression in mouse models. Circulation 1999;99:105-10.

271. Tangirala RK, Tsukamoto K, Chun SH, Usher D, Pure E, Rader DJ. Regression of atherosclerosis induced by liver-directed gene transfer of apolipoprotein A-I in mice. Circulation 1999;100:1816-22.

272. Okon M, Frank PG, Marcel YL, Cushley RJ. Secondary structure of human apolipoprotein A-I(1-186) in lipid-mimetic solution. FEBS Lett 2001;487:390-6.

273. Bergeron J, Frank PG, Emmanuel F, Latta M, Zhao Y, Sparks DL, Rassart E, Denefle P, Marcel YL. Characterization of human apolipoprotein A-I expressed in Escherichia coli. Biochim Biophys Acta 1997;1344:139-52.

274. McManus DC, Scott BR, Franklin V, Sparks DL, Marcel YL. Proteolytic Degradation and Impaired Secretion of an Apolipoprotein A-I Mutant Associated with Dominantly Inherited Hypoalphalipoproteinemia. J Biol Chem 2001;276:21292-302.

275. Markwell MA, Haas SM, Bieber LL, Tolbert NE. A modification of the Lowry procedure to simplify protein determination in membrane and lipoprotein samples. Anal Biochem 1978;87:206-10.

276. Sakr SW, Williams DL, Stoudt GW, Phillips MC, Rothblat GH. Induction of cellular cholesterol efflux to lipid-free apolipoprotein A-I by cAMP. Biochim Biophys Acta 1999;1438:85-98.

277. Fournier N, Atger V, Paul JL, Sturm M, Duverger N, Rothblat GH, Moatti N. Human ApoA-IV overexpression in transgenic mice induces cAMP-stimulated cholesterol efflux from J774 macrophages to whole serum. Arterioscler Thromb Vasc Biol 2000;20:1283-92.

278. Pownall H, Pao Q, Hickson D, Sparrow JT, Kusserow SK, Massey JB. Kinetics and mechanism of association of human plasma apolipoproteins with dimyristoylphosphatidylcholine: effect of protein structure and lipid clusters on reaction rates. Biochemistry 1981;20:6630-5.

279. Sparks DL, Phillips MC, Lund-Katz S. The conformation of apolipoprotein A-I in discoidal and spherical recombinant high density lipoprotein particles. 13C NMR studies of lysine ionization behavior. J Biol Chem 1992;267:25830-8.

280. Swaney JB, O'Brien K. Cross-linking studies of the self-association properties of apo-A-I and apo-A-II from human high density lipoprotein. J Biol Chem 1978;253:7069-77.

281. Albers JJ, Chen CH, Lacko AG. Isolation, characterization, and assay of lecithin-cholesterol acyltransferase. Methods Enzymol 1986;129:763-83.

282. Sparks DL, Anantharamaiah GM, Segrest JP, Phillips MC. Effect of the cholesterol content of reconstituted LpA-I on lecithin:cholesterol acyltransferase activity. J Biol Chem 1995;270:5151-7.

283. Huang W, Sasaki J, Matsunaga A, Han H, Li W, Koga T, Kugi M, Ando S, Arakawa K. A single amino acid deletion in the carboxy terminal of apolipoprotein A-I impairs lipid binding and cellular interaction. Arterioscler Thromb Vasc Biol 2000;20:210-6.

284. Sparks DL, Frank PG, Neville TA. Effect of the surface lipid composition of reconstituted LPA-I on apolipoprotein A-I structure and lecithin: cholesterol acyltransferase activity. Biochim Biophys Acta 1998;1390:160-72.

285. Qin S, Kawano K, Bruce C, Lin M, Bisgaier C, Tall AR, Jiang X. Phospholipid transfer protein gene knock-out mice have low high density lipoprotein levels, due to hypercatabolism, and accumulate apoA-IV-rich lamellar lipoproteins. J Lipid Res 2000;41:269-76.

286. Ehnholm S, van Dijk KW, van 't HB, van der ZA, Olkkonen VM, Jauhiainen M, Hofker M, Havekes L, Ehnholm C. Adenovirus mediated overexpression of human phospholipid transfer protein alters plasma HDL levels in mice. J Lipid Res 1998;39:1248-53.

287. Applebaum-Bowden D, Kobayashi J, Kashyap VS, Brown DR, Berard A, Meyn S, Parrott C, Maeda N, Shamburek R, Brewer HB, Jr., Santamarina-Fojo S. Hepatic lipase gene therapy in hepatic lipase-deficient mice. Adenovirus-mediated replacement of a lipolytic enzyme to the vascular endothelium. J Clin Invest 1996;97:799-805.

288. Davidson WS, Arnvig-McGuire K, Kennedy A, Kosman J, Hazlett TL, Jonas A. Structural organization of the N-terminal domain of apolipoprotein A-I: studies of tryptophan mutants. Biochemistry 1999;38:14387-95.

289. Van Allen MW, Frohlich JA, Davis JR. Inherited predisposition to generalized amyloidosis. Clinical and pathological study of a family with neuropathy, nephropathy, and peptic ulcer. Neurology 1969;19:10-25.

290. Rader DJ, Gregg RE, Meng MS, Schaefer JR, Zech LA, Benson MD, Brewer HB, Jr. In vivo metabolism of a mutant apolipoprotein, apoA-IIowa, associated with hypoalphalipoproteinemia and hereditary systemic amyloidosis. J Lipid Res 1992;33:755-63.

291. Booth DR, Tan SY, Booth SE, Hsuan JJ, Totty NF, Nguyen O, Hutton T, Vigushin DM, Tennent GA, Hutchinson WL. A new apolipoprotein Al variant, Trp50Arg, causes hereditary amyloidosis. QJM 1995;88:695-702.

292. Moriyama K, Sasaki J, Matsunaga A, Arakawa K. Identification of two apolipoprotein variants, A-I Kaho (Asp 51-->Val) and A-I Lys 107 deletion. J Atheroscler Thromb 1996;3:12-6.

293. Soutar AK, Hawkins PN, Vigushin DM, Tennent GA, Booth SE, Hutton T, Nguyen O, Totty NF, Feest TG, Hsuan JJ. Apolipoprotein AI mutation Arg-60 causes autosomal dominant amyloidosis. Proc Natl Acad Sci U S A 1992;89:7389-93.

294. Booth DR, Tan SY, Booth SE, Tennent GA, Hutchinson WL, Hsuan JJ, Totty NF, Truong O, Soutar AK, Hawkins PN, Bruguera M, Caballeria J, Sole M, Campistol JM, Pepys MB. Hereditary hepatic and systemic amyloidosis caused by a new

deletion/insertion mutation in the apolipoprotein AI gene. J Clin Invest 1996;97:2714-21.

CURRICULUM VITAE

BRIAN R. SCOTT

SUMMARY

Master's degree in biochemistry with extensive experience in protein expression, purification and characterization. Experience generating and utilizing adenovirus gene therapy vectors. Strong background in enzyme kinetics. Excellent training in the use of various chromatographic methods of protein separation. Extensive prior use of molecular biology techniques including PCR, mutagenesis and cloning. Excellent oral presentation skills and a solid publication history. Self-motivated, resourceful and creative individual with strong analytical, problem solving, decision making and interpersonal skills. Bilingual – French and English.

POST-SECONDARY EDUCATION

Jan. 2002 **MASTER'S DEGREE CANDIDATE – BIOCHEMISTRY**
University of Ottawa

May 1999 **BACHELOR'S DEGREE – BIOCHEMISTRY**
University of Ottawa

Areas of Study:

- Lipoprotein Metabolism
- Genetics
- Pharmacology
- Computer Applications
- Business
- Molecular Biology
- Organic Chemistry
- Toxicology
- Spectroscopy
- Statistics

WORK EXPERIENCE

Jan. 2000-
May 2000 **TEACHING ASSISTANT**
University of Ottawa

May 1997- **UNDERGRADUATE RESEARCH STUDENT**
May 1999 Ottawa Heart Institute

Jan. 1997- **LABORATORY TECHNICIAN**
May 1997 Ottawa Hospital – Department of Pathology and Laboratory Medicine

SKILLS AND KNOWLEDGE ACQUIRED THROUGH TRAINING AND EXPERIENCE

- Extensive experience in protein expression and purification in *E. coli* and in cultured eukaryotic cells
- Chromatographic methods of protein separation including ion-exchange, affinity, gel filtration and high pressure liquid chromatography (HPLC)
- Performed enzyme kinetic analysis and used statistical and graphing software to interpret results
- Use of monoclonal/polyclonal antibodies including the development of large scale radioimmunoassays and ELISA
- Development of ligand binding assays both *in vitro* and in cell culture
- Employed many genetic and molecular biology techniques including DNA sequencing, cloning, use of restriction enzymes and polymerase chain reaction (PCR)
- Experience in virology and the use of adenovirus gene therapy vectors
- Prior training in the Workplace Hazardous Materials Information System (WHMIS)
- Experience in training and teaching other laboratory staff
- Excellent oral presentation and scientific writing skills
- Solid communication skills in both French and English

ACADEMIC ACHIEVEMENTS

Master's Thesis

Structure-Function Relationships of Human Apolipoprotein A-I: Role of the Amino-Terminal Amphipathic Alpha-Helices

Our research, conducted at the Ottawa Heart Institute, focused on apolipoprotein A-I (apoA-I), the predominant protein constituent of high density lipoproteins (HDL), and the mechanisms by which this protein protects against the development of atherosclerosis. To this end, wild-type apoA-I and various deletion mutants thereof were expressed and purified from *E. coli* and characterized using a multitude of structural biochemical studies and enzymatic analysis. In addition, using an *in vivo* approach, similar proteins were transiently expressed in apoA-I deficient mice using recombinant adenovirus vectors. The HDL formed containing the wild-type and mutant forms of apoA-I were isolated and used for biochemical analysis. This work was presented at 2 research conferences and was recently published in the Journal of Biological Chemistry.

Publications

Scott, B.R., McManus, D.C., Franklin, V., McKenzie, A.G., Neville, T., Sparks, D.L., Marcel, Y.L. (2001) The N-terminal globular domain and the first class A amphipathic helix of apolipoprotein A-I are important for lecithin:cholesterol acyltransferase activation and the maturation of high density lipoprotein *in vivo*. *J. Biol. Chem.* 276, 48716-48724

McManus, D.C., Scott, B.R., Franklin, V., Sparks, D.L., Marcel, Y.L. (2001). Proteolytic degradation and impaired secretion of an apolipoprotein A-I mutant associated with dominantly inherited hypoalphalipoproteinemia. *J. Biol. Chem.* 276, 21292-302.

McManus, D.C., Scott, B.R., Frank, P.G., Franklin, V., Schultz, J.R., Marcel, Y.L. (2000). Distinct central amphipathic alpha-helices in apolipoprotein A-I contribute to the in vivo maturation of high density lipoprotein by either activating lecithin-cholesterol acyltransferase or binding lipids. *J. Biol. Chem.* 275, 5043-51.

Research Scholarships

Natural Sciences and Engineering Research Council (NSERC) of Canada Post-Graduate Scholarship
Ontario Post-Graduate Research Scholarship
NSERC Undergraduate Research Scholarship
Bill Schultz Undergraduate Research Scholarship – Heart & Stroke Foundation of Ontario

Recent Presentations

Apr. 2001 **LIPOPROTEIN AND ATHEROSCLEROSIS GROUP SEMINAR**
A detailed review and analysis of my research was presented to the Lipoprotein research group at the Ottawa Heart Institute.

Apr. 2001 **2001 OTTAWA HEART INSTITUTE RESEARCH COMPETITION**
Presentation entitled 'The Contribution of the Amino-Terminus of Apolipoprotein A-I to Reverse Cholesterol Transport' was presented as part of the students' competition during this annual research event.

Mar. 2001 **DEPARTMENTAL SEMINAR**
Oral research presentation given to the professors and students of the Department of Biochemistry, Microbiology and Immunology at the University of Ottawa.

Oct. 2000 **2000 CANADIAN LIPOPROTEIN RESEARCH CONFERENCE**
A poster presentation entitled 'The In Vivo Characterization of the Amino-Terminus of Apolipoprotein A-I' was delivered at this annual research conference.

COMPUTER SKILLS

- Working knowledge of Windows operating systems
- Proficient in Microsoft Word, Excel and Powerpoint
- Experience using scientific graphing software (ex. Sigmaplot)

PERSONAL ATTRIBUTES

- Works well under pressure within a fast-paced environment
- Able to coordinate and prioritize workload to meet stringent deadlines
- Fast learner; can grasp and apply new procedures/techniques quickly
- Interact cooperatively within a team environment
- Adapt readily to the demands of the position, including new challenges and work environments

HOBBIES AND INTERESTS

- Coaching high school volleyball
- Tutoring
- Golf, kayaking, squash and running
- Hiking and camping

CONTRIBUTIONS OF COLLABORATORS

Dan C. McManus

Dr. McManus generated the Wt and Δ7-65 apoA-I Ad5 constructs used for the *in vivo* characterization of the amino-terminus of apoA-I.

Vivian Franklin

Ms. Franklin expressed and purified the His-Wt apoA-I protein and performed the purification steps for all other His-apoA-I deletion mutants.

Andrea G. McKenzie

Miss McKenzie helped to generate the His-Δ210-243 apoA-I construct and optimize the conditions of its expression.

Phillippe Frank

During the course of his Ph.D studentship, Dr. Frank established the conditions for the purification of histidine-tagged apoA-I in our laboratory.

Christie G. Brouillette and Jeffrey A. Engler

The histidine-tagged Δ1-65 apoA-I cDNA cloned into the pGEMX prokaryotic expression vector was generously donated by Drs. Brouillette and Engler for this work.

Peter Rippstein

Mr. Rippstein was involved in the electron microscopic examination of the HDL samples isolated from apoA-I deficient mice. He performed the carbon coating of the formvar grids and provided some general tutelage as to the use of the microscope.